The destruction of ultradian and circadian rhythms

Mansour Awadh Alanazi, BSc, MSc

Department of Physics

Lancaster University

A thesis submitted for the degree of

Doctor of Philosophy

December, 2024

Declaration

I declare that the work presented in this thesis is, to the best of my knowledge and belief, original and my own work. The material has not been submitted, either in whole or in part, for a degree at this, or any other university.

Mansour Awadh Alanazi

Abstract

One of the most generally recognised rhythms observed across various living creatures is the circadian rhythm, a recurrent biological activity lasting around 24 hours. It is said to have evolved in reaction to the regular environmental alternation of light and darkness. Pacemaker cells, which are thought to be critical in generating the circadian rhythm, have been identified in suprachiasmatic nucleus (SCN) in 1972. However, there is ongoing discussion about whether the circadian rhythm is a truly basic rhythm generated in the SCN, or whether alternative mechanism are involved in its modulation.

Arousing stimuli, such as scheduled feeding, running wheel access, or methamphetamine (MA) administration, represent non-canonical circadian processes. Here, we investigate the circadian rhythm in genetically modified mice with the *Per1/2/3* genes knocked out, resulting in a disturbance of this rhythm, as *Per1/2/3* genes are essential components of the mammalian canonical circadian mechanism. Additionally, the effect of MA, a potent central nervous system stimulant, was evaluated on *Per1/2/3* genes knock out mice. As a reference, a group of wild-type mice was also recorded. In each case wheel running activity was recorded every minute for a period of 4 to 9 weeks. The investigation aimed to deduce whether rhythms remained when the clock genes were disabled and how MA affects them.

Nonlinear time-series analysis methods, specifically developed for analysis of oscillatory processes with time-varying frequencies, where used to analyse the recorded time series. We show that MA restores the circadian rhythm and increases the total power. Moreover, the rhythm gets more irregular with MA administration compared to the wild-type case. Additionally, MA introduces a new circabidian rhythm at around 40 hours.

In addition to the power analysis, couplings between rhythms on different timescales were considered. Firstly, harmonic analysis was performed to deduce which of the observed oscillations result from independent modes. This analysis revealed that,

in all *Per1/2/3* knock out mice not exposed to MA, there is a harmonic relationship between the 7 and 3.5 hour cycles. Following this, to elucidate the coupling between the remaining independent modes, bispectral analysis and dynamic Bayesian inference were applied. The *Per1/2/3* knocked out mice exposed to MA exhibited coupling between ∼24 hours and ∼1 hour oscillations, while in the *Per1/2/3* knocked out mice not exposed to MA a coupling between ∼8 hours and ∼1 hour oscillations was observed.

This study revealed the relationship between oscillators in the absence of a canonical circadian clock as well as the effect of MA. Power and coupling analyses provide a useful approach for understanding the functional significance of behavioural rhythms. Such investigations are vital, as disruptions in circadian rhythms are implicated in various diseases, including cancer, obesity, and mood disorders.

Based on the obtained results a phenomenological model was developed. It elucidates the dynamic characteristics of circadian rhythms in *Per1/2/3* knockout mice, particularly focusing on the alterations induced by methamphetamine exposure. The model captures the time-varying nature of oscillations and their interactions, providing insights into the underlying mechanisms of circadian regulation and potential implications for behavioural health.

Publications

The following manuscripts are currently under review:

- Samuel J.K. Barnes, Mansour Alanazi, Shin Yamazaki & Aneta Stefanovska. Methamphetamine alters the circadian oscillator and its couplings on multiple scales in Per1/2/3 knockout mice. *PNAS Nexus, 2024 (in revision).*

Parts of the work have been presented at the following scientific meetings or workshops:

- Mansour Alanazi, Samuel J.K. Barnes, Shin Yamazaki & Aneta Stefanovska. The effect of methamphetamine administration on ultradian, circadian and infradian rhythm. *Lancaster Biosciences Network, Symposium. 13 July 2023. Lancaster University, Lancaster, UK.* Poster presentation.

- Mansour Alanazi, Samuel J.K. Barnes, Shin Yamazaki & Aneta Stefanovska. The destruction of ultradian and circadian rhythms. *time-series analysis of noisy data, Workshop. 13–15 September 2023. Lancaster University, Lancaster, UK.* Poster presentation.

Glossary and abbreviations

IAAFT Iterative amplitude - adjusted Fourier transform. A method used for generating surrogates of a signal.

PSD Power spectral density. A method used to describe the distribution of power into frequency components composing that signal.

WFT Windowed Fourier transform. Time-frequency representation.

WT Wavelet transform. Time-frequency representation.

TFR Time-frequency representation. It is a view of a signal (taken to be a function. of time) represented over both time and frequency.

FT Fast Fourier transform. A fast algorithm for the computation of the Fourier.

DFT Discrete Fourier transform. transform, which transforms a signal from the time domain to the frequency domain.

DBI Dynamical Bayesian Inference. A method used to determine whether a pair of oscillators within a system.

SCN Suprachiasmatic Nucleus A cluster of cells located in the brain's anterior hypothalamus that is responsible for coordinating circadian rhythmicity in mammals.

MASCO The methamphetamine-sensitive circadian oscillator.

FEO Food-entrainable oscillator

MA the methamphetamine Drug.

DD Constant darkness.

LD 12 hours light and 12 hours dark.

Acknowledgements

I would like to thank my supervisor Professor Aneta Stefanovska for her help and unwavering support throughout my PhD. Without her help, support and time I would not have completed this thesis. I am very grateful for her unreserved support throughout my thesis, guiding me with her knowledge, experience and enthusiasm. Many thanks to prof. Shin Yamazaki and his research group (University of Texas South Western, Dallas, TX) for providing me the data.

With abundant love and affection, my sincerest gratitude goes to my beloved kind mother, and my ever supportive father, "My Lord, have mercy upon them as they brought me up [when I was] small" (Holy Quran, Isra 17:23-24).

To my wife, whose strength and encouragement have been my constant source of inspiration, I owe a debt of gratitude that words cannot fully express. To my children (Moath, Maria and Tamim), who bring immeasurable joy and motivation into my life, I thank you for your cheerful smiles and unwavering belief in me.

A special gratitude for the scientific assistance and kind friendship goes to Samuel J.K. Barnes for his encouragement, unconditional support and discussions during my PhD journey.

I would also like to thank everybody that has made the department a serene atmosphere throughout the years, especially my co-researchers in the office: Dr. Hala Siddiq, Juliane Bjerkan, Dr. Sultan Alatawi, Dr. Yunus Abdulhameed and Dr. Joe Adams.

Many thanks go to my government, Saudi Arabia, and my sponsor, Northern Border University, which never hesitated to support me financially and academically.

Contents

List of Figures

List of Tables

1. Introduction

In many natural and life-related fields, cyclic and repeating events are common. These behavioural and physiological patterns and processes can be divided into two groups based on the mechanisms that initiate and govern them. Certain behavioural and physiological cycles are directly caused by changes in the external environment. These externally generated alterations in behaviour and physiology are known as "masking" effects and are caused by stimuli such as light, temperature, or social interaction [1]. Additional cycles are governed by intrinsic biological systems such as tissue clocks and cellular oscillations. These events are known as biological rhythms, and they can last from milliseconds to months or even years. They have been seen in the behaviour and physiology of many species, and this diversity is important in maintaining strong and operational biological systems [4].

Biological rhythms are divided into three types based on their duration or cycle length. The first type consists of *infradian rhythms*, which are rhythms that repeat for more than 24 hours, ranging from many days to months. The second category of rhythms includes those with about 24-hour cycles, known as *circadian rhythms*, which is encompassed everyday patterns of rest and activity in humans, as well as the release of melatonin. Melatonin is a hormone generated by the pineal gland, and its secretion reaches its highest point during the dark hours of the day [5, 6]. The third type comprises *ultradian rhythms*, which are rhythms that last shorter than 24 hours. They can have periods ranging from milliseconds to several hours [4]. Circadian rhythms are distinct from the other two types of biological rhythms. They are distinguished

by a relatively short time of around 24 hours, as opposed to ultradian and infradian rhythms, which contain a diverse spectrum of biological rhythms exhibited with varying durations.

Actigraphy, a method for monitoring physical activity patterns over extended periods ranging from days to several weeks, serves as a cost-effective, non-invasive, and ecologically valid approach in studying sleep-wake patterns in humans, see figure 1.1 as an example. This technique holds particular promise for investigating circadian abnormalities in individuals with insomnia. While the American Academy of Sleep Medicine (AASM) does not mandate actigraphy for diagnosing insomnia, it acknowledges it as an optional tool for examining suspected circadian disruptions in this population [7].

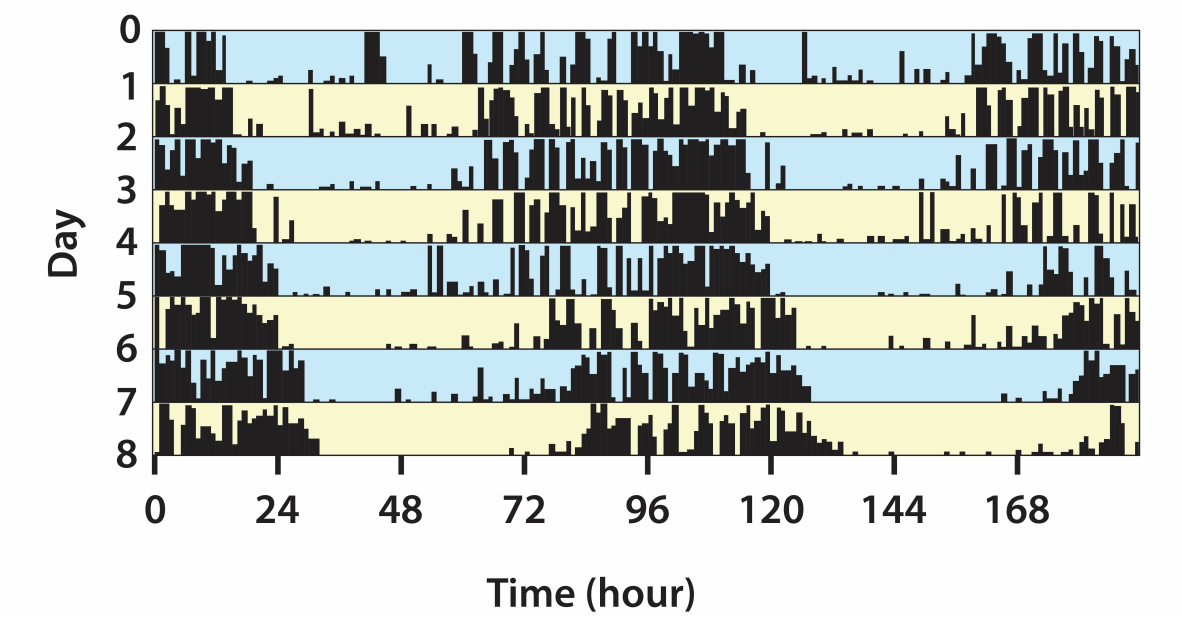

Figure 1.1: Example of actigraphy data for the circadian component. The y-axis indicates the days, and the black lines represent the rhythms. The x-axis shows the time in hours.

However, the results from studies utilizing actigraphy to explore whether circadian disruptions are a consistent characteristic of insomnia have been notably inconclusive

[8, 9]. This lack of consensus could be attributed to two potential factors: (i) circadian disruption may not routinely manifest as a feature of insomnia by the time it becomes chronic, or (ii) the methodology, and more likely, the statistical analysis employed, may lack the sensitivity required to detect subtle yet significant levels of circadian disruption if present. A notable challenge in employing actigraphy for sleep disorder diagnoses is the difficulty in identifying and eliminating artifacts in the data [10]. This ongoing challenge underscores the need for refined methodologies and analytical approaches in utilizing actigraphy for a more accurate and insightful examination of circadian disruptions in insomnia.

The traditional approach for examining circadian rhythms involves cosinor analysis [11]. This method measures the 24-hour circadian cycle and other specific shorter or longer periodic cycles. It does this by evaluating how well the experimental data align with a pre-determined model made up of overlapping cosine functions. Cosinor analysis is effective in determining key circadian parameters like mesor (the rhythm-adjusted mean), amplitude (the extent of rhythm variation), period (the duration of one cycle), and acrophase (the peak time of the rhythm). This technique allows for a detailed assessment of these parameters, providing insights into the underlying mechanisms of circadian rhythms and their variations under different conditions [11, 12, 13, 14]. Yet, when dealing with data that exhibit irregular patterns or whose statistical characteristics change over time (known as nonstationary time series) [15, 16, 17], such as those with a prevailing trend or data where amplitudes, frequencies, or phases vary with time, it becomes significantly more challenging, if not impossible, to accurately describe using models based on periodic functions. These complexities necessitate more advanced analytical approaches. In cases where the data deviate from regular, predictable patterns, traditional models like those based on cosine functions may not capture the full extent of the variability and complexity inherent in the data. Therefore, exploring alternative models or methods that can accommodate these variations, like advanced statistical techniques or machine learning algorithms, might be necessary.

These alternative approaches could provide a more nuanced understanding of irregular or nonstationary data, leading to more accurate and comprehensive insights into the underlying phenomena [18]. Moreover, a drawback of cosinor analysis is its struggle to effectively represent irregular or changing patterns in time series data. If a physiological time series shows inconsistencies, such as variations in amplitude, frequency, or phase over time, cosinor analysis might not accurately depict these aspects. Furthermore, it may fall short in detecting rhythm fragmentation, which is the breakdown of a regular circadian rhythm due to events like daytime sleeping or nighttime activity. Consequently, Although cosinor analysis is useful for assessing the 24-hour circadian cycle and other regular cycles, it may not fully capture the complexities of irregular or dynamically changing physiological rhythms. [18].

In this thesis, we aim to explore the behavioral rhythms that persist in a biological system even when the standard circadian clock mechanisms are switched off and external cues are absent. Modeling biological systems is challenging, and simplifications often lead to the loss of key features. Within these systems, oscillators can display varying frequencies, phases, amplitudes, and interactions. As a result, we need to employ innovative numerical techniques to unravel their intricate dynamics. The time series data collected from continuous behavioral monitoring have been examined using a unique set of methods designed to resolve multi-oscillatory dynamics over time. These algorithms focus on using both phases and amplitudes from the signals, which is advantageous because amplitudes alone are more susceptible to noise and artifacts. Importantly, our method does not depend on the assumption that phases or frequencies are constant[19, 20].

1.1 Aims and objectives of the work

The main goal of this thesis is to investigate the behavioral rhythms that remain in a biological system after the canonical circadian timekeeping mechanism is disabled

and in the absence of external stimuli. These methods are tailored to enable the time-resolved analysis of multi-oscillatory dynamics, capturing the intricate and evolving nature of biological systems [19]. The algorithms used for analyzing biological systems focus on both the phases and amplitudes of the signals, instead of relying solely on amplitudes, which are more susceptible to noise and artifacts. Importantly, these algorithms do not make the assumption that phases or frequencies remain constant. This approach allows for a more accurate and nuanced understanding of the dynamic and often fluctuating nature of biological oscillators, capturing the real-time variability and complexity inherent in living systems.

To address and answer the following questions:

1. Can circadian rhythm persist even when clock genes are knockout?
2. Does methamphetamine administration cause a disruption in the rhythm of the mice?
3. Does the system retain a memory of past disturbances under varying conditions?

1.2 Outline of thesis

Chapter 2 delves deeply into the subject of circadian rhythms, examining their physiological impacts and the significant role played by the suprachiasmatic nucleus (SCN) and clock genes. Key areas of focus in this chapter include:

Physiological manifestations of circadian rhythms: Detailing how these rhythms influence various bodily functions, including sleep patterns, hormonal secretion, and metabolic processes.

Suprachiasmatic nucleus (SCN) and nlock genes: Exploring the SCN's position as the central regulator of circadian rhythms in mammals and the function

of clock genes in maintaining these rhythms at a cellular level.

Molecular mechanisms: Investigating the molecular basis of circadian rhythms, including the feedback loops and genetic expressions involved.

Peripheral oscillators: Understanding how cells outside the SCN, known as peripheral oscillators, contribute to circadian regulation in different body parts.

Pacemakers and response to methamphetamine: understanding how circadian pacemakers, including the SCN, respond to external stimuli like methamphetamine, and the implications of this response.

Disruption of circadian rhythms: Discussing the causes and effects of circadian disruption, including environmental factors, lifestyle choices, and exposure to certain substances, and how these disruptions impact overall health and well-being.

Chapter 3 outlines the experimental protocol and details the behavioral data being investigated. It includes:

Description of the experimental protocol: This section provides a thorough explanation of the procedures, settings, and conditions under which the experiments were conducted, ensuring clarity on how the behavioral data was collected.

Behavioral data information: The chapter presents comprehensive information on all behavioral data under investigation, including the types of behaviors observed, the conditions under which these behaviors were recorded, and the specific parameters measured.

Introduction to analytical methods: Here, the chapter introduces the methodologies employed to analyze the collected data.

Chapter 4 presents an analysis of the data and the results obtained, and **Chapter 5** presents the model which focuses on the dynamics of circadian rhythms and their alterations following methamphetamine exposure in *Per1/2/3* knockout (KO) mice.

Chapter 6 discusses the results presented in chapter 4.

Chapter 7 summarises the work presented in the thesis and outlines possible directions for future research.

Detailed information about the results of systematic analysis is provided in the supplementary material and ethics approval from Prof. Shin Yamazaki, which is available in PURE, together with the measured data used in the analysis.

2. Biophysical review

2.1 Circadian rhythms

Circadian rhythms are biological cycles that occur over a 24-hour period and regulate behaviors and physiological processes like sleep, body temperature, and metabolism [21]. The fact that circadian rhythms are endogenous was definitively demonstrated by NASA scientists and astronauts who discovered that rhythmicity in the fungus Neurospora crassa is preserved in constant darkness during a space flight in which all geophysical cues are removed.[1, 21]

The fungus kept the same circadian patterns in space as it did on Earth. This established the presence of an internal biological timekeeping system, and the hunt for the underlying mechanisms began in earnest [1, 22]. Scientists established three key properties of circadian rhythms: they are self-sustained, meaning they persist even in constant conditions; they can be synchronized by environmental cycles, such as light and dark; and they maintain a consistent 24-hour period across a range of temperatures. These properties form the basis for understanding circadian rhythms in organisms [23]. Moreover, when circadian rhythms continue to cycle without external cues, such as light or other timing signals, they are referred to as free-running. This means that the internal biological clock of an organism maintains a cycle close to 24 hours even in the absence of environmental influences. The term "*free-running*" describes the ability of circadian rhythms to persist independently of external factors. The phase of a rhythm

acts as a prominent point within the cycle, such as its peak or trough parameters as illustrated in figures 2.1 and 2.2.

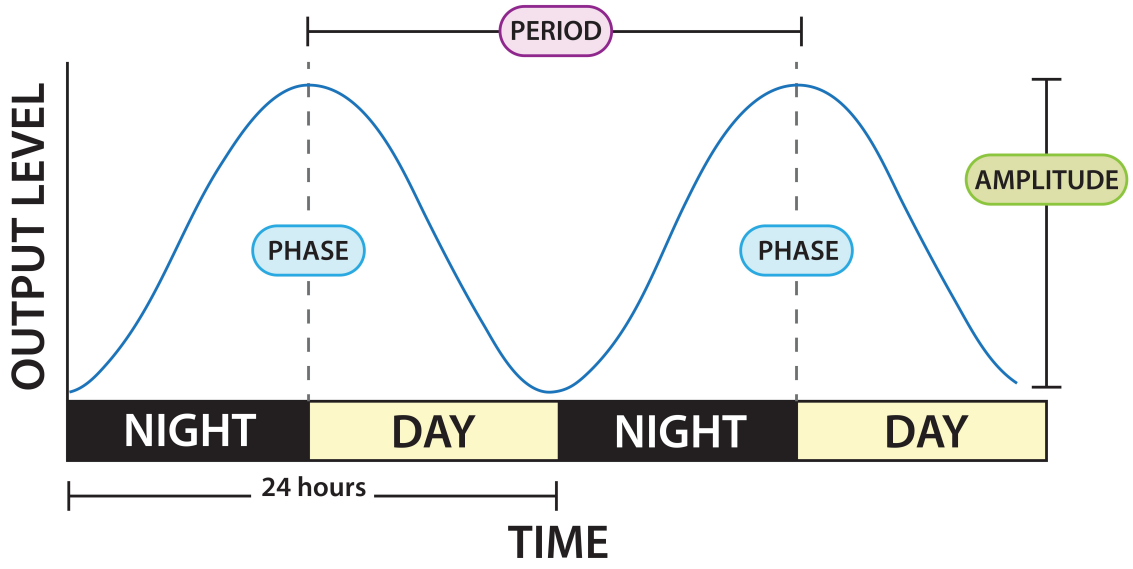

Figure 2.1: Modified from [1]. The amplitude, phase, and period of circadian rhythms are three crucial factors to consider. The amplitude is the difference in output level between the rhythm's peak and trough values. The phase is the timing of a reference point in the rhythm cycle in relation to a definite event. The period is the time interval between two reference points in the rhythm.

Because the period is rarely exactly 24 hours, a minor mismatch between the organism and its environment happens on a regular basis. Through daily phase shifts, the circadian clock is synchronised to the external cycle. This synchronisation enables us to match our rhythms to external timing cues like the light-dark cycle. When these cues vary, as when travelling across time zones, our circadian rhythms undergo phase shifts to realign with the new environmental cues, a process called as entrainment [1]. Many stimuli can cause rhythms to phase shift; however, the magnitude of the phase

shift is dependent on when the signal is delivered during the cycle. The most obvious signal in circadian entrainment is light, and light pulses have been used to construct phase response curves. These represent phase-dependent-resetting responses to light and are important tools for predicting how an organism would entrain to changes in the environmental light-dark cycle or light intensity.

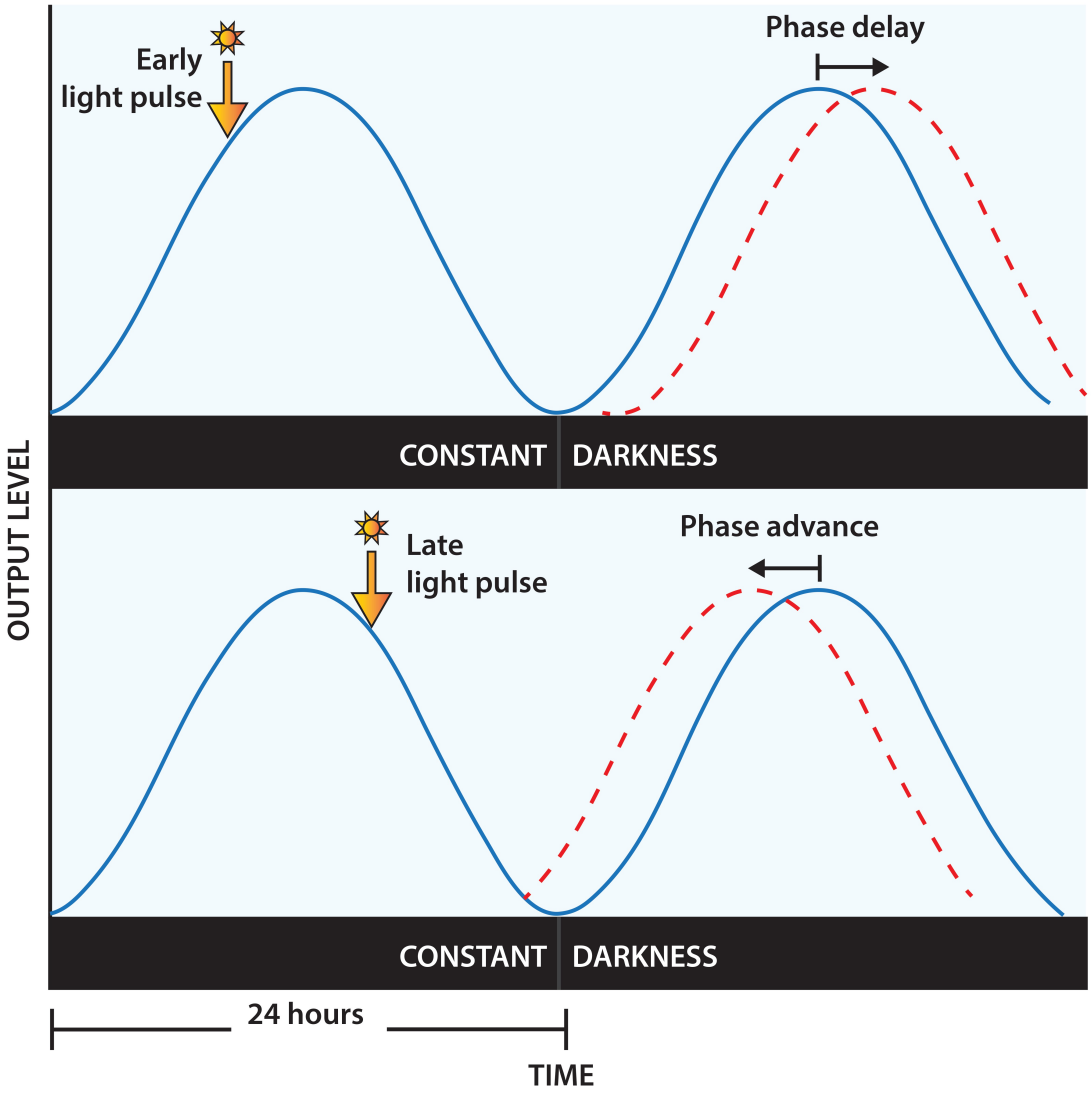

Figure 2.2: Modified from [1]. Illustration of an early-morning light pulse exposure that produces a delay in the commencement of the rhythm (top panel: phase delay, blue arrow), with the phase occurring later than predicted (solid line, expected phase; dotted line, delayed phase after light exposure). In contrast, late-night exposure to a light pulse leads to an earlier commencement of the rhythm (bottom panel: phase advance, blue arrow), where the phase arrives earlier than expected .

2.1.1 The physiological expression of circadian rhythms

The circadian rhythm is the most obvious and well-studied of all the biological rhythms, and practically every aspect of human physiology will show at least some degree of circadian control. This is true even though all biological rhythms are evident in human functioning. Sleep, temperature, and a variety of hormonal markers, most notably melatonin levels, are frequently researched examples of phase markers that can be used to determine the timing of the circadian cycle [24].

2.1.1.1 Temperature

Since it was originally observed in the 19th century, the circadian rhythm of core body temperature (CBT) has been the subject of extensive research ever since it was discovered to be a physiological phenomenon [25]. The temperature of an average human's body rises by around 0.5 degrees Celsius during the course of a day, reaching its lowest point in the morning and rising to its highest point in the late afternoon and evening [26]. It is common for an individual's core body temperature to drop to its lowest point during the second part of the sleep cycle, and this temperature drops to its nadir, which is one of the major markers for circadian rhythms, around two hours before the individual's habitual waking time. The paraventricular nucleus and the hypothalamus are responsible for the underlying control of temperature change. They do this by modifying the activity of the autonomic nervous system.

Changes in CBT can be brought about by a variety of external variables, such as smoking, drinking alcohol, and alterations in one's routine; biological factors, such as advancing age and illness; and physiological processes, such as physical activity and metabolic rate [27, 28].

2.1.1.2 Melatonin

Melatonin, a neurohormone secreted by the pineal gland, plays a crucial role in the regulation of circadian rhythms and the promotion of sleep. It is responsible for regulating the sleep/wake cycle, as well as other circadian and some biological rhythms. Additionally, melatonin works as an immunostimulator and cytoprotective agent [29]. The cyclical release of hormones is an ubiquitous characteristic observed in all vertebrate species [30]. Melatonin's circadian rhythm can travel through the bloodstream and reach every cell in the body because it is a hormone that circulates. It is likely that these receptors reside on the membranes of all cells whose activity must be synchronised by the melatonin rhythm [31], which is a demonstration of the significance of this regulation. The widespread distribution of melatonin receptors [32, 33] is a demonstration of the importance of this regulation.

Melatonin activities are pleiotropic, which means that it influences several phenotypic qualities that appear to be unrelated to one another. Nuclear receptors and various additional binding sites and chemical interactions are also responsible for mediating these effects. Because melatonin can affect cellular processes independently of receptors, it is possible that membrane mediators are not necessary for the hormone to have an effect on circadian gene expression in peripheral cells. This would be the case if melatonin could control these processes. Since its production is instantly inhibited by light, all animals that emit melatonin do so at night. It has been demonstrated that the melatonin rhythm provides an optimal marker of circadian phase in humans [34], specifically if samples (saliva, blood, or urine) are obtained in low light and controlled posture settings. Since light melatonin onset is easily quantifiable in saliva just before bedtime. Despite their potential diagnostic utility, melatonin tests are neither a quick nor widely accessible approach. In 1963, Wurtman et al [35, 36] made an important discovery about the impact of the circadian melatonin rhythm on reproductive physiology. They found that the administration of melatonin resulted

in a decrease in the weight of the ovaries in female rats. There exists empirical evidence indicating that melatonin has an impact on the reproductive capacity of numerous species. Moreover, it has been observed that the secretion pattern of melatonin, which is regulated by exposure to light, directly impacts reproductive function [36].

2.1.1.3 Activity

One of the most apparent manifestation of the circadian rhythms is the pattern of activity. The understanding of the characteristics of the circadian system, the influence of zeitgebers in achieving optimal synchronisation with the 24-hour day, and the mechanisms involved in sleep regulation has resulted in the formulation of rigorous methodologies for studying circadian rhythms and activity. These research have established the benchmark methods for determining circadian amplitude and phase, and have determined the physiological or hormonal markers that are most effective for this purpose. The current problem consists of developing simple markers that may be used ambulatorily and which provide a good estimate of the phase of the circadian cycle.

Long-term measurements taken over the course of at least one 24-hour cycle are necessary for chronobiology. Polysomnography is the neurophysiological method that is considered to be the gold standard for detecting sleep; nevertheless, it is also quite expensive, requires that the individuals attend a sleep laboratory, and uses advanced technology for interpreting the results. The latest microchip technologies make it possible to collect non-invasive data continuously over the course of many days. Data loggers are what actigraphy monitors are called, and they record digitally integrated measures of a person's gross motor activity. They keep track of the amount of white light exposure, activity levels, and are a valid measure of the activity status of healthy populations [7]. Actigraphy properly is a non-invasive technique used to assess cycles of activity and rest over several days to several weeks. compared with polysomnography which is a test used to diagnose sleep disorders, and shown robust inter unit reliability

and good validity [37]. The research was carried out by Pollak and colleagues [38] on adults using two commercial devices.

Polysomnography is a test used to diagnose sleep disorders usually performed during the night, while actigraphy is a non-invasive technique used to assess cycles of activity and rest over several days to several weeks.

2.2 Suprachiasmatic nucleus (SCN)

During the 1970s, researchers conducted ablation studies in an effort to pinpoint the location of the biological clock within the brain. Through the targeted destruction of specific brain regions using minimal electric current, scientists determined that damage to a particular area within the hypothalamus disrupted the normal daily rest-activity rhythms of animals. This groundbreaking research directed their focus toward a specific region, namely the anterior hypothalamus, which appeared to house the biological clock.

Identification of the precise location of the internal circadian clock occurred nearly simultaneously in two independent laboratories while examining rats. Robert Moore's laboratory provided the original breakthrough. Given that light cues are the key signals for establishing the circadian rhythm in animals, it was only natural to look at areas associated with light reception. Moore's tract tracing research showed a previously unknown bidirectional connection from the retina to the hypothalamus, a portion of the brain not directly related to vision. The hypothalamus, notably the suprachiasmatic nucleus (SCN) located above the optic chiasm, was identified as the brain region that receives information about environmental light [22, 39].

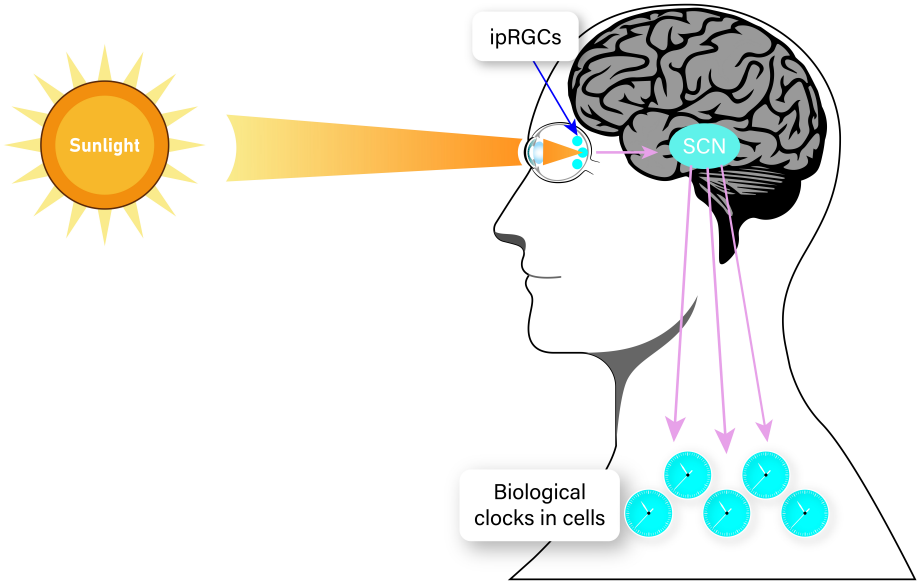

Figure 2.3: Modified from [2] illustrating an entrainment of the circadian rhythm to the 24-hour environmental light-dark cycle. Temporal information in the form of sunlight enters through the eyes and is transmitted to the SCN. The SCN then passes on this information to the rest of the circadian body clocks throughout the body.

The SCN plays a crucial role in maintaining the alignment of phases among different tissues in the body. Its role as the central circadian pacemaker involves the synchronization of various oscillators present throughout the brain and the body. Instead of forcing rhythmicity upon cells that naturally lack it, the SCN serves as a coordinator, harmonizing the rhythms of other timekeeping mechanisms. To put it in perspective, the SCN functions much like the conductor of an orchestra, ensuring the harmonious timing of various components. With this understanding, the circadian system can be envisioned as a hierarchical structure, with the SCN occupying the highest position [1, 40].

In order to ensure the optimal operation of the circadian timing system, it is imperative to maintain synchronisation among all the circadian clocks throughout the

body, as well as align them with the 24-hour day. This crucial task is carried out by the suprachiasmatic nucleus (SCN), which serves as the master circadian pacemaker (5). Similar to other types of cells [41], SCN neurons have the ability to establish self-sustained circadian rhythms [42]. However, SCN neurons possess distinctive characteristics that are significant in several ways. Initially, the cells in question get direct visual input from the retina, enabling them to align their activity with the diurnal rhythm [43] 2.3. Additionally, these organisms possess unique coupling systems that are organised based on topography. This enables them to maintain synchronisation with each other even under conditions of perpetual darkness [44]. Furthermore, these organisms exhibit a distinct circadian rhythm in the frequency of neuronal firing. This rhythm enables them to synchronise other cells in the body through several direct and indirect channels [45]. Therefore, the suprachiasmatic nucleus (SCN) serves as the central pacemaker that regulates the synchronisation, or entrainment, of secondary cellular oscillators to the light/dark cycle. Moreover, due to internal coupling, the suprachiasmatic nucleus (SCN) is capable of producing a synchronised output signal even in the absence of a light/dark cycle.

This phenomenon explains the presence of "free-running" circadian rhythms, which last around 24 hours, in both physiological and behavioural processes that persist under constant environmental conditions. However, it is important to note that the suprachiasmatic nucleus (SCN) encompasses more than a mere collection of interconnected oscillator cells that receive light input and produce synchronised rhythmic output. Despite the ability of SCN neurons to oscillate autonomously, their functionality is mostly dependent on collaborative interactions within the tissue, relying more on input from neighbouring cells to form rhythmic patterns compared to fibroblasts [46]. The SCN pacemaker is capable of generating output signals with diverse phases to various tissues through the presence of phase diversity among its constituent cells [47]. Moreover, alterations in the phase connections among neurons in the suprachiasmatic nucleus (SCN) have the potential to modify the intensity or shape

of rhythmic outputs at the level of the entire organism.

This phenomenon can explain the impact of persistent exposure to light [48], variations in day length throughout the year [49], and certain genetic mutations that influence the coupling of SCN neurons [50]. The suprachiasmatic nucleus (SCN) has a higher level of precision in generating rhythmic output signals compared to individual cells [51]. The rhythmic output of SCN is demonstrated to have greater resilience to genetic alterations compared to individual cells [52]. Welch et al examined examines the role of the suprachiasmatic nucleus (SCN) as a central regulator of circadian rhythms, with a specific emphasis on its cellular autonomy and network characteristics [53].

2.3 Clock genes

The initial discovery of a gene responsible for the circadian rhythm was made in Drosophila, specifically the period (*Per*) gene [54]. Subsequent investigations have also brought to light another gene implicated in the circadian rhythm: the timeless (*Tim*) gene [55, 56, 3]. In mammals like mice, the use of chemical mutagenesis techniques facilitated the identification of the initial clock genes. One such gene is the circadian locomotor output cycles kaput *Clock* gene, and mutations in this gene were found to extend the rest-activity cycle. Further research in mouse circadian regulation led to the identification of additional clock genes. These included the brain and muscle ARNT-like protein 1 (*Bmal1*) gene, which acts as a partner to *Clock*, along with the *Per1* and *Per2* genes. Additionally, the cryptochrome-1 (*Cry1*) and *Cry2* genes, responsible for encoding proteins involved in blue light reception in non-mammalian species, were also discovered in the context of circadian regulation [57, 3].

Melatonin, primarily produced by the pineal gland, is crucial for managing the sleep-wake cycle and other circadian rhythms. Its release is carefully regulated by the suprachiasmatic nucleus (SCN), which receives light-dark cycle information from the retina. At night, when light levels are low, the SCN prompts the pineal gland

to secrete melatonin, inducing drowsiness and facilitating rest. In contrast, during daylight hours, when light levels are elevated, melatonin secretion is inhibited. [58, 59] Melatonin's involvement in circadian oscillatory rhythms, especially as a neuroendocrine regulator of molecular oscillatory systems, has been documented in previous research [58, 59, 60, 61]. Experiments conducted with animal models have demonstrated that melatonin plays a role in governing the circadian expression of various clock genes. These include *Per1* and *Per2*, *Bmal1*, reverse erythroblastosis virus, *Clock*, and *Cry1*, and this regulation extends to both central and peripheral tissues that are responsive to melatonin. Melatonin can also coordinate circadian oscillations in the cardiovascular system by influencing the circadian rhythmic expression of Per1 and Bmal1 in the rat heart [62]. Melatonin stimulates the expression of Cry1 while suppressing the expression of other clock genes in the pituitary gland of sheep [63].

In the case of humans, counterparts of *Clock*, *Bmal1*, *Per*, and *Cry* genes have been identified. Notably, the *Clock* gene, which is the sole cloned circadian rhythm gene, is situated on chromosome 4 [64]. Additionally, there exist other clock genes responsible for circadian regulation, including retinoic acid receptor-related orphan receptor and casein kinase-1. These genes are involved in regulating the transcription of the *Bmal1* gene. In fact, clock genes are expressed in many cells and tissues throughout the body, allowing for the coordination of circadian rhythms at the systemic level. Various peripheral tissues, such as the liver, heart, kidney, and skin, possess their own circadian clocks, which contribute to the regulation of local physiological processes. [65]

2.4 The molecular mechanism of the cellular circadian clock

The identification of various clock genes paved the way for the development of a molecular clock model, which operates through a feedback loop spanning 24 hours

[66]. The molecular mechanisms underpinning circadian rhythms exhibit considerable similarity across different species. These mechanisms encompass enhancer elements, repressor elements, and control circuits that encompass processes like phosphorylation-dephosphorylation, methylation, acetylation reactions, and the formation of specific protein dimers [67, 68]. In mammals, the molecular circadian system operates within the central clock located in the hypothalamus, specifically in the suprachiasmatic nuclei, as well as in secondary clocks found in the brain and various peripheral organs. When the retina perceives light, it triggers alterations in the transcription of specific circadian rhythm genes within the master clock. This demonstrates the body's capacity to adapt to shifts in the photoperiodic environment. The master clock serves to synchronize multiple peripheral circadian oscillators, although the precise mechanisms involved in this synchronization are still not fully understood [3]. The molecular circuitry of the circadian clock appears to involve, in a broad sense, two categories of mechanisms. First mechanism is the transcriptional which govern the regulation of genes at the DNA level and the second one is post-transcriptional which oversee processes occurring after transcription, downstream of gene expression as described in figure 2.4 [69, 3].

Transcriptional mechanisms can be summarized through autoregulatory feedback loops. The primary negative feedback loop relies on a combination of positive and negative elements. In mammals, the positive elements consist of two proteins, the *CLOCK* and *BMAL1* transcription factors, which form heterodimers. The two negative elements are also proteins, *PER* and *CRY*. Within a neuron of the suprachiasmatic nucleus, the levels of *PER* and *CRY* are low in the morning. At this time, the *CLOCK-BMAL1* complex maximally activates the transcription of *Per* and *Cry* genes. Nevertheless, the *PER* and *CRY* proteins don't accumulate right away because they are inherently unstable. This characteristic prevents the cycle from being prematurely disrupted. Over the course of the day, they gradually become more stable through interactions with other proteins. Subsequently, they form heterodimers and ultimately relocate into the nucleus [70]. Once in the nucleus, they inhibit the

transcriptional activity of the *CLOCK-BMAL1* heterodimer, consequently halting their own transcription [71, 72]. As the activity of the *Per* and *Cry* genes diminishes, the production of PER and CRY proteins also decreases. Their concentration peaks at the onset of the night and subsequently declines. Simultaneously, the *CLOCK-BMAL1* heterodimer gradually recovers its activity during the nighttime. Therefore, the fundamental molecular mechanism of the circadian clock primarily revolves around a feedback loop composed of a positive element represented by the CLOCK-BMAL1 heterodimer and a negative element represented by the PER-CRY heterodimer [3]. A full cycle of this loop takes approximately 24 hours to complete. Moreover, *CLOCK* and *BMAL1* heterodimers are also responsible for the daily transcription of numerous clock-controlled genes (CCGs) across various peripheral tissues [73, 74, 75].

Post-transcriptional mechanisms The effective operation of the circadian loop necessitates the eventual degradation of *PER* and *CRY* proteins after they have fulfilled their role. While they are inhibiting the positive elements (*CLOCK* and *BMAL1*), the initiation of a new cycle remains hindered. Multiple post-transcriptional processes, therefore, influence the capacity of *PER* and *CRY* to interact with *CLOCK* and *BMAL1*. The most thoroughly explored element is the modification of these proteins via phosphorylation and dephosphorylation mechanisms. Several kinase proteins target PER and/or CRY, and each of these two proteins can be phosphorylated at multiple locations. These alterations either accelerate or slow their transit to the proteasome. Ubiquitin tags proteins that are destined for destruction. Post-transcriptional mechanisms governing the clock proteins within the primary molecular loop are essential for maintaining the functionality of intracellular trafficking and the degradation of clock proteins. These processes are critical for the proper operation of the molecular loop over a 24-hour period [76, 3].

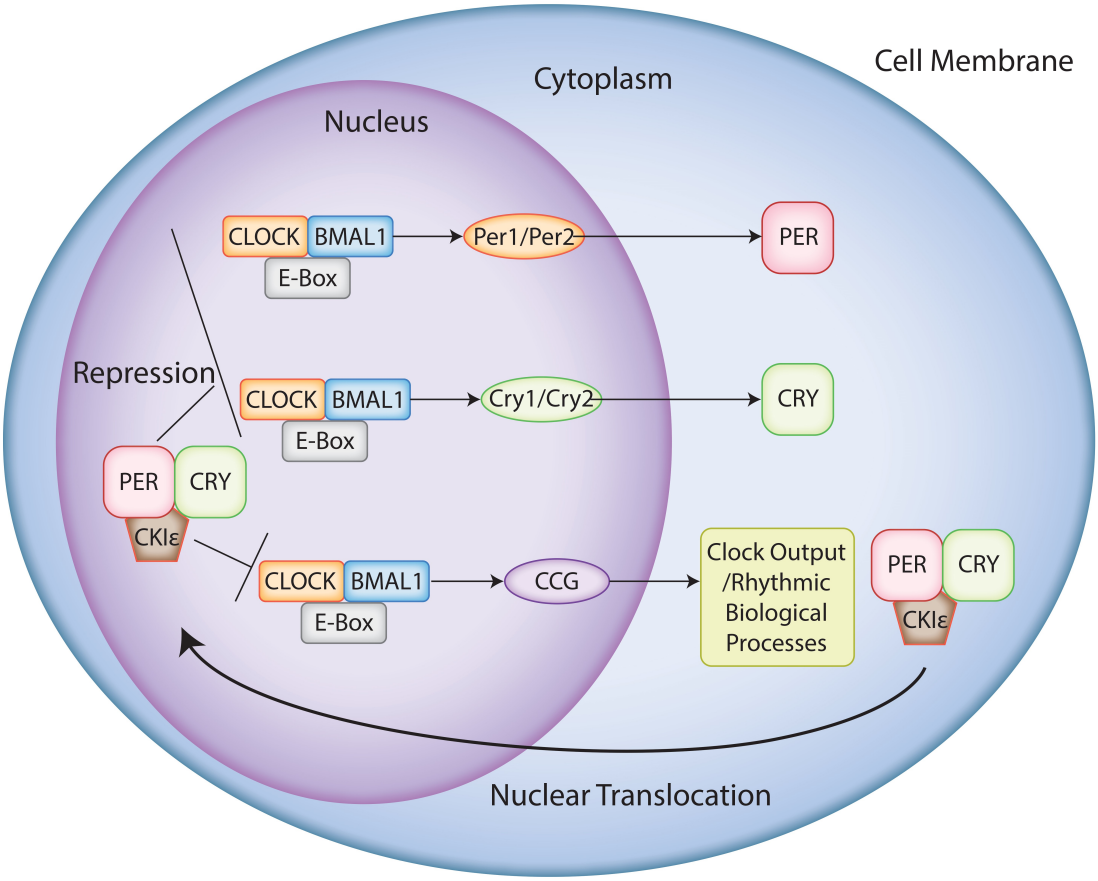

Figure 2.4: Modified from [3], illustrating that the mammalian cell-autonomous oscillator model *CLOCK* and *BMAL1* are transcriptional activators that promote the expression of *Cry* and *Per* genes. The protein products derived from these genes come together in the cytoplasm to create dimers that enter the core. Within the core, they serve two roles: firstly, repressing their own transcription by inhibiting *CLOCK*-*BMAL1*, and secondly, activates the *BMAL1* gene through a mechanism that has yet to be fully elucidated. Thus, these proteins form two regulatory loops, one negative and one positive. Also, these proteins activate clock-controlled genes (*CCG*), the products of which send rhythm information to the rest of the organism via the clock's output channels.

2.5 Peripheral oscillators

It is known that there are clocks in many additional peripheral tissues and cells, despite the fact that the SCN is the location of the central clock in the body. Organs and tissues like the liver, lungs, and heart each have their own clocks, but they must be synchronised to the exogenous solar time source by the SCN [77, 78]. The molecular mechanisms governing circadian clocks in peripheral tissues mirror those of the SCN clock. These mechanisms entail the rhythmic activation of clock genes like *BMAL1*, *Per*, and *Cry*, which establish interconnected feedback loops at the transcriptional and translational levels. These oscillations drive circadian fluctuations in gene expression and cellular functions within peripheral tissues. Peripheral oscillators play a vital role in aligning physiological functions in individual tissues with systemic signals, including feeding-fasting cycles, hormone variations, and activity rhythms. This synchronization is crucial for maintaining optimal tissue performance and overall well-being [79].

This has been demonstrated in mice with a lesion in the SCN, in which the peripheral clocks no longer synchronise with one another, neither between the same organ in different animals nor between various organs in the same animal [78]. while extended rhythms can still be found in the explanted peripheral tissues of animals that have had their SCN lesioned. Guo et al. [80] conducted a series of fascinating studies in which they lesioned the SCN in hamsters and assessed endogenous peripheral clock transcripts. In this investigation, rhythms were lost in all of the tissues that were examined, which was a slightly different finding compared to the one that Yoo et al. [78] observed. However, the replacement of the SCN was only successful in restoring these rhythms in some tissues (liver and kidney) and not others (heart and skeletal muscle). According to these findings, the responses of peripheral organs to signals originating from the SCN are distinct, and the liver and kidney must be getting their timing cues from a different source than the rest of the body. Such as signals that are born in the blood or even signals that are fed. However, due to the fact that these results indicate that caution is

required when utilising a 'peripheral' model to analyse the clock, it is imperative that this be done. It is more likely that individual tissues will respond independently as opposed to as part of a population [80].

The SCN acts as a core oscillator, entraining peripheral oscillators to the external environment [81]. This occurs in response to internal cues from hormones (such Gcs) or neurons, as well as external cues like the need to eat (known as "zeitgebers"), a situation in which daylight feeding of a nocturnal rodent will reverse the phase of the peripheral clocks relative to that of the SCN, which is mostly unaffected by the situation [82]. Another potential zeitgeber is the natural cycle of the surrounding temperature, as temperature rhythms have been shown to produce oscillation in cultivated Rat-1 fibroblasts [83]. The process of entrainment is essential since human cells do not possess direct light sensitivity. However, lesser eukaryotic animals like Drosophila and ZebraFish have peripheral tissues that are light-sensitive, and hence, they may not necessarily rely on entrainment [84]. Similar to the suprachiasmatic nucleus (SCN), peripheral clocks exhibit temperature compensation within the typical temperature range observed in mammals, which spans from 33°C to 42°C. The rationale behind this phenomenon remains ambiguous; nonetheless, numerous animal species possess the ability to reduce their body temperature, a physiological state referred to as torpor, under specific circumstances. Moreover, hibernation serves as the primary mechanism for significant temperature reduction in animals. However, despite the reduced metabolic activity during this period, it remains crucial for the animal to awaken at an opportune moment, such as during the Spring season, necessitating the maintenance of a functional internal clock [81].

2.5.1 An additional pacemaker outside the SCN responsive to methamphetamine

Methamphetamine (MA), is a stimulant that acts on the central nervous system. It causes intoxication in those who consume it as a result of an increase in the stimulation of dopamine and norepinephrine receptors in the brain. The effects of using MA, which include alertness, euphoria, and a sensation of well-being, last for a far longer period of time than those of a comparable nature that arise from using cocaine, and the drug is metabolised by the body at a significantly slower rate. MA is a derivative of amphetamine, which was initially synthesised in 1887 by a German scientist and researched in depth for the first time in the early 1930s. Amphetamine is a sympathomimetic medication that stimulates the sympathetic branch of the autonomic nervous system. Its chemical structure is comparable to that of the sympathomimetic ephedrine. As bronchial airway dilatation is one of the effects of amphetamine, the drug was first used in medicine in 1932 as a nasal spray for the treatment of asthma. Subsequent research revealed that the medication was also effective in providing relief from narcolepsy, lowering activity levels in hyperactive youngsters, reducing appetite, and making it possible for people (such as students and truck drivers) to remain awake for longer stretches of time. In the 1930s and 1940s, amphetamine was utilised in the treatment of a wide variety of additional illnesses and disorders. These conditions and disorders included schizophrenia, addiction to morphine, smoking tobacco, low blood pressure, radiation sickness, and even chronic hiccups [85].

In addition to being smoked, sniffed, or inhaled through the nose, MA can also be injected, referred to as "crystal" or "meth" or "speed." The manner in which a person takes MA plays a role, at least in part, in determining the timing and strength of the "rush" that comes with the usage of the substance. This "rush" is brought on by the release of high levels of dopamine into the brain, which is a result of taking MA. When MA is smoked or injected, the effects are virtually instantaneous; when

snorted, they take around five minutes, and when swallowed, they take about 20 minutes. Increases in blood pressure, body temperature, heart rate, and breathing rate are some of the immediate physiological changes that are related with the use of MA. These changes are comparable to those that are induced by the fight-or-flight reaction. Negative side effects include increased anxiety, insomnia, violent tendencies, paranoia, and hallucinations. Other negative side effects include a high body temperature, stroke, cardiac arrhythmia, stomach cramps, and shivering [86, 85].

The SCN of the hypothalamus is where the mammalian brain's most important circadian pacemaker is located [87, 88]. Methamphetamine, on the other hand, has the ability to restore circadian rhythmicity in patients whose SCNs have been destroyed by a lesion or inhibited by exposure to persistent strong light, conditions that lead to irregular locomotor behaviour. At a molecular level, methamphetamine exerts its impact on circadian rhythms chiefly by modulating neurotransmitter systems and cellular signaling pathways integral to circadian regulation [87]

In addition, there are other circadian pacemakers that regulate locomotor activity rhythms but do not rely on the SCN or the typical molecular timekeeping mechanism. These extra-SCN pacemakers can be activated by various stimuli, including methamphetamine/amphetamine, restricted food availability (known as the food-entrainable oscillator or FEO), and rewarding activities like wheel-running or palatable meals. These findings suggest that the mammalian circadian system is more complex than previously thought, involving multiple pacemakers with different regulatory mechanisms [23].

Jennifer et al. [89] has studied an oscillator of the circadian rhythm that is sensitive to the substance methamphetamine, which is a psychostimulant. The study outlines a number of experiments that were conducted to study the characteristics of the MASCO (methamphetamine-sensitive circadian oscillator). In one set of tests, mice that were missing certain genes or had mutations in those genes were used. These genes are part of the conventional circadian machinery. When administered with methamphetamine, the

researchers discovered that these animals displayed circadian locomotor rhythms. This finding indicates that MASCO can induce behavioral rhythms even without the SCN and independently of the molecular feedback loops that underpin traditional circadian rhythms. In another experiment, the participation of canonical clock genes in the MASCO mechanism was tested by modifying or knocking out these genes in order to evaluate whether or not they were engaged. The findings of these tests shed light on the molecular mechanisms that are responsible for circadian rhythmicity and the possible function that MASCO plays in the addiction to psychostimulants.

In 1982, Ikeda and Chiba conducted a study on the effects of various psychotropic drugs on the circadian locomotor activity rhythms in Fischer rats. They found that low-dose d-amphetamine administered in the drinking water had significant effects on the locomotor activity rhythm. This resulted in an elevated activity bout at the end of the activity period, followed by a free-running rhythm with a longer period. They proposed the existence of at least two circadian oscillators in rats, with one oscillator being more sensitive to amphetamine than the other [23].

The discovery made by Ken-Ichi Honma's group revealed that the activity rhythm induced by psychostimulants like methamphetamine is controlled by a circadian oscillator located outside of the SCN. The circadian oscillator outside the SCN, often activated by MASCO, operates independently but can interact with the SCN by influencing rhythms under specific conditions, like restricted feeding schedules. While the SCN is the primary light-entrained circadian regulator, MASCO can maintain rhythms even when SCN function is compromised. However, MASCO and the SCN can show synchronized rhythms when both are active, although they are governed by different environmental cues (e.g., light for SCN, methamphetamine, or feeding for MASCO). Thus, they represent separate but sometimes interacting pathways for circadian regulation [79]. They found that low-dose methamphetamine had similar effects on activity rhythms in rats as d-amphetamine, and this rhythm persisted even in rats with SCN lesions. The methamphetamine-induced rhythm dissociates from the

SCN-controlled rhythm, free-runs in light-dark cycles, and can also be entrained by restricted feeding [23].

Taufique et al. [90] have discussed the genetics and functional significance of the methamphetamine-sensitive circadian oscillator (MASCO). Their finding was in the absence of the SCN, mice with SCN lesions and no methamphetamine treatment exhibit irregular or frequent locomotor activity, indicating the absence of a discernible MASCO output rhythm. This suggests that MASCO is a weak oscillator on its own and cannot sustain a continuous activity rhythm without the presence of methamphetamine. However, when methamphetamine is administered to mice with SCN lesions, a robust free-running activity rhythm with a prolonged period of 26 to 30 hours emerges. This indicates that MASCO becomes a strong oscillator with a longer period when methamphetamine is present. Conversely, without methamphetamine treatment, the SCN remains a strong oscillator while MASCO is weak. This leads to a strong coupling between the SCN and MASCO, resulting in an activity rhythm with a period of approximately 23.7 hours in constant darkness (DD) conditions. In constant light (LL) conditions, the SCN oscillator is still stronger than MASCO, but the period of the resulting activity rhythm is lengthened to about 26 hours.

Tataroğlu et al. [91] have discussed the presence of an SCN-independent oscillator that contributes to behavioral rhythmicity in mammals, which challenges the completeness of the model of mammalian circadian organization that posits the SCN as the main pacemaker that orchestrates synchrony among the circadian oscillators present in almost all tissues and is chiefly responsible for the generation of rhythms in locomotor activity. The study investigates the effects of methamphetamine (MAP) on the circadian wheel-running activity of intact, SCN-lesioned, or constant light (LL)-treated mice. The doses of methamphetamine used were 0.0025%, 0.005%, 0.0065%, 0.0075%, or 0.01% weight in volume (w/v). Food, water, or methamphetamine-containing water was available ad libitum unless otherwise stated. In conculsion, there is evidence of an SCN-independent oscillator, MASCO, that contributes to behavioral rhythmicity in

mammals. The study suggests that MASCO interacts with the SCN in a strain, sex, and dose-dependent manner in intact mice. Additionally, MASCO induces robust free-running locomotor rhythmicity in SCN-lesioned mice, which persists for up to 14 cycles after methamphetamine is withdrawn.

2.6 The disruption of circadian rhythms

The circadian system has undergone evolutionary adaptations in order to allow animals to anticipate and take advantage of regular alterations in the external environment. This adaptation optimises the physiological and behavioural functions of organisms to specific periods of the day [92]. Nevertheless, contemporary society, characterised by its constant activity and availability, presents countless instances in which our way of life clashes with our inherent biological rhythms. These instances include shift work and the disruption caused by travelling across different time zones, commonly known as jet-lag. In addition, the utilisation of artificial light leads to the exposure to light during unsuitable periods, encompassing nocturnal illumination as well as the exposure to light emitted by mobile devices, such as smartphones, tablets, and computers. The repercussions of circadian disturbance and aberrant light exposure on human health are currently a subject of increasing concern. Individuals who are consistently exposed to such circumstances may experience difficulties in their performance, sleep disturbances, emotional disruptions, and gastrointestinal issues. It is widely believed that these symptoms have an impact on approximately 5-10 % of individuals engaged in shift employment.

Treatments aim to synchronise the internal circadian rhythm with the external environment by many methods, including scheduled exposure to light or darkness, strategic napping, and the administration of pharmaceutical interventions, such as melatonin or caffeine [93, 94, 95, 92]. Given the rising prevalence of artificial light sources, it is anticipated that such issues are poised to escalate in the forthcoming years.

In order to examine the mechanisms that contribute to the negative health consequences of circadian disruption, an expanding body of research has explored the impact of abnormal light exposure on cognitive function. These studies have utilised rodents that are housed under non-standard light-dark cycles. Nevertheless, these atypical LD cycles may potentially exert their influence through other mechanisms.

Certain situations lead to exposure to light during the typical subjective night, while others lead to a discrepancy between an individual's internal circadian clock and the external environmental time, necessitating a continuous adjustment of the phase. The hypothesis posits that the discrepancy between circadian rhythms and external environmental cues may underlie the adverse effects associated with circadian disturbance [94]. There has been a suggestion that the discrepancy between circadian rhythms and external factors may serve as the underlying cause for the adverse effects of circadian disruption [94]. Supporting evidence for this claim can be found in research where animals demonstrate compromised well-being when exposed to non-24-hour environmental settings [94]. The most compelling evidence is derived from studies on longevity. In these studies, it has been observed that wild-type mice exhibit a decrease in lifespan when subjected to non-24 hour light-dark cycles [96]. Additionally, tau mutant hamsters have been found to experience shortened longevity under 24 hour settings, but display normal lifespan when exposed to persistent darkness [97, 98].

The aforementioned results suggest that the efficacy of a circadian clock is contingent upon its synchronisation with the period of the surrounding environment. One potential alternate explanation regarding the negative consequences of circadian disruption posits that such circumstances lead to internal desynchrony. This refers to a situation in which the circadian clocks in various tissues, or even distinct parts of the brain, may become misaligned or lose their rhythmicity altogether. As a consequence, this can lead to poorer performance. The phenomenon of internal desynchrony has been observed in mice as a consequence of scheduled feeding. This leads to a lack of synchronisation between the clocks in the SCN and the hippocampus, which in turn impairs learning

and memory. Additionally, in rats subjected to 22-hour light-dark cycles, internal desynchrony occurs within specific groups of neurons in the SCN, resulting in behaviour similar to depression. The hypotheses of the mismatch between internal and external time and internal desynchrony are not mutually exclusive and may both have a role in the adverse consequences of circadian disturbance [92].

Tahara et al [99] discussed age-related circadian disorganization caused by sympathetic dysfunction of peripheral clock regulation. The study sheds light on the changes that occur in the adaptation of peripheral clocks to external signals with age. The effects of age-related impairment of the peripheral clock on stress, exercise, and food stimuli are discussed. The circadian clock plays a critical role in maintaining homeostasis, preventing disease, and limiting the deleterious effects of aging. By maintaining a robust circadian clock, individuals may be better able to resist the negative effects of aging and maintain their health and well-being as they age.

There exists a correlation between disturbances in the circadian rhythm and other age-related ailments, such as obesity, cancer, and dementia. The phenomenon of ageing is correlated with a reduction in the diurnal fluctuations observed in the sleep-wake cycle, body temperature, and hormone secretions. The manifestation of age-related deterioration in the timing signal from the suprachiasmatic nucleus (SCN) has been documented in the neuronal firing rhythms and membrane characteristics of SCN cells. Furthermore, it was observed that the molecular clock exhibited regular oscillations in the aged suprachiasmatic nucleus (SCN) in vivo. However, a more rapid drop in oscillation was observed in cultured SCN derived from aged mice compared to those derived from young mice. Several research have been conducted to assess the oscillations of the molecular clock in aged peripheral tissues. In several of these investigations, luciferase reporter transgenic mice or rats were utilised to examine the expression of core clock genes (*Per1* and *Per2*) in liver, lung, pineal gland, and kidney tissues obtained from both young and old animals. Hence, perturbations to the circadian rhythm can potentially contribute to the progression of the ageing phenomenon and age-associated

ailments [99].

3. Measurements and methods of analysis

In this thesis, additional analysis was conducted to gain a deeper understanding and ensure the identification of existing rhythms throughout the experimental duration. This in-depth examination was crucial to determine the persistence and characteristics of rhythmic patterns under the experimental conditions. The signals that is investigated in this report was obtained from Shin Yamazaki, University of Texas Southwestern,Dallas, TX. In following agreement to use the data as well as ethics approval is provided as background of this work and all letters in the appendex (a,b).

3.1 Study 1: Behavioural rhythm across multiple conditions

These are the behavioral data from 8 triple knockout $Per1/2/3^{-/-}$ mice, each of which was observed over a period of 140 days. Table 3.1 shows the information of all mice and their gender. During the experiment and period of these days, all mice have gone through several different stages. Mice have stayed the first 8 days in 12 hour in constant darkness and 12 hour in constant light (12D:12L). The condition has moved to constant darkness and mice have stayed for 11 days, with same condition all mice has given (0.005%) methamphetamine in their drinking water and spent 26 days. Then the

condition has moved to constant lightness for 74 days, the first 22 days under the effect of the drug then the effect of the drug has finished and spent the rest in constant lightness. Finally the mice return back to constant darkness until the end of the experiment. Fig 3.2 illustrates the behavioral data of mouse 1 within the investigation during 140 days.

Table 3.1: Information of all mice and their respective genders that are currently under investigation.

Mice	**Gender**
Mouse 1 (PTKO-1002)	Male
Mouse 2 (PTKO-8780)	Male
Mouse 3 (PTKO-8840)	Female
Mouse 4 (PTKO-8844)	Male
Mouse 5 (PTKO-8896)	Female
Mouse 6 (PTKO-8898)	Female
Mouse 7 (PTKO-8845)	Male
Mouse8 (PTKO-8975)	Female

Table 3.2: Meaning of abbreviations.

abbreviation	**Meaning**
LD	12 hours in constant light and 12 hours in constant dark
DD(1)	Constant darkness.
MA & DD(1)	Methamphetamine drug in constant darkness.
MA & LL	Methamphetamine drug in constant lightness.
LL	Constant lightness.
DD(2)	Constant darkness.

Moreover, animals were singly housed in cages (length × height × width: 29.5 × 11.5 × 12 cm) with unlimited access to a running wheel (diameter 11 cm), food (unless otherwise indicated), and water. The cages were placed in light-tight, ventilated boxes in light/dark conditions (light intensity: 200–300 lx) or in constant darkness (as indicated for each experiment). Cages were changed every 3 wk. Wheel-running activity was continuously recorded every minute by computer and initially analyzed using ClockLab software (Actimetrics).

Figure 3.1: Illustration of the wheel which enables the mice to run inside the cage.

The same PC recorded the number of revolutions of the running wheel. Figure 3.2 shows the time series of mouse 1 and how its behaviour during 140 days. During the investigation, the PC recorded nan values due to some issue that have interrupted the recording, and this happened for all mice at the same time. Since this issue happened for a low percentage of data points, the time series could later be utilized as an input for analysis, with no impact on the general outcome.

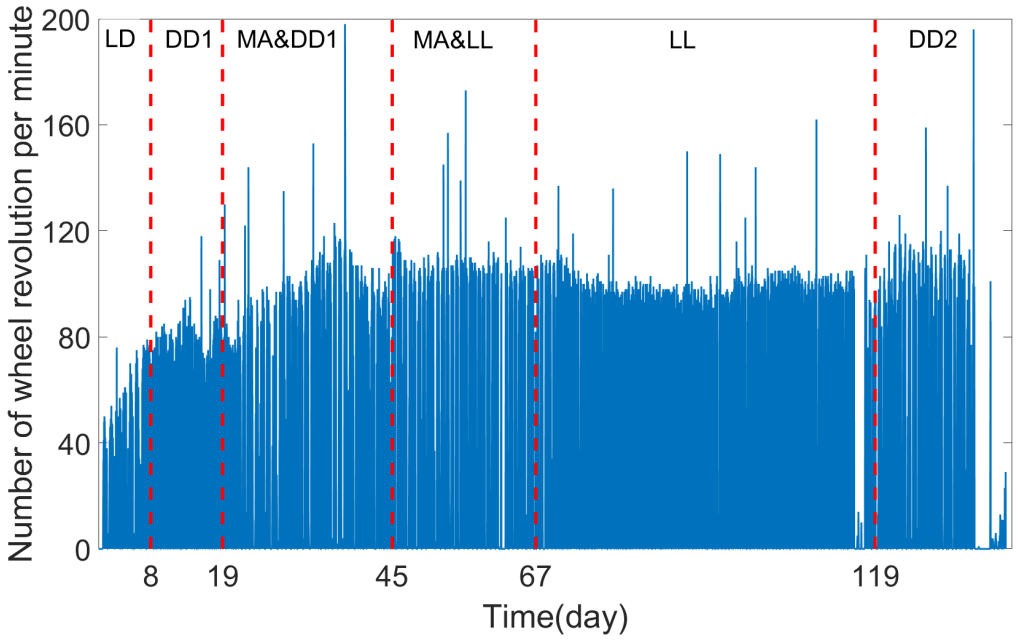

Figure 3.2: The behavioral data obtained from mouse 1, depicting the number of revolutions of a running wheel per minute recorded over a span of 140 days. The red lines on the graph indicate the start/end of a given condition.

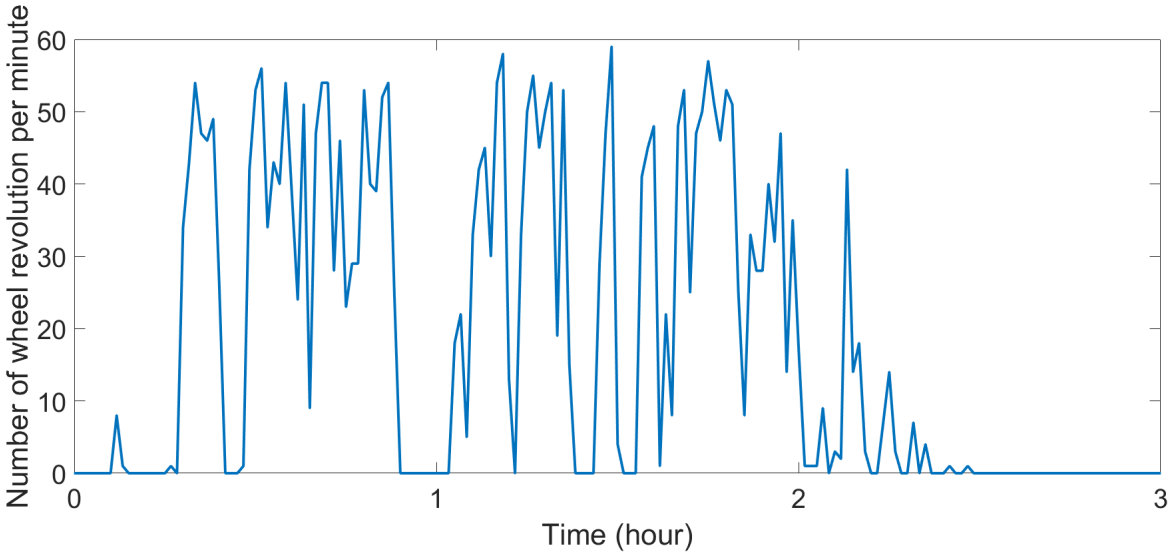

Figure 3.3: A 3 hours segment of 140 days of Murine behavioural data. The number of revolutions of a running wheel was recorded every minute.

3.2 Study 2: Comparing wild type and per knock-out mice under identical condition

3.2.1 A. Wild-type mice

In this study, three wild-type mice with active clock genes were observed over 32 days while being kept in constant darkness to investigate their circadian rhythms. Figure 3.4 illustrates the behavioral data of mouse 1 within the investigation during 32 days, and 4.11 also ilusrates the 3 hours segment of 32 days.

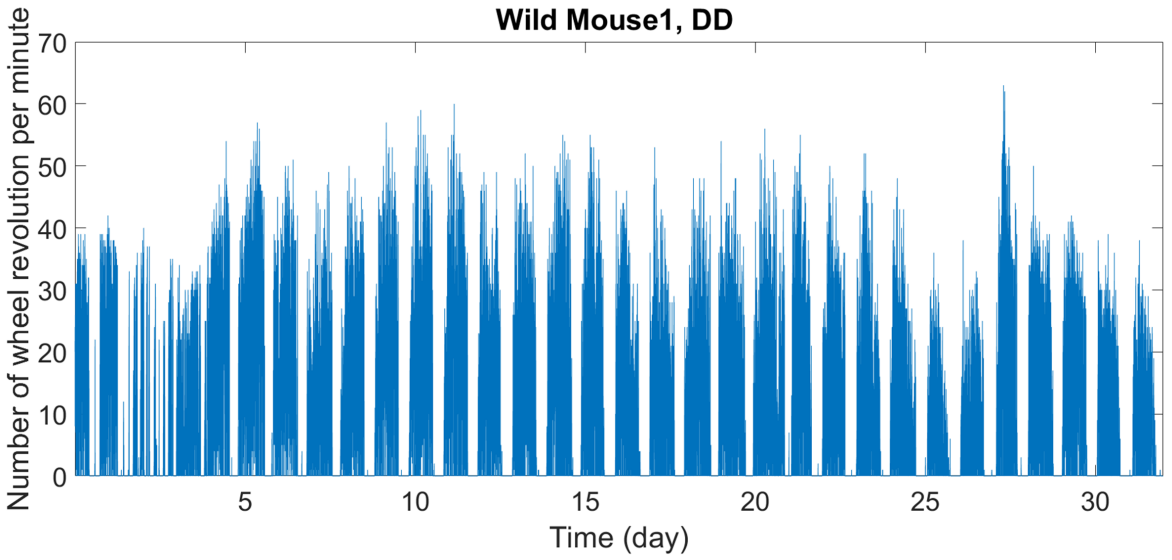

Figure 3.4: The behavioral data obtained from wild mouse 1, depicting the number of revolutions of a running wheel per minute recorded over a span of 32 days.

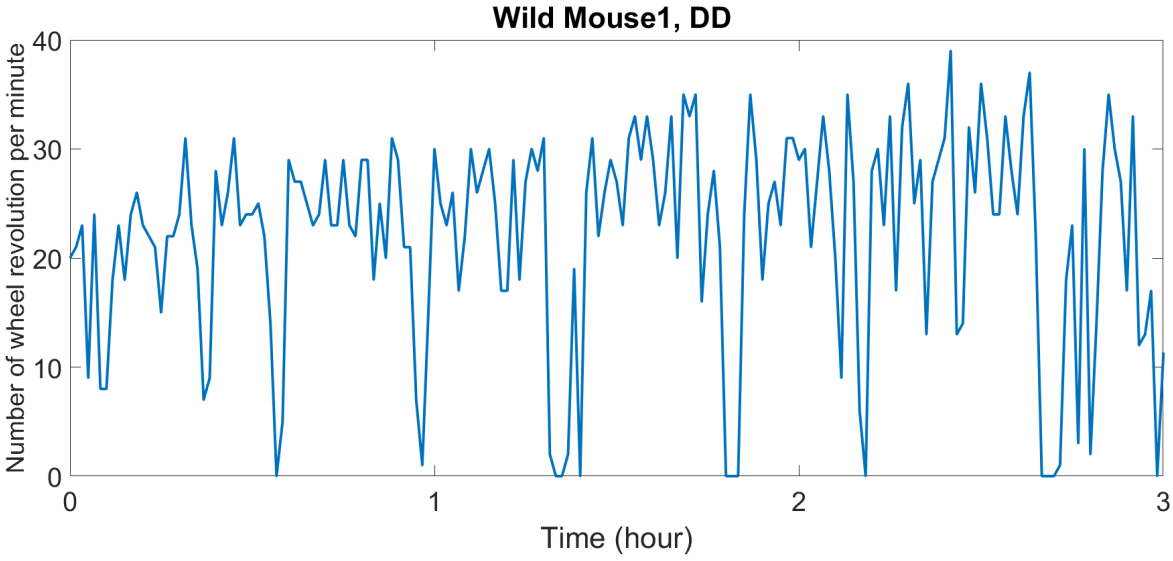

Figure 3.5: A 3 hours segment of 32 days of Murine behavioural data. The number of revolutions of a running wheel was recorded every minute.

3.2.2 B. Knocked out mice in constant darkness

This investigation focused on six triple knockout $Per1/2/3^{-/-}$ mice over a span of 45 days, during which they were maintained in constant darkness. Figure 3.6 illustrates the behavioral data of mouse 1 within the investigation during 45 days, and 3.7 also ilusrates the 3 hours segment of 45 days.

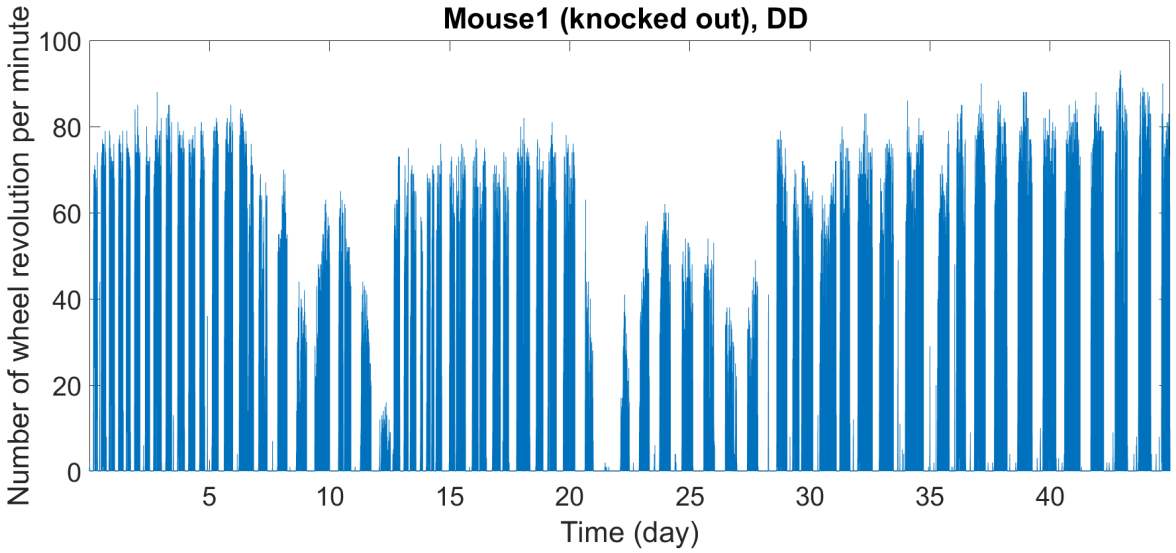

Figure 3.6: The behavioral data obtained from mouse 1, depicting the number of revolutions of a running wheel per minute recorded over a span of 45 days.

Figure 3.7: A 3 hours segment of 45 days of Murine behavioural data. The number of revolutions of a running wheel was recorded every minute.

3.3 Study 3: Evaluating the effect of MA administration utilising longer recording

3.3.1 A. Knocked out mice in light-dark and constant darkness

The experiment monitored seven mice for a duration of 93 days under two distinct environmental conditions. Initially, they spent 26 days in a Light-Dark (LD) cycle, after which they were transitioned to constant darkness for the remaining of the experiment. Throughout this period, the clock gene in all the mice was inactivated. Figure 3.8 illustrates the behavioral data of mouse 1 within the investigation during 93 days, and figure 3.9 also illustrates the 3 hours segment of 93 days.

Table 3.3: Information of all mice included the study 3 (A) and their respective genders.

Mice	Gender
Mouse 1 (PTKO-8911)	Male
Mouse 2 (PTKO-9313)	Male
Mouse 3 (PTKO-9501)	Male
Mouse 4 (PTKO-9507)	Male
Mouse 5 (PTKO-9509)	Female
Mouse 6 (PTKO-9565)	Female
Mouse 7 (PTKO-9567)	Female

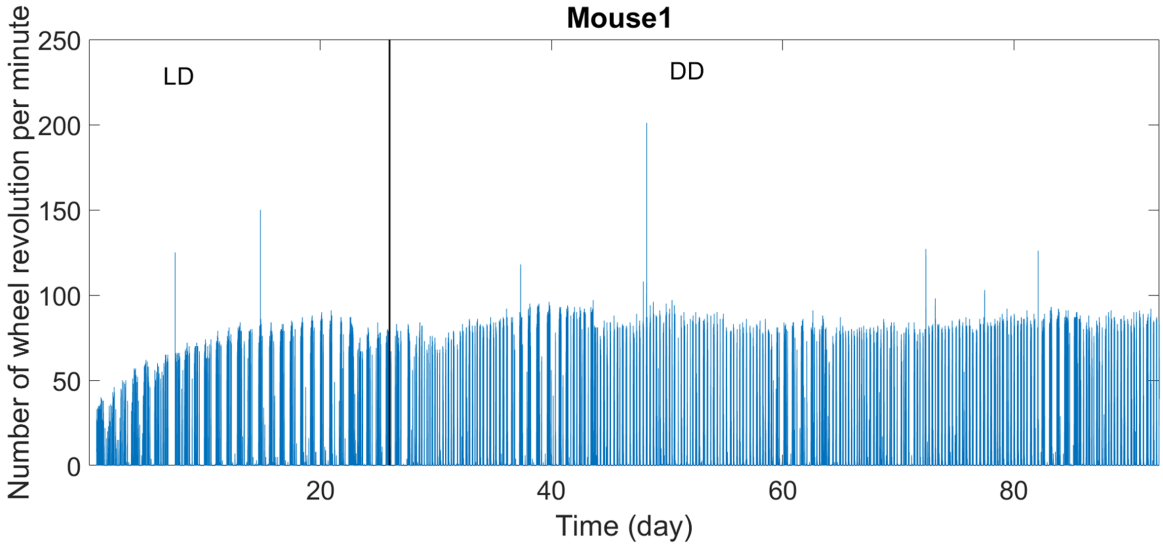

Figure 3.8: The behavioral data obtained from mouse 1, depicting the number of revolutions of a running wheel per minute recorded over a span of 93 days.

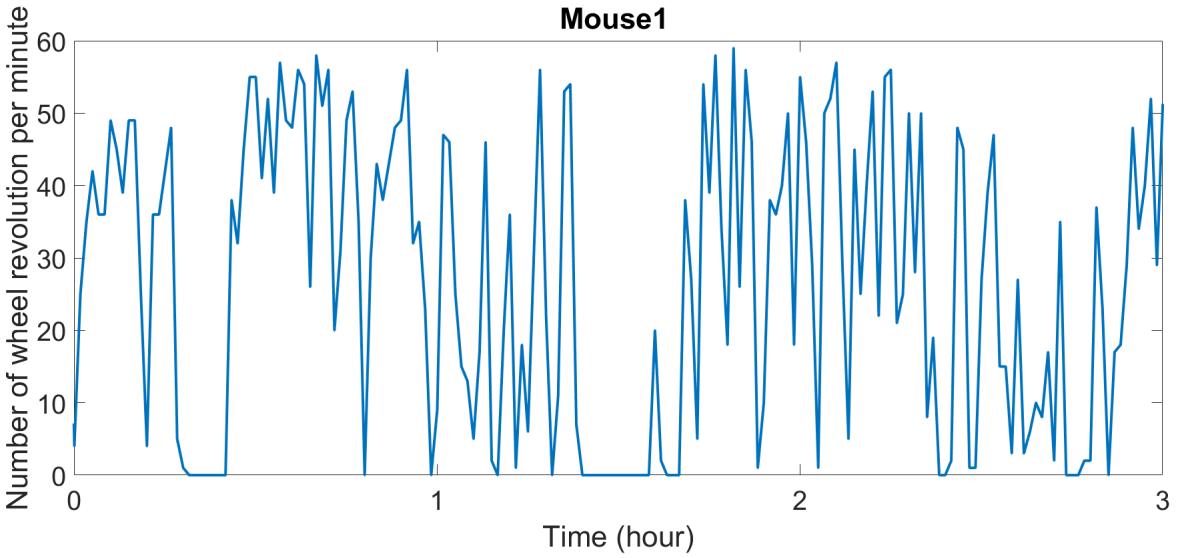

Figure 3.9: A 3 hours segment of 93 days of Murine behavioural data. The number of revolutions of a running wheel was recorded every minute.

3.3.2 B. Knocked out mice in light-dark, constant darkness, and methamphetamine administration

The experiment involved a longitudinal observation of five mice over the course of 135 days, subject to a series of environmental changes. Initially, the mice were placed under a Light-Dark (LD) cycle for the first 6 days. This was followed by a 26-day period in constant darkness. Subsequently, methamphetamine was administered via their drinking water, and the mice remained in the constant darkness condition for the duration of the experiment. Figure 3.10 illustrates the behavioral data of mouse 1 within the investigation during 135 days, and 3.11 also ilusrates the 3 hours segment of 135 days.

Table 3.4: Information of all mice included the study 3 (A) and their respective genders.

Mice	Gender
Mouse 1 (PTKO-7759)	Female
Mouse 2 (PTKO-7786)	Female
Mouse 3 (PTKO-8001)	Female
Mouse 4 (PTKO-8003)	Female
Mouse 5 (PTKO-8025)	Male

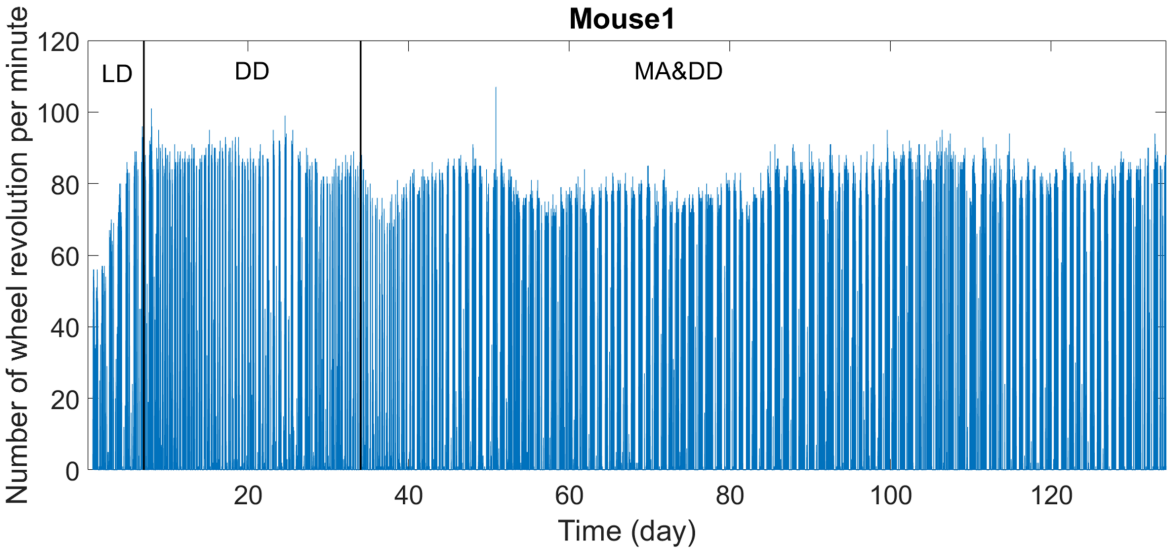

Figure 3.10: The behavioral data obtained from mouse 1, depicting the number of revolutions of a running wheel per minute recorded over a span of 135 days.

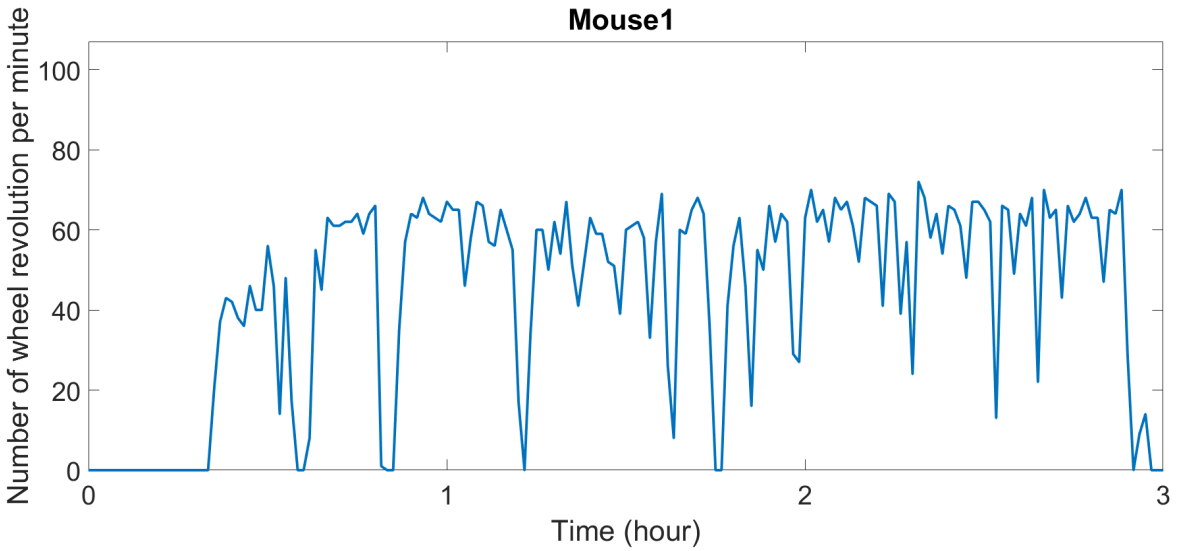

Figure 3.11: A 3 hours segment of 135 days of Murine behavioural data. The number of revolutions of a running wheel was recorded every minute.

3.4 Dynamical systems and methods for analysing them

3.4.1 Introduction

To acquire a better understanding of the underlying dynamics of any given system, several methods can be applied to the data it generates. Data obtained from the system can be investigated using methods that enable the temporal resolution of its oscillatory dynamics. This temporal resolution allows for a detailed analysis of the system's periodic behaviors, oscillations, or rhythmic patterns over time. By examining the data at different time scales, researchers can extract valuable information and statistical features from the data. This includes measures such as mean, variance, distribution properties, correlations, spectral characteristics, and other statistical descriptors. These extracted features provide insights into the underlying dynamics of the system and aid in understanding its behavior, variability, and statistical properties. Rather than just amplitudes, the algorithms consider the amplitude, power, and phase aspects of oscillations. Furthermore, the algorithms in question take into account the signals' fluctuating frequencies and phases [100].

Dynamical systems are mathematical models that are used to explore how complex systems behave and evolve over time. They are capable of describing a wide range of events, from physical systems such as planetary motion to biological systems such as population dynamics or biochemical reactions. It can be described by the equation:

$$\frac{dx}{dt} = f(x). \tag{3.1}$$

Equation 3.1 defines the progress of continuous-time systems. Iterated maps can be employed when time is discrete [100], where f is a function that acts on the previous state of x; f describes the infinitesimal change in the state x in an infinitesimal time

interval t The concept of dynamical systems is related to a number of systems, such as the linear harmonic oscillator, the planetary system, and the simple pendulum. Dynamical systems that explicitly depend on time are referred to as *nonautonomous* systems. In contrast to autonomous systems, where the evolution of the system does not explicitly depend on time, nonautonomous systems have time-varying dynamics. A differential equation with explicit time dependency is the most basic mathematical representation of a nonautonomous system which is:

$$\frac{dx}{dt} = f(x, t). \tag{3.2}$$

System based on their mathematical qualities can be generically classified as linear or nonlinear. Linear systems are much easier to solve and have much simpler properties than nonlinear systems. A linear system's output evolution is proportionate to its input evolution. In nonlinear systems, however, such proportionality does not exist. Because most open systems are nonlinearly dynamical, they are challenging to analyse [101].

3.4.2 Stochastic and deterministic systems

Given complete information about a linear system at a specific moment, it becomes straightforward to ascertain the system's state at every subsequent moment. This characteristic facilitates the development of analytical solutions for the problem. This implies that it is feasible to comprehend all the characteristics of the system inside the framework of a linear model, without the need to observe the system's dynamics. In contrast, it is not feasible to analyse nonlinear systems, such as living systems, using the aforementioned approach. Although it is possible to derive certain aspects of nonlinear systems analytically, predicting the trajectory of such systems without the aid of computer simulations or examining real system dynamics is not practical. It is noteworthy that the complexity of a system is not the determining factor in this matter. A linear system can exhibit significant intricacy, while a nonlinear system can

possess relative simplicity. Nevertheless, the fundamental principles discussed herein are applicable to the analysis of both linear and nonlinear systems [20].

When a fluctuation results from the interactions and actions of a large number of variables or degrees of freedom, it is considered noisy or stochastic. As a result, complicated behaviour can be created by the impact of random external stimuli on a system. This can be modelled by including a noise term in the equations characterising a system's time series. The properties of the noise in the system are separate from the system's underlying dynamics. This distinction permits stochastic systems to be treated as open systems.

A deterministic system is one that uses differential equations to explain how it changes over time. It does not use any random factors to forecast its future behaviour. Because probabilistic systems contain random elements, their evolution cannot be predicted with precision. In a deterministic system, on the other hand, if we know the initial state of the system at a certain moment, we can predict the events that will occur in the system without any uncertainty.In chaotic systems, which are deterministic autonomous systems, small differences in initial conditions may result in exponential divergence in the resulting trajectories.

3.4.3 Oscillatory systems

An oscillatory system refers to a dynamic system where the solutions are confined within certain limits but do not settle into a steady equilibrium state. An oscillatory system, as a type of dynamical system, can be described as a physical system that naturally exhibits oscillations. These oscillations are a result of disturbances to the system's equilibrium state (Hopf bifurcation) and are inherent to the system's characteristics. From a biological perspective, numerous oscillatory systems are present within a human or other living organisms, where they continuously interact with each other. All physiological processes in a biological system not only interact

with other processes within the system but also constantly exchange matter and energy with their environment. As a result, they exhibit oscillatory behavior. The characteristics of oscillatory systems are influenced by the activities taking place within them. These systems are classified as nonlinear because their behavior cannot be accurately represented by linear equations. Instead, they require nonlinear equations for a proper description. Importantly, the principle of superposition, which applies to the combination of two or more oscillators, does not hold true for nonlinear systems comprised of interacting oscillators.

3.5 Relationship between biological systems and dynamical systems theory

3.5.1 Nonlinearity

For a linear system, if all its fundamental properties are known at a specific moment, it is always feasible to estimate the system's state at that time, making analytical solutions to the system possible. This means that it is possible to understand all the properties of a linear system without the need to observe its dynamics continuously over time. Although it is possible to calculate some characteristics of these systems analytically, fully understanding the trajectory of a real nonlinear system typically requires monitoring its dynamics over time or simulating it. It's important to note that this challenge is not tied to the complexity of the system. However, these underlying principles of analysis still apply regardless of the complexity when examining either type of system. The implications of nonlinearity can indeed be quite significant. Not only does it introduce mathematical complexities, but it also results in phenomena such as hysteresis. This refers to a situation where the path a system takes moving from one state to another differs from the path it follows when returning to the original state. This difference in trajectories illustrates why the direction of time is crucial

in analyzing nonlinear systems, as the system's behavior can vary depending on the sequence of events and the direction of change [19].

3.5.2 Openness

The nonlinearities mentioned earlier can be seen as manifestations of a unique characteristic of living systems: their status as thermodynamically open systems that exchange energy and matter with their environment. In contrast, many major theories of dynamical systems often assume that the systems are closed, meaning they are autonomous and can be fully described by their internal state.

Contrary to closed systems, living systems are inherently open and non-autonomous, indicating that both their state and the factor of time are essential in describing their dynamics. Consequently, the incorporation of time-dependent variables becomes an unavoidable aspect when analyzing the dynamics of living systems. This reflects the continuous interaction of living systems with their environment and the time-sensitive nature of their responses and adaptations [19, 100].

3.6 Inverse approach to dynamical systems

Describing real-world system circumstances frequently necessitates a more realistic framework involving non-autonomous differential equations. However, analysing these equations is complicated and has proven to be problematic in many circumstances, resulting in failed attempts. A critical stage in the implementation of a deterministic description is phase space analysis. It is commonly used to rebuild the attractor in phase space. This technique is suitable for autonomous systems that do not explicitly rely on time, but it does not take into account time-dependent attractors [102]. Additional dimensions in phase space are necessary to solve the problem of these systems' time dependence. This complicates the situation. In solving dynamical systems, the inverse problems technique comes in handy, which involves determining the unknown inputs or

parameters of a dynamical system based on observed outputs or behaviour. It can be used to measure the system directly or to simulate it using a set of differential equations. The only difference between the two techniques is that the first is limited by the available data, whilst the second is limited by the approximations and simplifications made in the model.

Many signal analysis methods presume that the data's frequency distribution is constant. In nonautonomous systems, however, this is not the case. Nonstationarity is statistically represented as a change in either the mean or variance of a time series, or both [103]. One widely used approach to visualize the dynamic characteristics of a system's time series is by determining its frequency spectrum. The discrete Fourier transform (DFT) is a traditional approach for analysing time traces. However, applying the DFT to nonstationary time series results in distorted or deceptive power spectra. This limitation reduces its practical value as the computation of the power spectral density often results in a "$1/f$" spectrum, leading to the loss of critical information [103]. Various windowing methods, including the windowed Fourier transform (WFT) and wavelet transform (WT), have proven to be effective in analyzing time traces. The WFT method faces limitations because of its fixed window size, which significantly restricts its effectiveness in analyzing slow oscillations. In contrast, the WT method overcomes this limitation by introducing an adaptive window size, thereby offering a solution to address the issue [104]. The simultaneous visualization of the complete time-frequency representations of a signal proves highly valuable for observing the dynamic characteristics of the system and tracking their temporal evolution.

3.6.1 Time-domain

A signal obtained from a physical system can be initially represented in the time domain as time traces. However, the underlying dynamical properties of nonautonomous systems are often hidden within the data, making it challenging to visualize them

solely in time-domain representations. To reveal the system's dynamics, alternative methods are necessary. These methods involve analyzing the variations in frequencies and amplitudes of oscillations within the time series.

3.6.2 Preprocessing

Signal preprocessing is essential for efficient analysis, but it's advisable to minimize data manipulation. Time series data, especially when acquired experimentally from living systems, can exhibit anomalies. These artifacts may originate from equipment-induced movements or noises during the experiment. These artifacts influence the statistical characteristics of the recorded time series throughout the entire study duration, resulting in a noticeable trend. The ability to distinguish between undesirable and nonstationary inherent dynamics within a signal is paramount during analysis. An elementary approach involves scrutinizing the temporal signal longitudinally; conspicuous deviations from established norms or documented patterns may indicate undesirable trends stemming from factors like motion. Moreover, undesirable trends induced by motion may manifest as pronounced spikes within the time series when observed visually over time. To remove such undesirable trends, the signal is first detrended by removing the non oscillatory trends from the original signal. This is achieved by subtracting a best-fit cubic polynomial, see figure 3.12.

On the other hand, nonstationary dynamics inherent to the system (e.g., circadian rhythms oscillating approximately every 24 hours) can be detected through the application of time-frequency analysis methodologies. The act of eliminating this trend from a time series is referred to as 'detrending'. Finding trends in time series, identifying such trends, and then removing them from consideration are crucial steps in the data analysis process in virtually every industry. Preprocessing has evolved into an essential stage for the majority of statistical methods, including the computation of correlations and spectral analysis [105]

In pre-processing, filtering is still another important factor. If mean values are computed or frequency analysis is used to remove trends, then the data should be detrended. This is because the impacts of frequencies lower than the frequencies of interest in this research may have an influence on the outcome results. There are several different approaches that can be taken in order to buck a trend. It could be done theoretically or statistically, although it is often carried out in the temporal domain [106] [107].

Using a technique known as moving average to smooth out data is the best way to apply detrending. Calculating the statistical mean of the data that is contained within the window and utilising that number as the central point of the window is how this is defined. After that, the window is shifted by one data point in the subsequent step. After that, we compute the new mean, and so on and so forth. The change in amplitude that occurs as a result of applying this approach to the time series can be observed. Time series that have high frequency components, which are represented by amplitude fluctuations that fluctuate quickly, are averaged over and minimised. On the other hand, time series that have low frequency components, which are represented by the amplitudes of long-term trends, remain mainly constant.

It is worth emphasizing that the window length l is the pivotal parameter that governs the degree of smoothness in the resulting time series. larger windows, which correspond to increased smoothing, filter out low-frequency components. Moreover, when conducting frequency or time-frequency analysis, it is imperative to perform signal averaging and subsequently subtract it from the original signal [19]. However, it is essential to differentiate between smoothing and filtering. In the frequency domain, filtering involves the direct manipulation or removal of information. In contrast, the impact of time domain methods can be described as smoothing. Opting for time domain smoothing over filtering offers the advantage of preserving information at each stage, particularly when it comes to specific objectives in signal processing and noise reduction. It allows for precise targeting of unwanted noise or interference, enabling the removal or

attenuation of specific frequency components without affecting the underlying signal's relevant features.

Nevertheless, simple frequency domain filtering can eliminate Fourier components within a specific frequency range, sacrificing information and yielding suboptimal results when the time series contains non-sinusoidal components (i.e., the harmonics remain unaffected). Smoothing is applicable to nonstationary time series as it operates in the time domain and conserves all time-dependent information within the time series [19].

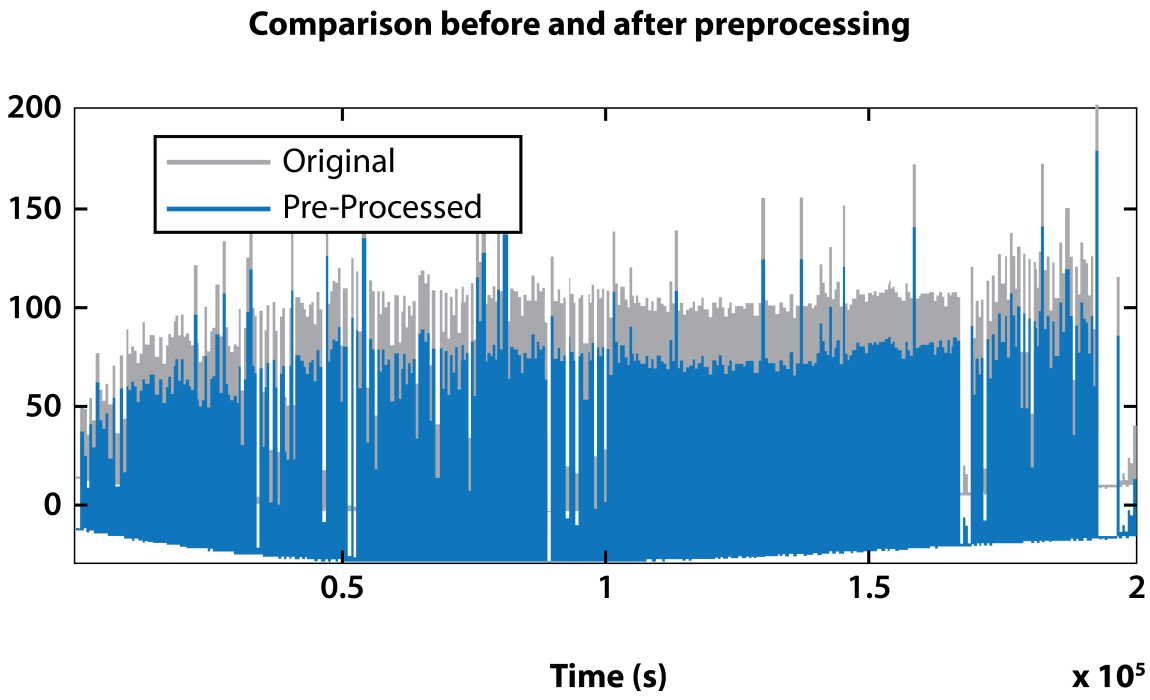

Figure 3.12: Comparison of behavioural data from Mouse 1, before and after preprocessing.

3.6.3 Phase

Biological system time series are influenced by noise from various sources, which are typically unstable. To gain a deeper understanding of the behavior of individual

elements within biological systems and the nature of their interactions, it is essential to develop and apply specialized analytical techniques [108]. In analyzing complex signals, one important but less commonly addressed topic is the study of the instantaneous phases of oscillations. A key aspect of this analysis involves separating 'amplitude' dynamics from 'phase' dynamics, which is crucial to much of the research. The concept of phase in this context is a generalized version of the one-dimensional phase used in simple harmonic oscillators [19].

$$x(t) = A\cos\left(2\pi f t + \phi_0\right), \tag{3.3}$$

The term "rotational frequency," which is uniquely related to linear frequency by the equation $\omega = 2\pi f$, is commonly used for convenience. The instantaneous phase of the system is represented by the cosine function. It represents the number of oscillations the system completes over time t since the start of measurements, as expressed in the argument of this function [108].

$$\phi(t) = 2\pi f t + \phi_0 = \omega t + \phi_0, \tag{3.4}$$

The instantaneous phase can never decrease over time, but it can increase at a variable rate. It is measured in either radians or degrees, which are uniquely related. The phase increases by 360 degrees, or 2π radians, during a complete oscillation cycle. In equation 3.4, ϕ_0 represents the initial phase of the oscillations. Oscillations with simple waveforms may not necessitate instantaneous phase analysis, but for complex signals, this information can be highly valuable in characterizing their features.

3.6.4 Frequency-domain

Prior to conducting frequency domain signal analysis, it is crucial to take into account the properties of the data. Data obtained as time series from any physical system can

be represented and analyzed in both the time domain and the frequency domain. In the time domain, the data is expressed as a function of time, $f(t)$, while in the frequency domain, the data is depicted as the distribution of the system's dynamics across different frequencies. The maximum observable frequency in the signal is equal to half of the sampling frequency (f_s) employed for data measurement, which is known as the Nyquist frequency. The time interval between two consecutive measurements is equivalent to the inverse of the sampling frequency. In other words, Δt is equal to 1 divided by the sampling frequency, represented as $\Delta t = 1/f_s$. The minimum detectable frequency relies on the duration of the data (L), where the lowest observable frequency (f_{min}) is equal to 1 divided by the length of the data ($1/L$). Consequently, the data must be longer than a single oscillation period, and it is not possible to differentiate between two oscillations if their frequency difference is smaller than the minimum frequency. One commonly employed method for visualizing signal dynamics is to represent them in the frequency domain. This representation enables the observation of how oscillations and variations are distributed across a potentially broad range of wavelengths.

The Fourier transform

In the field of physics, a physical process can be described and represented in either the time domain or the frequency domain. Conversely, the frequency domain representation describes the amplitude of the process, denoted as F, as a function of frequency, usually represented as F(f). Each of these representations provides distinct types of information about the same function. When time is measured in seconds, frequency is commonly measured in (Hz), representing the number of cycles per second. The discrete Fourier transform (DFT) is a technique utilized for signal analysis. It is typically introduced through the concept of Fourier series. The Fourier transform $F(\omega)$ of a non-periodic continuous function $f(t)$ is defined as:

$$F(\omega) = \int_{-\infty}^{\infty} f(t) e^{-i\omega t} dt \tag{3.5}$$

Where the Fourier series of a periodic function can be represented as an infinite series comprising sines and cosines.

$$f(t) = a_0 + \sum_{\omega=1}^{\infty} [a_\omega \cos(\omega t) + b_\omega \sin(\omega t)] \tag{3.6}$$

The angular frequency is donated as ω, while the Fourier coefficients are

$$a_0 = \frac{1}{T} \int_0^T f(t) dt, \tag{3.7}$$

$$a_\omega = \frac{2}{T} \int_0^T f(t) \cos\left(\frac{2\pi\omega t}{T}\right) dt, \tag{3.8}$$

$$b_\omega = \frac{2}{T} \int_0^T f(t) \sin\left(\frac{2\pi\omega t}{T}\right) dt. \tag{3.9}$$

The shape of the function $f(t)$ determines the specific values of these coefficients. Larger coefficients correspond to more prominent modes or their harmonic in the signal. The data obtained from the biological system will be used for discrete sampling. Therefore, the Fourier transform of a signal can be written as:

$$F(\omega) = \sum_{n=0}^{N-1} f(n) \exp \frac{-2\pi i \omega n}{N}. \tag{3.10}$$

This equation allows the conversion of a time series from the time domain to the frequency domain, transforming a time-dependent series into one dependent on ω. Essentially, any periodic components in the time series will manifest as peaks in the Fourier transform at frequencies corresponding to those periodic terms. When a time series contains frequencies beyond the observable range, issues arise with the Fourier transform. Low-frequency components ($< \frac{1}{L}$) no longer behave periodically and instead

appear as trends at these frequencies. Since the Fourier series of a non-periodic function is an infinite sum of sine and cosine waves, most low-frequency oscillations tend to accumulate at $\omega = 0$, while higher-frequency oscillations are distributed across the spectrum. Therefore, it's essential to remove any trends from the time series before performing a Fourier transform to ensure that the detected components within the observable frequency range have accurate amplitudes. Even for frequencies within the observable range, the Fourier transform poses challenges when used as a representation in the frequency domain. Figure 3.13 visually demonstrates the process by which the amplitudes of periodic components with different forms can be divided into modes that are scattered over the frequency domain. This is achieved through the utilisation of the transform's emphasis on sinusoidal components. Hence, there exists a potential for misclassification of higher frequency modes with significant amplitudes as distinct components within the time series.

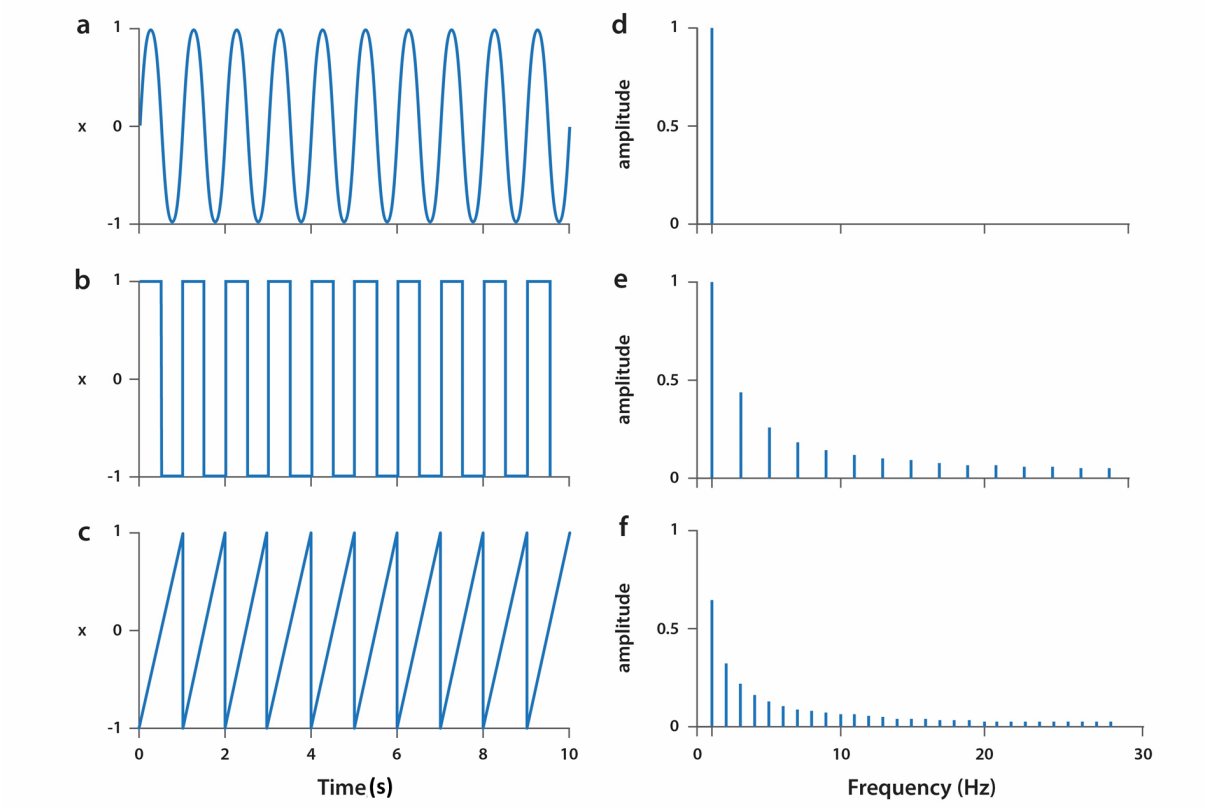

Figure 3.13: Time series of three different periodic functions: (a) A sine wave, (b) square wave and (c) sawtooth shape, as well as their one-sided Fourier transform amplitudes, are shown in panels (d), (e), and (f). The sampling frequency was 1000Hz

Power spectral density

The most commonly used approach for visualizing the dynamic properties of a signal is through the Fourier transform, which was discussed in the previous section regarding the frequency domain. This study can be utilised to ascertain the occurrence rate of deterministic processes that are observable in the time-series, achieved by identifying distinct and isolated spectral peaks. Alternatively, when the frequency vary significantly, the absence of peaks in the time-series can be utilised to identify it as "noise," where the spectral power demonstrates a linear gradient on a log-log plot of power spectral density (PSD) against frequency, see equation 3.11. An instance of a

time-series is classified as "white noise" when its PSD exhibits a continuous linear gradient. Conversely, it is categorised as "pink noise" when the power is directly proportional to $1/f^{\beta}$, where β is a value within the range of $(0, 2)$. Lastly, a time-series is labelled as "blue noise" when β falls within the range of $(-2, 0)$ [109].

The PSD for a discrete signal x(n)is given by the squared magnitude of the Discrete Fourier Transform (DFT) divided by the signal length N:

$$P\left(f_k\right) = \frac{\left|X\left(f_k\right)\right|^2}{N}, \tag{3.11}$$

where $X(f_k)$ is the DFT of $X(n)$ and f_k is the frequency corresponding to the k_{th} DFT bin.

The term "$1/f$ noise" is used to describe the shape of the spectral density, P(f), of a stochastic process that follows a specific pattern

$$P(f) = \frac{\text{constant}}{f^{\alpha}}, \tag{3.12}$$

Where f is frequency and $\alpha \geq 0$ and determines the functional dependence of the spectrum. Taking the logarithm of each side of Eq 3.12, we obtain

$$log(P) = -\alpha \log(f) + \log(\text{constant}), \tag{3.13}$$

α is determined by the gradient of the straight line (see figure 3.14) given by :

$$-\alpha = \frac{\sum_{k=0}^{N/2-1} \left(\log\left(f_k\right) - \mu_{\log(f)}\right)\left(\log\left(P_k\right) - \mu_{\log(P)}\right)}{\sum_{k=0}^{N/2-1} \left(\log\left(f_k\right) - \mu_{\log(f)}\right)^2}, \tag{3.14}$$

where $\mu_{\log(P)}$, $\mu_{\log(f)}$ are the mean values, N is The total number of data points (or frequency bins), f_k: The frequency value at index k and P_k: The power (or power spectral density) at the corresponding frequency f_k [110]. Table 3.5 shows the slope

values of all mice and the average value which is $\alpha = 1.21 \pm 0.08$. In the case of nonautonomous systems, a representation solely in the frequency domain is inadequate to capture all the information present in the signal. The characteristic feature of 1/f noise is its power spectral density, which rises as the frequency decreases. However, this representation does not convey information regarding the temporal variations or changes in the noise over time.

Unlike autonomous systems, nonautonomous systems exhibit a time-varying behavior, where their dynamics can change over time due to external inputs or internal mechanisms [109]. Consequently, to gain a comprehensive understanding of nonautonomous systems, it is essential to take into account both the frequency characteristics of the signal and how those characteristics evolve over time. By considering both the frequency content and its temporal variations, a more complete picture of the behavior of nonautonomous systems can be obtained. Certainly, the power spectral density (PSD) is a useful tool for analyzing the frequency content of a signal and determining the amplitude of each frequency component. However, it does not provide any information about the phase relationships between these frequency components. Additionally, the PSD representation lacks physical significance when it comes to understanding the mechanisms of frequency modulation.

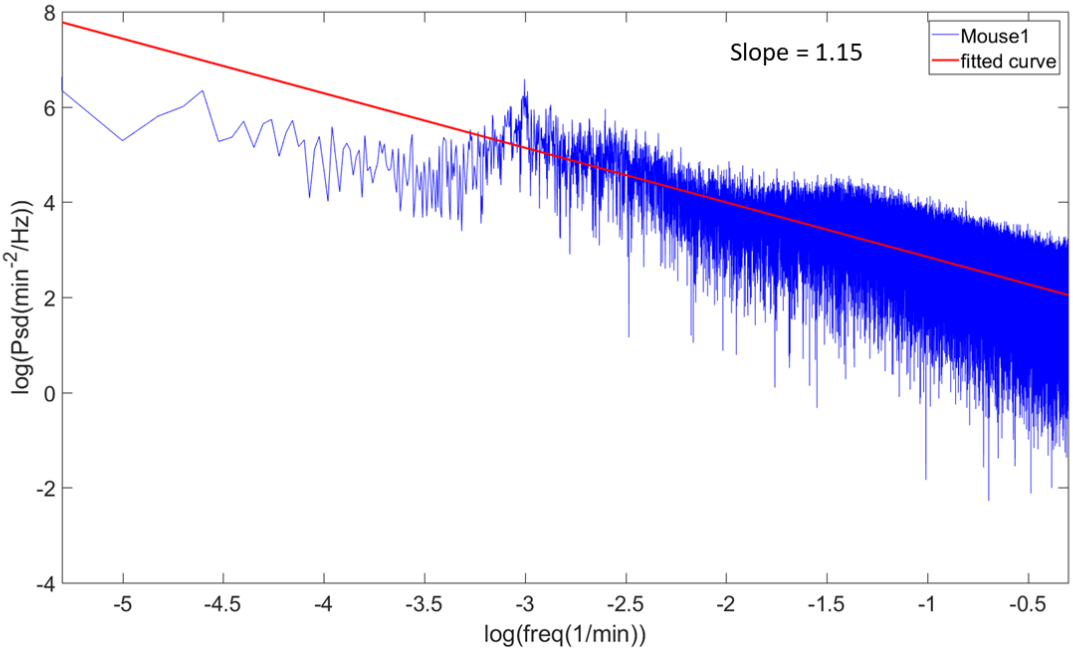

Figure 3.14: Power spectral density (PSD) of behavioural data of mouse 1 from study 1. The red line is obtained by calculating the y–intercept to fit the line. The obtained value α in this case is equal to 1.15.

Table 3.5: Values indicating the slope for all behavioral data recorded from all mice from study 1. The values slope provides information about the type of noise or the nature of the signal. It is considered pink noise as the value of the mean.

Mouse	**Slope**	**Mean ±S.D.**
1	1.15	1.21 ±0.08
2	1.04	
3	1.23	
4	1.30	
5	1.26	
6	1.22	
7	1.25	
8	1.22	

3.6.5 Time-frequency analysis

A physical signal can be represented in either the time domain or the frequency domain. Even while the methods for time domain decomposition offer some advantages that the Fourier transform does not, it would still be very helpful to have spectral approaches that could be successfully applied to the time series of sophisticated systems [111]. Although a Fourier transform is capable of revealing a great deal of information about a time series in the frequency domain, it can only be used to time series that contain components that are either periodic or stationary. Because non-stationary dynamics are only ever represented by discrete stationary components, this means that it is impossible for it to convey accurate information regarding the development of the components over time. As a consequence of this, a technique that monitors the phase and frequency of a number of different components as time passes is necessary.

It is not uncommon for physiological and real-world signals to be erratic in certain respects. By the way randomness or noise refers to unpredictable variations in a signal that can arise from various sources. Noise is typically considered to be a stochastic (random) process, and it can be characterized by its statistical properties. Non-stationarity refers to signals whose statistical properties change over time. In real-world systems, non-stationarity often arises from underlying trends, periodic components, or structural changes in the process generating the signal [19, 112, 113].

These oscillatory components exhibit a great number of amplitudes and/or frequencies that change over the course of time. The analysis of these variations in the time domain or through the use of Fourier transforms is challenging, but the beating of the heart is an excellent example. Although it is frequently centred around 1 Hz, the frequency of heart contractions is constantly fluctuating about this average. Because time and frequency are different dimensions, it is often more helpful to examine the qualities of a signal in both time and frequency at the same time. This can be accomplished by analysing certain projections of the signal onto a (two-dimensional)

time-frequency plane, which results in the creation of a chart that is known as a time-frequency representation (TFR). The analysis of multi component and nonstationary time series that contain time-varying spectral features lends itself particularly well to the practise of tracking the frequency content over time. This is because such time series may be tracked using TFR. A crucial part of TFR is its capacity to recover the oscillatory components of a signal, some of which may have time-varying characteristics [107].

We are concentrating our efforts in this study on the behavioural signals that were collected from mice. Due to the fact that these signals are non-stationary and non-linear, a time-frequency analysis that is founded on wavelet transforms is very suitable method for dealing with the complexity that they present. A wavelet-based extraction method was employed for the goal of determining the characteristic rhythms of these various signals, in addition to their temporal variability. This was accomplished by using TFR [114].

Windowed Fourier transform

The Windowed Fourier transform (WFT) or Short Time Fourier Transform (STFT) was developed as a solution to address the limitations of the standard Fourier transform and power spectral density. By using the STFT, it is possible to overcome the constraints of the Fourier transform when analyzing nonstationary signals and to create time-frequency representations of the signals [104]. The signal can be decomposed in a time-frequency plane by using STFT. The partition of this plane is stratified using rectangular or Gaussian cells with the same dimension. moreover,each cell in the time-frequency plane can be a rectangle, where the width corresponds to the duration of the time segment and the height corresponds to the frequency range being analyzed. Alternatively, cells can be shaped like Gaussian windows, which are bell-shaped curves. This approach can be used to give more weight to frequencies near the center of the window while tapering off toward the edges, allowing for smoother transitions in

frequency [115].

In living systems, the frequency composition of the recorded signal can gradually shift over time. In order to do research on this kind of signal, a short-time Fourier transform that uses a window that covers a brief period of time is necessary [116]. Within each of these time intervals, the frequency content of the signal is examined. This method splits the signal up into these time frames. The window is subsequently shifted along the signal, and the frequency content of the signal itself is examined, all in an effort to achieve time localization [111]. This method involves the evaluation of both the characteristic frequencies present in the signal and the corresponding time variations associated with those frequencies. The outcomes are presented in the format of a time-frequency representation. By employing the assumption of weak stationarity, it is possible to obtain insights into the frequency characteristics of the signal by taking an average across all windows [116]. The Short-Time Fourier Transform (STFT) can be mathematically stated as follows:

$$G_s(\omega, t) = \int_{-L/2}^{L/2} g(u-t) f(u) e^{\frac{-2\pi i \omega u}{l}} du, \tag{3.15}$$

where $f(u)$ represents a signal with a length of l, and $g(u)$ represents a rectangular function with a length of l that is zero outside $-l/2 \leq u \leq l/2$. The variable ω represents a chosen frequency for analysis, whereas the variable t represents an arbitrary shift in time. In addition to providing information on the frequency spectrum, the complex coefficients of the STFT also provide information on the phase of the components, which can be thought of as the location in the cycle in relation to time [19]. Note that if g(u) is a Gaussian function, the transform becomes known as the Gabor transform. This is something that should be kept in mind [117]. The following is a definition of the Gaussian window function:

$$g(u) = \frac{1}{\sqrt{2\pi} f_0} e^{-u^2/2f_0^2}. \tag{3.16}$$

When the resolution parameter f_0 is taken into consideration, the Gaussian window spread is what determines the trade-off between the time resolution and the frequency resolution of a WFT: When the f_0 resolution parameter has a smaller value, time changes are reflected more quickly; however, it becomes more difficult to differentiate between two components that are very close to one another in frequency [107].

The STFT method has its limitations due to a trade-off between time localization and frequency resolution. This trade-off arises from the uncertainty principle, which dictates that it is not possible to precisely determine both the frequency and the exact time of a signal simultaneously. Hence, the choice of window size is adjusted based on the specific requirements of the user, whether they prioritize better frequency resolution or better time localization. A larger window can provide improved frequency resolution but at the expense of poorer time localization, as the frequency resolution is directly related to the length of the window. Additionally, the linear frequency resolution of the STFT may not perform well in distinguishing distinct oscillatory modes, particularly when analyzing low-frequency components in the data [104].

Continuous wavelet transform

Recognizing the limitations of the fixed window size in the WFT, a solution was sought to overcome this constraint. The wavelet transform (WT) emerged as an optimal solution, as it permits the window size to vary inversely with the frequencies present in the data. This adaptive windowing approach entails using a wider window for very slow oscillations and a smaller window for very fast oscillations. The WT, when implemented in discrete steps, is referred to as the discrete wavelet transform (DWT). In this approach, the window is applied to different parts of the signal without any overlap between frequency bands. When this process is performed continuously, it is referred to as the continuous wavelet transform (CWT). The wavelet transform is

obtained from [20]

$$W_T(s,t) = \frac{1}{\sqrt{s}} \int_{-\infty}^{\infty} \psi \left(\frac{u-t}{s} \right) g(u) du, \tag{3.17}$$

where s is a scale parameter, t is a location on the signal in time and ψ is the mother wavelt. The wavelet transform (WT) employs same wavelet function stretched and contracted to examine the entire frequency interval of interest. It utilizes the scaling factor and time shifting to compute each scale. A small window (wavelet) is utilized for fast oscillations (high frequencies), while larger windows are used for slow oscillations (low frequencies). As a result, the time resolution at high frequencies is not constrained by the larger window required for detecting low frequencies [19].

When the wavelet basis employed is well-matched with the data, the convolution between the wavelet and the data yields a significant value. This enables the generation of a time-frequency representation of the entire signal by plotting time, frequency, and amplitude on a three-dimensional graph. The wavelet power spectrum can be determined by computing the integration of the squared magnitude of the wavelet transform across different frequencies [19, 20]

$$P_W(\omega,t) = \int_{\omega-\frac{d\omega}{dt}}^{\omega+\frac{d\omega}{dt}} |W_T(\omega,t)|^2 \, d\omega. \tag{3.18}$$

As a result, a vector representing the power of the entire time series is obtained, which can be plotted against frequency. This allows for the comparison of power spectra between different signals. This serves as a useful starting point in the analysis as it helps identify the frequency range of the primary oscillatory components within the signal being examined.

Wavelet types

Various wavelet forms exist, each possessing its unique properties and applications.

The preferred wavelet in this study is the lognormal wavelet, which offers higher resolution compared to the widely used Morlet wavelet [107]

$$\hat{\psi}(x) = \begin{cases} e^{-\frac{(2\pi f_r \log x)^2}{2}} & x > 0 \\ 0 & x \leq 0 \end{cases}, \tag{3.19}$$

where f_r is the frequency resolution which is a parameter that determines the trade-off between time localization and frequency resolution; the higher the value, the higher the frequency resolution and the lower the time resolution. Signals obtained from real systems have a finite length, while the Continuous Wavelet Transform (CWT) integrates over an infinite time range. As a result, the wavelet transform near the boundaries, close to t = 0 or when approaching the end of the signal, becomes undefined or ill-defined. To address this limitation, a technique called signal padding is employed. Padding involves extending the signal at both ends during the wavelet transform process, and then removing the added regions to retain only the original period of interest.

Different types of padding methods are available, including zero padding, periodic padding, and predictive padding. Despite the padding, a boundary effect can still be observed when the wavelet transform is performed near the edges of the original signal. The unaffected portion of the wavelet transform is referred to as the "cone-of-influence," indicating the region where reliable analysis can be conducted without being influenced by the boundary effects.

3.6.6 Ridge curve extraction

Ridge curve extraction is a technique used to extract the oscillatory modes or the trajectory of a time-varying frequency from the time-frequency representations of the data [118, 119]. It traces the highest amplitude peaks in a given frequency band. This is achieved by finding the greatest amplitude of an oscillatory component at each point in time. By combining the time-frequency representation with a time-averaged power plot, it becomes possible to visualize the oscillatory components along with

their corresponding frequencies. These frequency bands should cover the entire extent of the oscillatory component, including the peak as well as the surrounding blurring caused by the uncertainty principle. To ensure accuracy, it is important to focus on extracting a single oscillatory component from the selected frequency band. The frequency band for each mode in the spectrum can be determined by examining both the time-frequency representation and the average amplitude spectrum. The minima observed in the amplitude spectrum were utilized as reference points to establish initial boundaries between different oscillatory components. These boundaries were further adjusted based on the analysis of the time-frequency representation to prevent any overlap between the oscillatory components.

Occasionally, missing data due to measurement errors leads to periods where there is no information present. In this case, the ridge extraction algorithm may be unable to trace the mode due to the lack of information, causing fluctuations to a different value. However, these anomalies are transient and the ridges typically return to follow the mode after this period. As such, these fluctuations have little impact upon the further analysis. Figure 4.3 gives an example of the chosen boundaries for ridge extraction, and the ridges for each oscillation in each mouse are shown in the appendix.

3.6.7 Detection of high harmonic components

Since WT inherits the issue of high harmonics resulting from nonlinearity and provides time-dependent phase information, it enables the detection of relationships between oscillations and the identification of harmonics in any mode of the signal [120]. The method introduced by Sheppard et al. [120] allows for the differentiation between genuine modes and harmonics of non-sinusoidal oscillations. This approach utilizes the mutual information between harmonics that exhibit the same dynamics and involves surrogate testing.

3.6.8 Couplings

3.6.8.1 Bispectral analysis

The bispectral analysis is a valuable tool for detecting couplings between different oscillatory modes within a time series, such as those observed in the wheel-running activity of mice. In this study, we employ autobispectral analysis to explore the potential phase couplings between modes in the time series data. The focus is on determining whether two different oscillatory modes are phase-locked, which implies a dynamic relationship between them, contributing to the overall rhythmic behaviour [121, 122].

The method used is the wavelet bispectrum, denoted as $B_w(s_1, s_2)$, which measures the extent of phase coupling between oscillations at scales s_1 and s_2 over time. Mathematically, this is expressed as:

$$B_w(s_1, s_2) = \int_T W_T(s_1, \tau) W_T^*(s_2, \tau) W_T(s_1 + s_2, \tau)\, d\tau, \tag{3.20}$$

where $W_T(s, \tau)$ represents the wavelet transform of the signal at scale s and time τ, and W_T^* is its complex conjugate. The integration is performed over a time interval T, where the scales s_1 and s_2 satisfy the condition:

$$\frac{1}{s_1} + \frac{1}{s_2} = \frac{1}{s}. \tag{3.21}$$

This formula enables us to quantify how much coupling is present between two oscillatory modes at different scales over a certain time period.

In addition to the bispectral analysis, surrogate analysis is employed to verify the significance of the results. Surrogate data are generated to test whether the observed couplings are statistically significant or could occur by chance, ensuring the robustness

of the phase coupling measurements.

3.6.8.2 Dynamical Bayesian Inference (DBI)

Estimating the relationship that exists between the two components and the manner in which they are connected can be done using method called **Dynamical Bayesian Inference (DBI)** [123]. Within a system, the frequencies and amplitudes of specific oscillators are able to shift throughout the course of time. Then, the ways in which they interact with various other components might likewise change over time. In point of fact, dynamical Bayesian inference (DBI) identifies the couplings between oscillators as functions of time; thus, this method can be utilised to comprehend the real nature of what is beneath a system [123, 124, 125].

It is based on Bayes' theorem, which uses knowledge of the evolution of the system to forecast the future condition of the system. DBI is able to determine the model of the dynamical system for a given pair of oscillators by analysing the coupling functions between them. These functions are responsible for the interaction that occurs between two oscillators [126]. As an approximation, differential equations can be written as follows, with the joint phase dynamics decoupled (unidirectionally) from the overall dynamics. This works well when the coupling is weak.

$$\begin{cases} \dot{\phi}^1(t) = q_1\left(t, \phi^1(t), \phi^2(t)\right) \\ \dot{\phi}^2(t) = q_2\left(t, \phi^1(t), \phi^2(t)\right) \end{cases}, \tag{3.22}$$

where ϕ^1, ϕ^2 are instantaneous phases of a given oscillatory mode, as defined by ridge extraction [118], q_1 is the coupling function from ϕ^1 to ϕ^2, and q_2 is the coupling function from ϕ^2 to ϕ^1. This method enables the detection of bidirectional coupling functions,q_1, q_2, which tell us how the phase of one oscillator influences the phase of another, also known as phase coupling, as defined in [123, 126].

Due it is assumed that the oscillator frequencies vary slowly, the coupling function is assumed to also vary slowly over time. This is due of the assumption that the

oscillator frequencies vary slowly. Therefore, the time-independent estimates of the coupling strength, denoted by $q_i^{t_n}(\phi^1, \phi^2)$, are computed during designated time periods. To compute the coupling strength within each time window, it is necessary to first determine if the phase of one component is influenced by the phase of the other component or vice versa. In order to obtain precise findings,the size of the window is chosen so that it encompasses at least 10 cycles of the lowest frequency of interest. This is to ensure we have sufficient information for accurate determination of the dynamics of each window (cite toturial). The approximating coupling functions $q_i^{t_n}$ can be selected to lie inside the span of some finite number of Fourier basis functions. The equation that describes $q_i^{t_n}$ for all pairs of phases (ϕ^1, ϕ^2) at a time t_n is provided by

$$\begin{aligned} q\left(\phi^1, \phi^2\right) = a_0 + \left(\sum_{j=1}^{K} b_j \cos\left(j\phi^2\right) + c_j \sin\left(j\phi^2\right)\right) \\ + \left(\sum_{i=1}^{K}\sum_{j=-K}^{K} d_{ij} \cos\left(i\phi^1 + j\phi^2\right) + e_{ij} \sin\left(i\phi^1 + j\phi^2\right)\right), \end{aligned} \tag{3.23}$$

for the values of the parameters $a_0, b_j, c_{j,} d_{ij}$ and e_{ij}. Within each window, a statistical inference procedure is used to determine the coupling function between signals with phases $(\phi^i(t), \phi^j(t))$ in accordance with Bayes' theorem [127]. When determining the interaction between two oscillators, there are a total of $(2K+1)^2$ degrees of freedom for each of the two functions $(\phi^i(t), \phi^j(t))$ when using a certain K-value, which is referred to as the Fourier order. This K is selected as a second-order Fourier coefficient, and it is used to define the number of degrees of freedom. The set of K prevents the introduction of an excessive number of degrees of freedom, which can cause overfitting and lead to inaccurate predictions. Following the computation of the result in a particular time window, the propagation constant $p \geq 0$ will decide the extent to which the result will impact the calculation of the window that comes after it. When the value of p is increased, it indicates that the result has a greater bearing on the computation that takes place in the following window. Having a value of p that is excessively high for

coupling functions that fluctuate over the course of time can restrict the accuracy of the results.

The strength of the coupling that exists between one signal and another is measured across each time interval as

$$\begin{aligned} \epsilon_{21} &= \|q_1\left(\phi_1, \phi_2\right)\| \\ \epsilon_{12} &= \|q_2\left(\phi_1, \phi_2\right)\| \end{aligned} \tag{3.24}$$

Where $q_1(\phi_1, \phi_2)$ and $q_2(\phi_1, \phi_2)$ are the coupling functions. Each of these values $\epsilon_{j\to i}$ is simply equal to the Euclidean norm of the $(2K+1)^2$-dimensional vector of coefficients in the Fourier expression for $q_i^{t_n}$. Eqs. (3.24) are rewritten

$$\epsilon_{j\to i} := \left(\int_0^1 \int_0^1 \left[q_i^{t_n}(\phi_1, \phi_2) - a_0^{(i)}\right]^2\right)^{\frac{1}{2}}, \tag{3.25}$$

where $a_0^{(i)}$ defines the constant term in the Fourier expression for $q_i^{t_n}$. In point of fact, the angular velocity of the phase oscillator i at time t ought to be constant if it is not being influenced in any way by an additional oscillator j. Through the utilisation of the surrogates approach, the importance of the coupling strength $\epsilon_{2\to 1}$ from ϕ^2 to ϕ^1 is investigated. For the purpose of determining whether or not the apparent coupling between two oscillators is statistically significant, surrogates are utilised.

DBI offers a framework that is more adaptable and may be used to estimate the coupling between nonlinear and nonstationary signals. In this method the underlying dynamics of the signals are modelled as a probabilistic process. Bayesian inference is then used to estimate the parameters that explain the coupling between the signals. Moreover,DBI is a more reliable method for estimating the coupling between signals in noisy and complicated systems since it can also use prior knowledge about the system and can incorporate uncertainty in the measurements. This makes DBI a more desirable method, see figure 4.20.

3.7 Statistical tests

The reason we have applied non parametric tests is due the non Gaussian nature of the distribution in the data as we later show in figure 4.4.

3.7.1 Wilcoxon signed-rank and sum-rank tests

The use of wavelet transform and windowed Fourier transform techniques allows for the determination of time-averaged power in signal analysis, which holds greater physical significance compared to frequency spectra obtained via the standard Fourier transform, particularly for data stemming from nonautonomous dynamical systems. These systems, characterized by their time-dependent behavior, require analytical methods that can account for the temporal variations in their signal power. By employing these advanced transforms, researchers can capture the dynamic changes over time, providing a more accurate representation of the system's behavior [128, 129, 130].

This enhanced analytical capability is especially valuable when conducting statistical hypothesis testing. The time-averaged power serves as a robust metric for such tests, offering a solid foundation for the application of non-parametric tests like the Wilcoxon signed-rank test, which is used for paired samples to assess the differences between matched pairs. Similarly, when dealing with two independent samples, the rank-sum test (also known as the Mann-Whitney U test) can be applied. These tests do not assume a normal distribution of the data, making them more versatile for a range of data types and particularly suitable for the non-linear and non-stationary data typically observed in nonautonomous systems. When we obtain bivariate data, specifically (x(t), y(t)), from an identical population P and both data sets are measured in the same units, such as millivolts, it becomes possible to compare the spectra derived from these measurements. Let's consider that we aim to evaluate the null hypothesis, which states that, at each frequency value, the median of the signed differences between the spectral values from the two data sets is zero.

Furthermore, if we assume that the distribution of the signed differences is symmetrical around a certain value, then the Wilcoxon signed-rank test is an appropriate method to use for this hypothesis testing (sum of the ranks of the paired differences). In the context of the thesis, the Wilcoxon signed-rank test was employed, requiring that both datasets under comparison have an identical number of samples, equivalent length, and the same sampling frequency. For the results of this test to be deemed statistically significant, a p-value threshold of less than 0.05 was established. The significance threshold of p=0.05 is a benchmark that is widely accepted in statistical testing. This indicates that there is a probability of less than 5% that the observed differences occurred by chance. This threshold ensures the accuracy of the findings by reducing the possibility of making Type I errors, which occur when the absence of an effect is wrongly interpreted as evidence against the null hypothesis [128, 129, 130].

For instances where the datasets being compared originate from two distinct populations, the null hypothesis posited for testing stipulates that the median time-averaged power at a given frequency f for the initial population is identical to that of the second population. Under these circumstances, the appropriate statistical test to utilize is the rank sum test. In such analyses, it is not a requirement for the datasets to share an equal number of samples. The criterion for statistical significance in this scenario is once again established as a p-value of less than 0.05 [128, 129, 131]..

3.7.2 Surrogates

Surrogates can be characterised as synthetic indicators that are employed to examine the potential presence of a specific characteristic within systems. The individuals in question exhibit patterns of behaviour similar to those observed within the system being examined, although they do not possess ownership rights over the property subject to inquiry. There exist a multitude of surrogates that can be employed for diverse applications [132]. The primary signal from any given system, referred to as the "real"

signal, is treated in an identical manner to its surrogate signals. Upon implementing the selected methodology on the initial signal as well as the surrogate set, a comparison is made between the outcomes derived from the original data and the distribution of results produced from the surrogates. If there is a statistically significant difference between the original data and the surrogate set, at a certain confidence level determined by the chosen statistical threshold, it can be inferred that the original system possesses the specific attribute of interest. However, if the test lacks adequate strength, then the system cannot be considered as possessing such a quality. Surrogates are employed as a means to assess the statistical significance of findings derived from the examination of wavelet phase coherence and dynamical Bayesian inference. In dynamical Bayesian inference, the surrogates approach is employed to assess the statistical significance of the estimated connection between two oscillators. The surrogates test offers a means to assess the relative magnitude of the coupling strength. The surrogate test employed for dynamical Bayesian inference involves the utilisation of cyclic phase permutation (CPP). The signals will oscillate within the range of 0 and 2π. The signal is partitioned into full cycles, which are randomly rearranged, while the partial cycles at the start and finish stay unchanged.

Surrogates are employed in order to evaluate a null hypothesis at a predetermined level of significance α, where α is a significance level that falls within the interval (0, 1). To conduct a one-sided test, it is recommended to generate $1/(1-\alpha)-1$ surrogates. Similarly, for a two-sided test, it is advisable to generate $2/(1-\alpha)-1$ surrogates. The null hypothesis can be rejected when there is a significant deviation between the value of the statistic obtained from the data being analysed and the distribution of values derived from the surrogate data. Alternatively, it is possible that the outcome may not occur as indicated by previous research [133]. In order to enhance the discriminatory capacity, it is vital to augment the quantity of surrogates.

In this thesis, for the bispectral analysis, 19 iterative amplitude adjusted Fourier transform (IAAFT) surrogates were used. This approach involves adjusting the

amplitude of the Fourier-transformed data to create surrogates that maintain the original amplitude distribution while randomizing the phase information. This allows for the evaluation of non-linear interactions and dependencies in the data. For DBI analysis, 19 cyclic phase permutation surrogates were generated. This method randomizes the phase behavior of the original time series data while preserving the overall structure and distribution of the data.

4. Results

This chapter presents the analysis and findings derived from the data collection methods and protocols detailed in Chapter 3. Initially, we will discuss the specific frequency bands of interest and the implementation of the ridge extraction technique to analyze them. Following this, we provide evidence of the circadian rhythm presence, highlighting the variations observed in the rhythm when methamphetamine is administered versus when it is not. Additionally, we explore and present the harmonic relationships and coupling dynamics that occur in both scenarios: with methamphetamine and without it.

4.1 Study 1: Behavioural rhythm across multiple conditions

4.1.1 Frequency bands

In this thesis, the time series are wavelet-transformed in order to recover the oscillatory components across time. This transformation takes place in the time-frequency domain. Because of its higher resolution, the lognormal wavelet is the preferred type of wavelet to use. The signal is processed using a wavelet transform, where each portion of the signal that overlaps with the wavelet is converted into the frequency domain. Adjustments are made to the wavelet as it moves across the signal to capture both time and frequency information. According to the findings of this investigation, the

value of the f_r parameter that offered the best possible trade-off was 1.8. In order to ensure that ridges are extracted for the entirety of the recording process, zero padding was added to the entirety of the time-frequency representation for all mice.

It was discovered by applying the wavelet transform to the data that the *Per1/2/3* triple knockout mice, when subjected to a range of different conditions, demonstrated how methamphetamine has enhanced the rhythm after being administered to the mice. This was the case after the mice were given the drug. The exact identical time-frequency representation was obtained for each of the mice, even though they were all examined using the same technique, figure 4.1 illustrates one mouse which is number 4. Violin plots for the various periods of each oscillation are shown in the figure 4.4 illustrates the violin plots which have been created to display the range of oscillation periods as presented in the table 4.2, for all of the mice (1-8). These plots were generated based on frequency ridges obtained through the process of ridge extraction. The use of violin plots provides a visual summary that not only shows the distribution of these periods across the sample of mice but also highlights the probability density of the data at different values, offering a more nuanced understanding of the oscillatory behavior in the study.

In order to extract ridges, the boundaries that are chosen must contain the full oscillatory component under investigation and no other components. These boundaries are represented by dashed lines. Figure 4.3 gives an example of the chosen boundaries for ridge extraction. The ridges for each oscillation in each mouse are shown in the Appendix. The time sequence of maximum amplitude peaks in time-frequency space within the defined frequency interval is what gives rise to ridge curves. The values that are displayed in table 4.1 were obtained by calculating the average frequency value of the ridges, which were taken from the time-frequency representation through the process of ridge extraction.

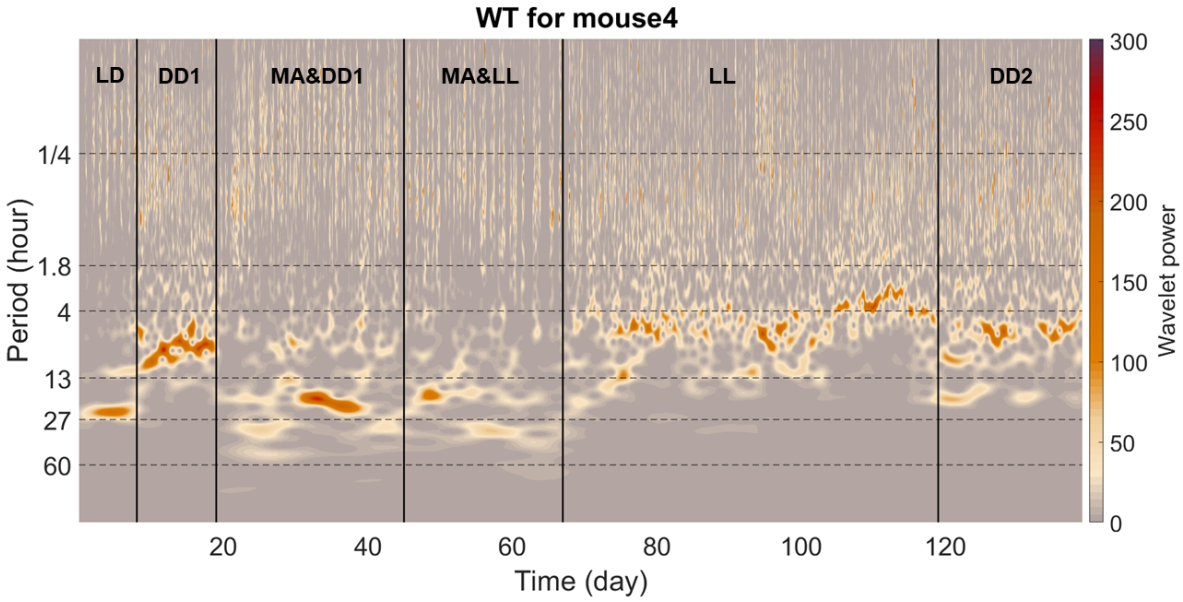

Figure 4.1: Time-frequency representation obtained via the wavelet transform of behavioural data from mouse 4. The vertical black lines indicate the start/end of a given condition, (as all of the abbreviation described in chapter 2), where the horizontal dashed black lines indicate the frequency band of interest.

Interval	Period (hour)
1	27 - 60
2	13 - 27
3	4 - 13
4	1.8 - 4
5	¼ - 1.8

Figure 4.2: Identification the band of interest and their associated values.

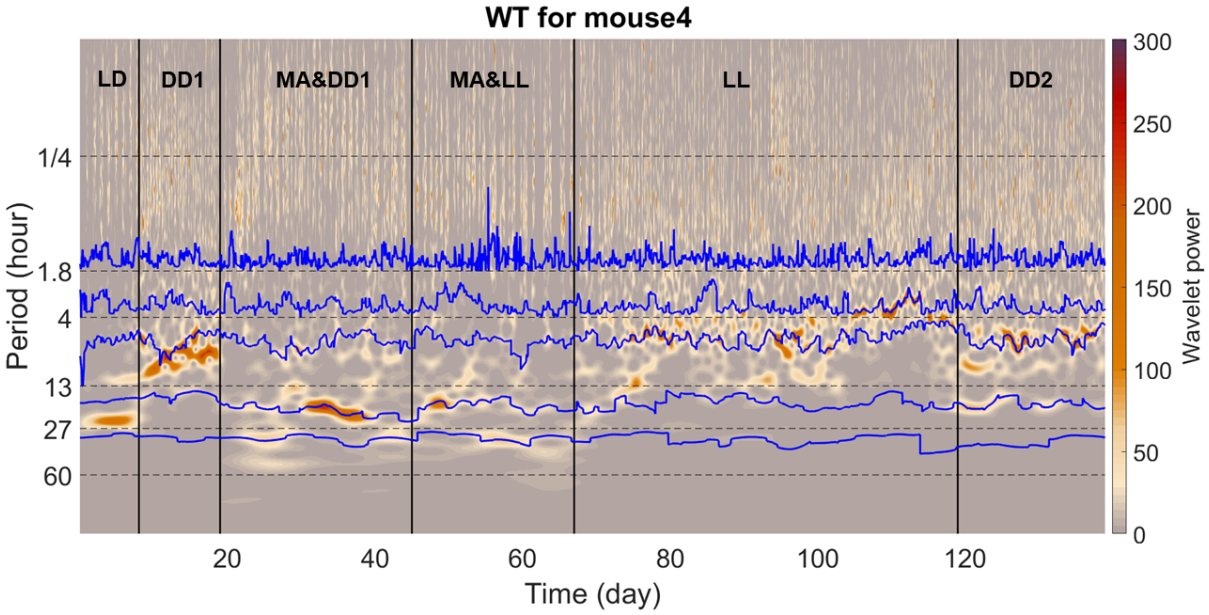

Figure 4.3: The method for extracting ridges from a time-frequency representation, and the extracted ridges. The wavelet transform is performed on the behavioral data of mouse 4.

	1	2	3	4	5
Mouse 1	37.0 ± 5.0	18.6 ± 2.0	10.7 ± 1.3	3.3 ± 0.5	1.5 ± 0.9
Mouse 2	35.0 ± 5.0	18.3 ± 2.5	9.6 ± 1.6	3.3 ± 0.4	1.5 ± 0.7
Mouse 3	34.2 ± 4.0	20.1 ± 3.0	10.3 ± 1.3	3.2 ± 0.4	1.4 ± 0.5
Mouse 4	32.7 ± 2.8	17.9 ± 2.1	5.9 ± 6.0	3.3 ± 0.6	1.5 ± 0.6
Mouse 5	35.2 ± 3.4	20.1 ± 2.6	7.3 ± 1.2	3.2 ± 0.3	1.5 ± 0.4
Mouse 6	40.2 ± 3.9	18.7 ± 3.2	7.8 ± 9.0	3.3 ± 0.4	1.4 ± 0.3
Mouse 7	35.0 ± 4.3	18.4 ± 3.5	9.0 ± 1.6	3.3 ± 0.5	1.5 ± 0.8
Mouse 8	34.5 ± 4.1	19.1 ± 2.5	9.5 ± 1.8	3.3 ± 0.4	1.4 ± 0.3
Mean	35.5 ± 1.3	18.8 ± 6.2	8.7 ± 3.8	3.3 ± 0.2	1.5 ± 2.1
Median	35.0 ± 1.3	18.3 ± 6.2	8.7 ± 3.8	3.3 ± 0.3	1.5 ± 2.1

Table 4.1: The oscillatory components were located by first determining the mean frequency value of the ridges, followed by calculating the standard deviation of those values. This was done by extracting the ridges from the time-frequency representation using the ridge extraction method.

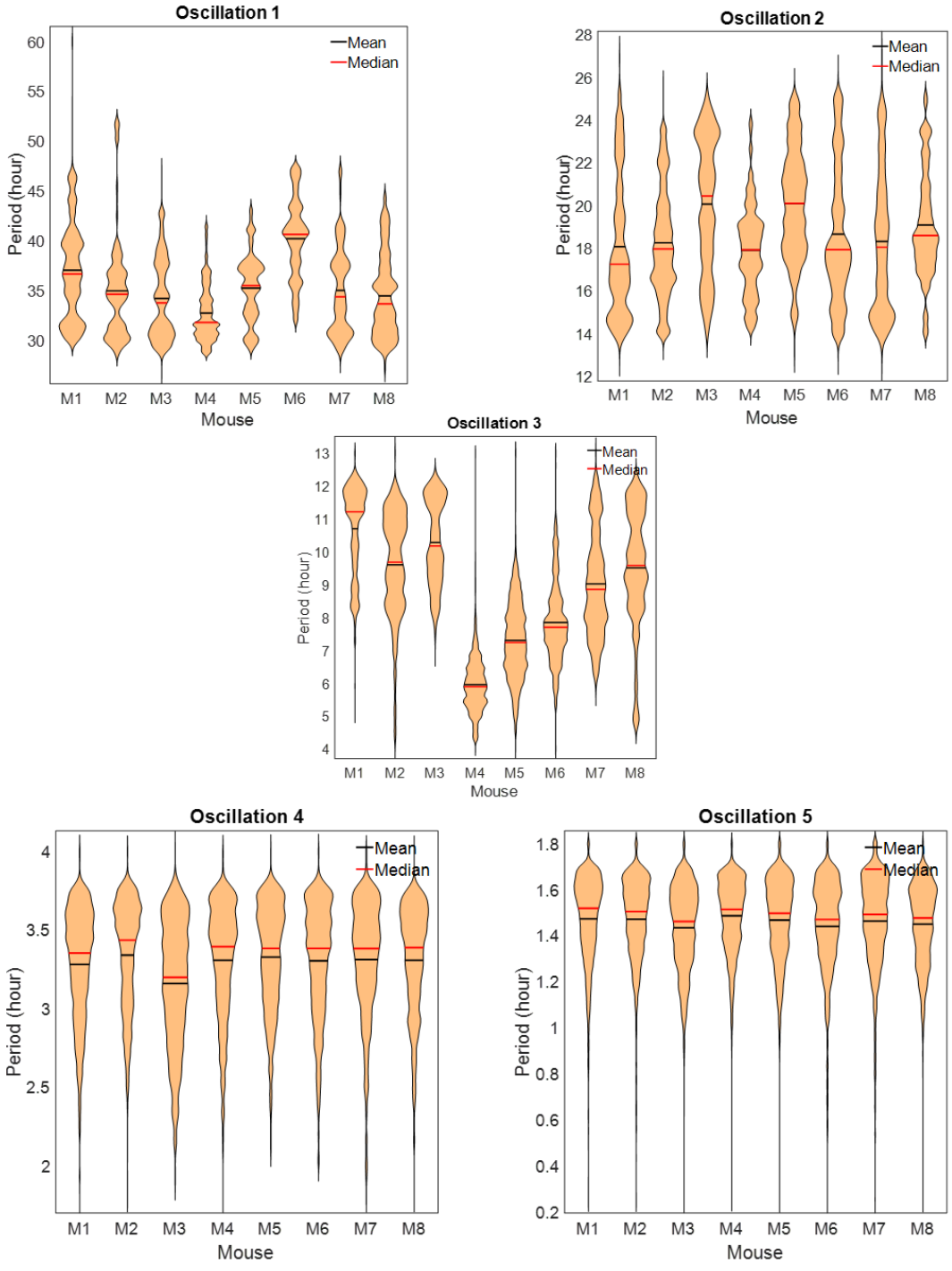

Figure 4.4: Violin plots representing oscillation periods (1-6) for all mice (numbered 1-8) were derived using frequency ridges from ridge extraction. The significant variability in oscillation 3 could be due to genetic, environmental, or experimental factors.

4.1.2 Circadian rhythms can persist even when clock genes are knocked out

The wavelet transform analysis conducted on the behavioral data has yielded a noteworthy finding— the 24-hour circadian rhythm persists even in the absence of the clock gene. This intriguing revelation emerged during a meticulous examination of the data using the wavelet transform, providing valuable insights into the robust nature of circadian regulation within the system.

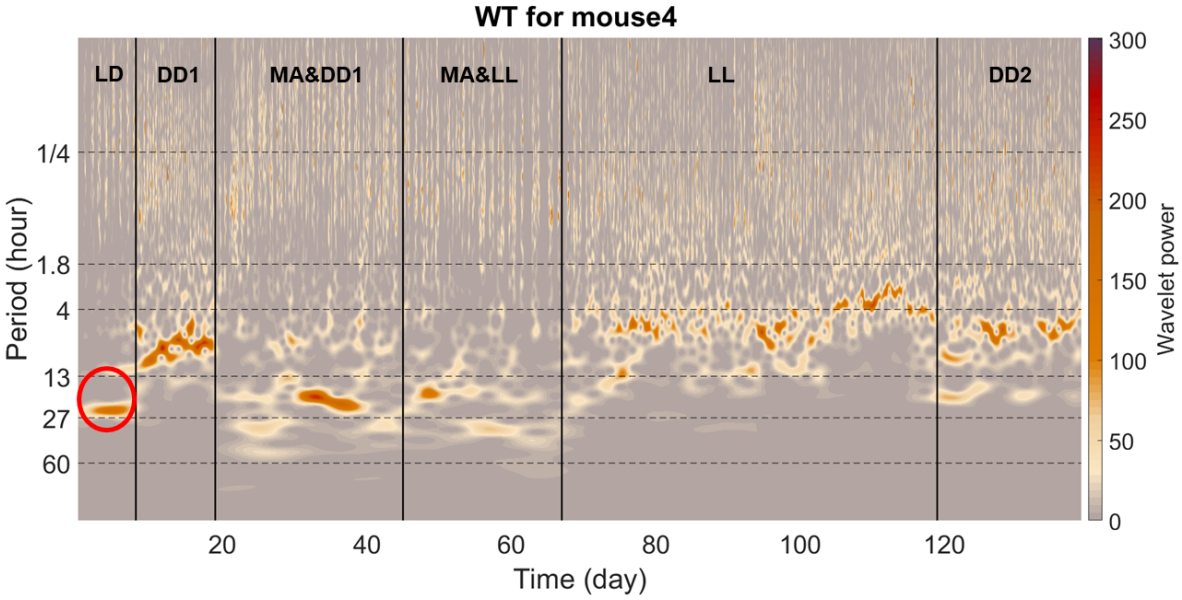

Figure 4.5: Time-frequency representation obtained via the wavelet transform of behavioural data from mouse 4. The red circle indicates the circadian rhythm. The vertical black lines indicate the start/end of a given condition, (as all of the abbreviation described in chapter 2), where the horizontal dashed black lines indicate the frequency band of interest. The wavelet transform is applied using the lognormal wavelet and a frequency resolution parameter of 1.8.

Figure 4.5 illustrates the time-frequency representation of mouse 4's behavioral data, offering a visual representation of the observed phenomenon. The conspicuous red circle

within the plot distinctly marks the presence of a rhythm in the LD condition. This clear and identifiable rhythm showcases the resilience of the circadian cycle, emphasizing its sustained regularity despite the absence of the clock gene. Given the intrinsic nature of this circadian phenomenon, there is a compelling interest in delving deeper into its dynamics. To further unravel the intricacies of this persistent circadian rhythm, we are motivated to extend our investigation by analyzing additional datasets characterized by long-term recordings under similar conditions.

4.1.3 Group average power across all conditions

We now present the average power across a period spectrum under three different conditions over six days of recording which are LD, DD, and MADD as it is illustrated in figure 4.6. The peaks in the figure indicate periods where there is a high average power, which suggests that under these conditions, the subjects show a significant amount of activity or expression with a specific rhythm. For instance, under LD conditions, there are peaks corresponding to the circadian rhythm (around 24 hours), while under DD conditions, these rhythms might free-run with a slightly different period due to the absence of light cues.

The DDMA condition provides critical insights into the impact of methamphetamine on biological rhythms. Methamphetamine is a potent central nervous system stimulant that can profoundly disrupt normal biological and circadian rhythms. We observe that the DDMA condition exhibits a distinctive pattern in comparison to the LD and DD conditions. Specifically, the shape and position of the peaks in the power spectrum are notably different. The peaks represent periods where there is a heightened average power, indicating more intense or frequent activity in the biological variable being measured.

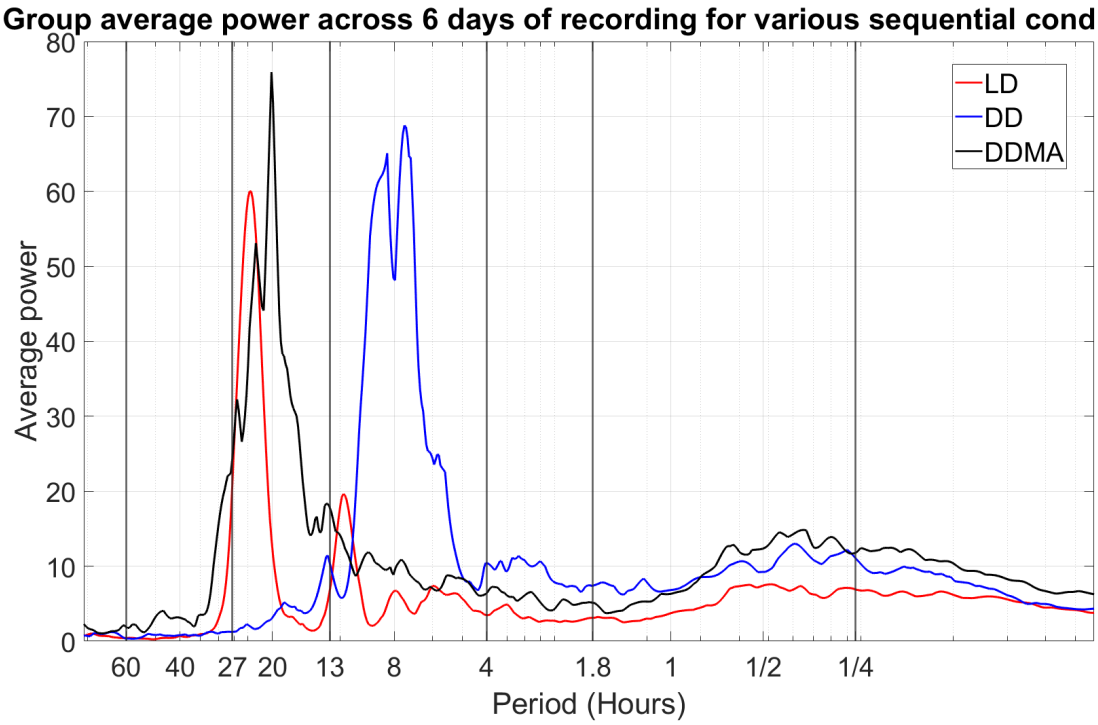

Figure 4.6: Average power across a period spectrum under three different conditions over six days of recording. The x-axis shows the period in hours, on a logarithmic scale.

4.1.4 The system retains the memory following the MA administration

When performing a wavelet transform analysis of behavioral data influenced by MA, as shown in Figure 4.1. Moreover, Figure 4.7 presents a comparative analysis of the average power in DD conditions, measured before (DD1) and after (DD2) the administration of MA to mice. This comparison is designed to illustrate the effects of MA on the biological rhythms or activities being studied.It becomes apparent that the system retains a form of 'memory' after the cessation of the drug's effects. This observation is made clearer in this figure. Before MA administration, the DD condition serves as a baseline, representing the natural rhythms of the mice in the absence of light cues and the drug. The system's inherent tendency to revert to its original rhythmic patterns

that were present before the introduction of methamphetamine. Despite the significant disruption caused by the drug, which is detectable in the altered frequency and power of the behavioral rhythms, the system shows an inclination to re-establish its baseline state once the influence of the drug is removed.

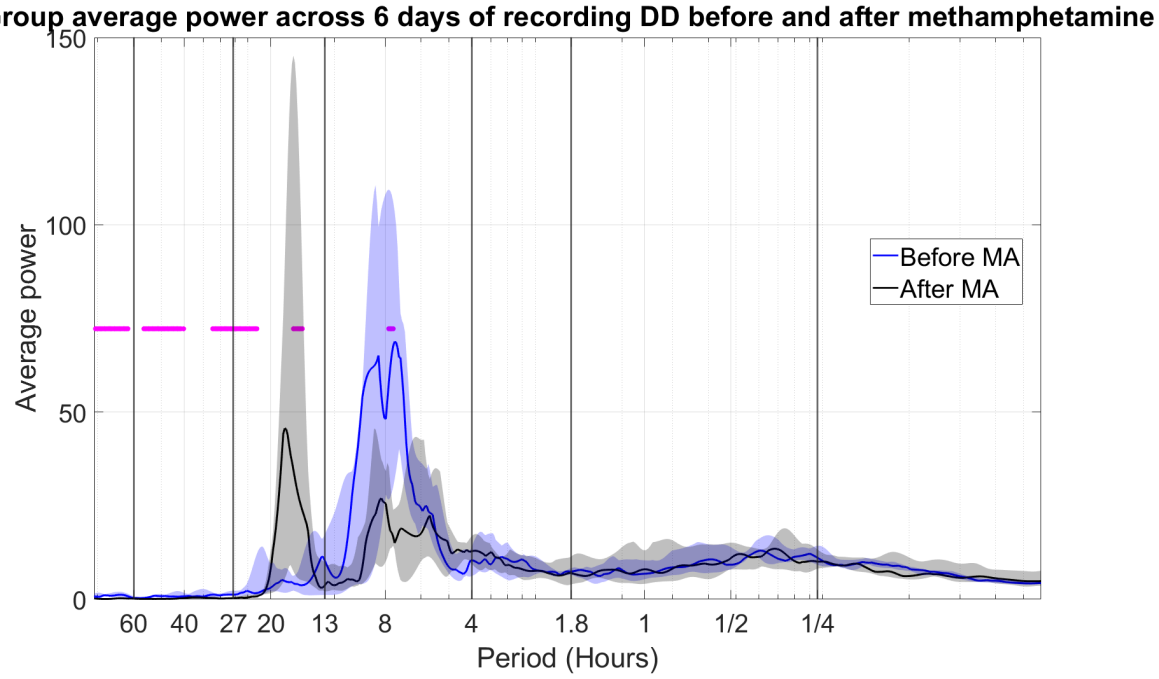

Figure 4.7: Average power across a period spectrum under three different conditions over six days of recording. Pink horizontal lines indicate the significant differences between conditions with (p-value < 0.05). The shaded area in the plot represents the variability around the average power values, typically shown as confidence intervals. By displaying these intervals, the plot provides a visual indication of the uncertainty or variability in the power measurements across different periods, helping to highlight where significant differences might exist. The x-axis shows the period in hours, on a logarithmic scale.

Pink horizontal lines indicate the significant differences between conditions with (p-value < 0.05). The shaded area in the plot represents the variability around the average power values, typically shown as confidence intervals. By displaying these

intervals, the plot provides a visual indication of the uncertainty or variability in the power measurements across different periods, helping to highlight where significant differences might exist.

4.1.5 Hyperactivity following methamphetamine administration

As we compute the total power across all six conditions, it's important to note that we limited the calculation to a span of 6 days for each of these conditions. This decision aligns with the duration of the LD condition, which also spans 6 days, influencing our choice of the 6-day limit for analysis. The influence of methamphetamine administration is prominently evident upon examining these mice, as depicted in Figure 4.8. The series of violin plots within the figure encapsulates the total power across six experimental conditions. A detailed examination reveals distinct alterations in rhythmicity following the administration of methamphetamine to the mice, notably observed in conditions MA & DD(1) and MA & LL. Moreover, the figure shows that there is a significant difference between DD(1) and MADD(1), but not between DD(2) and MADD(1), which can be attributed to the system's memory, as discussed in the previous subsection.

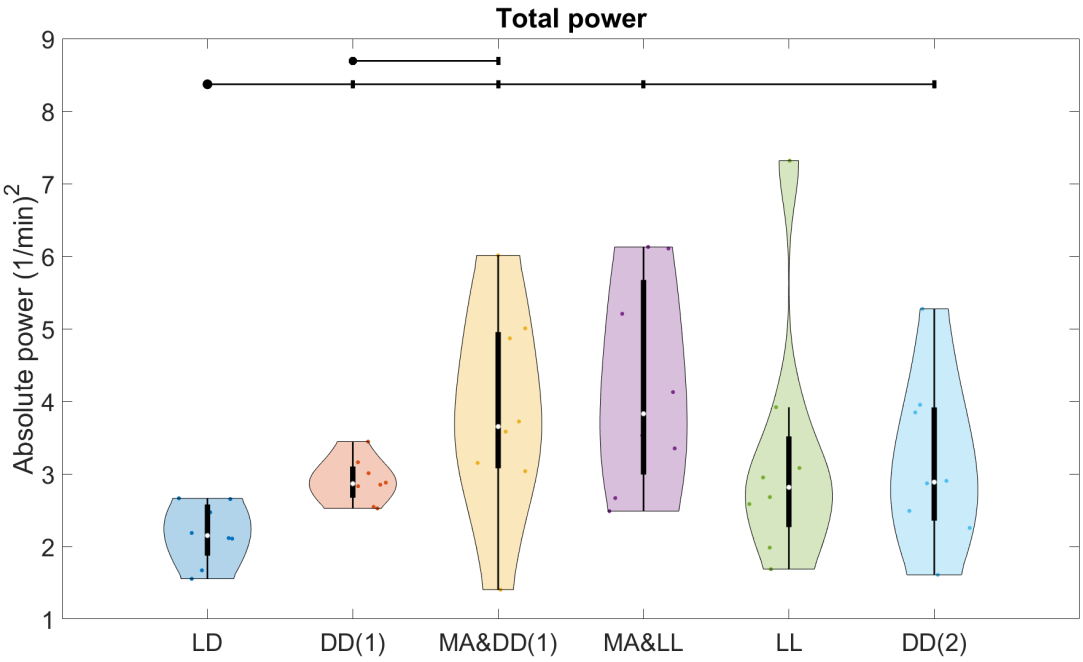

Figure 4.8: Violin plot for the total power in the 6 conditions, evaluated over a 6 day interval. Black horizontal lines indicate the significant differences between conditions with (p-value <0.05). After performing the Wilcoxon rank test, the lines above the violin plots indicate which conditions were compared, and the results of those comparisons typically show whether there was a significant difference in the distributions of those conditions.

Administering methamphetamine to the mice restored the 24 rhythm for MA & DD and following the administration of the methamphetamine condition, the circadian rhythm had a significantly increased the total power in the 1/13 - 1/27 hr band, see figure 4.9. The plots provide a visual representation of how methamphetamine influences the intensity and regularity of the mice's circadian rhythms. It is anticipated that the mice's circadian rhythms will be disrupted in both instances because of the gene deletion.

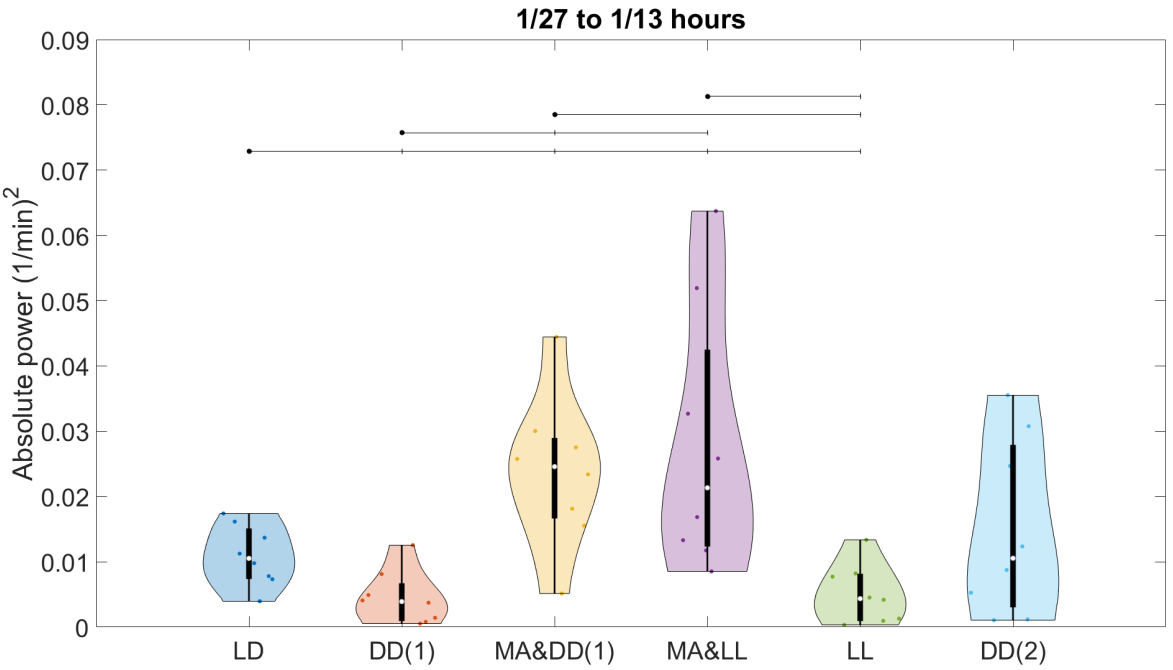

Figure 4.9: Violin plot for the absolute power for the frequency band (1/27 hours to 1/13 hours) for all conditions and across all mice evaluated over a 6 day interval. Black vertical lines indicate the significant differences between conditions with (p-value <0.05). After performing the Wilcoxon rank test, the lines above the violin plots indicate which conditions were compared, and the results of those comparisons typically show whether there was a significant difference in the distributions of those conditions.

Moreover, the figure 4.10 provides representation of the total power within the frequency band spanning from 1/27 to 1/60 hours. A notable observation is the clear emergence of a new rhythm following the initiation of methamphetamine administration.. This visual depiction enhances our understanding of the impact of methamphetamine on the rhythmic patterns within the specified frequency range. However, since this study was conducted over a period of only six days, there wasn't sufficient time to comprehensively assess the effects of a rhythm falling between the 27 and 60-hour period. Therefore, we conducted an additional studies (2 and 3) with a longer recording period to obtain more comprehensive insights.

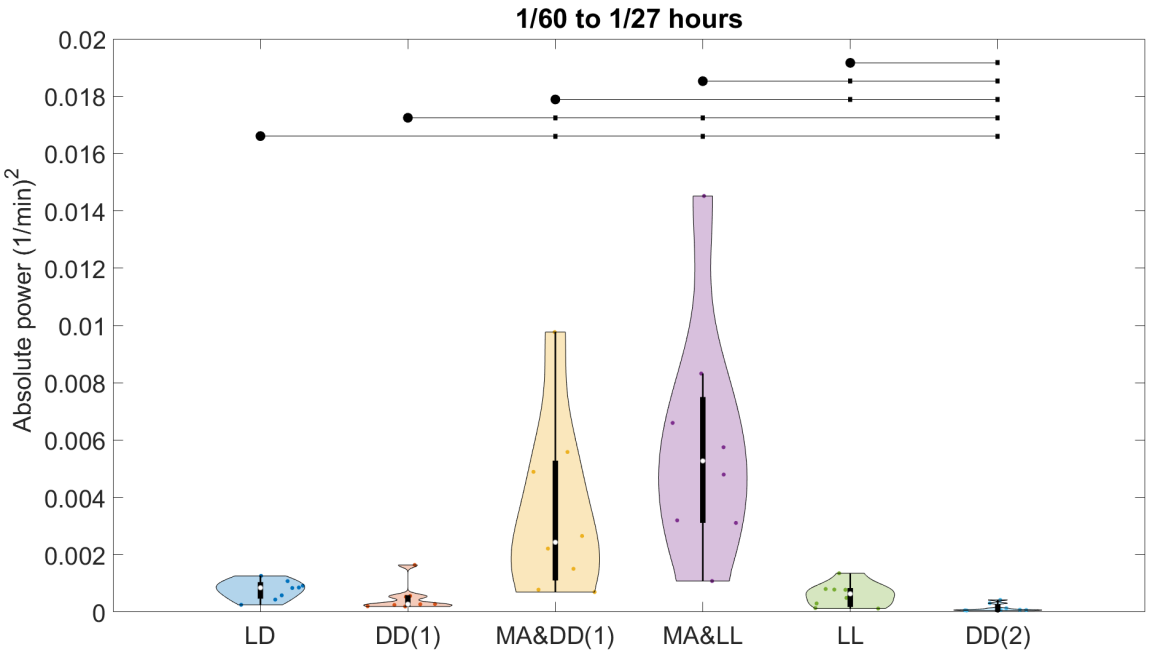

Figure 4.10: Violin plot for the absolute power for the frequency band (1/60 hours to 1/27 hours) for all conditions and across all mice evaluated over a 6 day interval. Black horizontal lines indicate the significant differences between conditions with (p-value <0.05). After performing the Wilcoxon rank test, the lines above the violin plots indicate which conditions were compared, and the results of those comparisons typically show whether there was a significant difference in the distributions of those conditions.

4.2 Study 2: Comparing wild type and per knock-out mice under identical condition

In this section we are comparing between wild mice and knocked out mice in the same condition (DD). We have performed wavelet transform for both wild-type mice which is illustrated in figure 4.11. These mice have intact Per genes, which contribute to the regulation of the circadian clock. The wavelet transform of their activity under constant darkness conditions usually shows a stable and consistent rhythm, aligned with the expected 24-hour circadian cycle. This stability implies that the internal

clock is functioning normally, driving regular patterns of behavior and physiology even without external light cues to synchronize it.

Per gene knockout mice which is illustrated in figure 4.12, the absence of one or more Per genes results in a marked disruption of the circadian rhythm. The wavelet transform in this case often reveals that the rhythm is not only inconsistent but may also lack the 24-hour periodicity typically observed in wild-type mice. The irregularity can manifest as a rhythm with a shorter or longer period, or as a complete fragmentation where no clear periodic pattern can be discerned. While circadian rhythms can emerge in the absence of Per genes, these genes are essential for ensuring the stability, precision, and adaptability of the circadian system, as well as for mitigating potential health risks associated with disrupted rhythms.

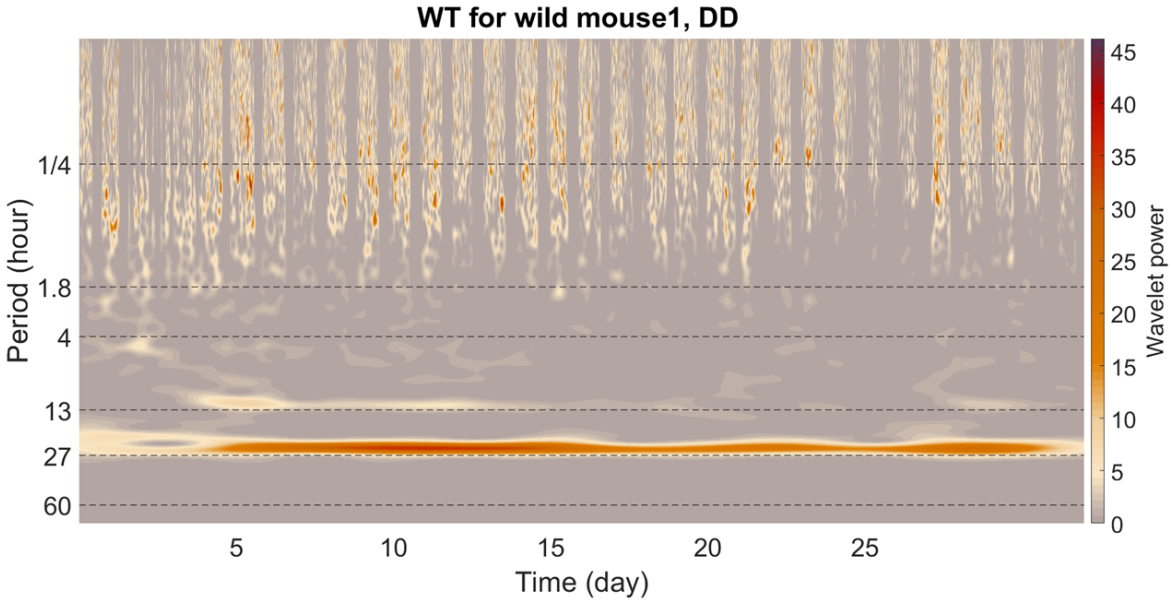

Figure 4.11: Time-frequency representation obtained via the wavelet transform of behavioural data from a wild mouse in constant darkness over 32 days (study 4). The wavelet transform is applied using the lognormal wavelet and a frequency resolution parameter of 1.8.

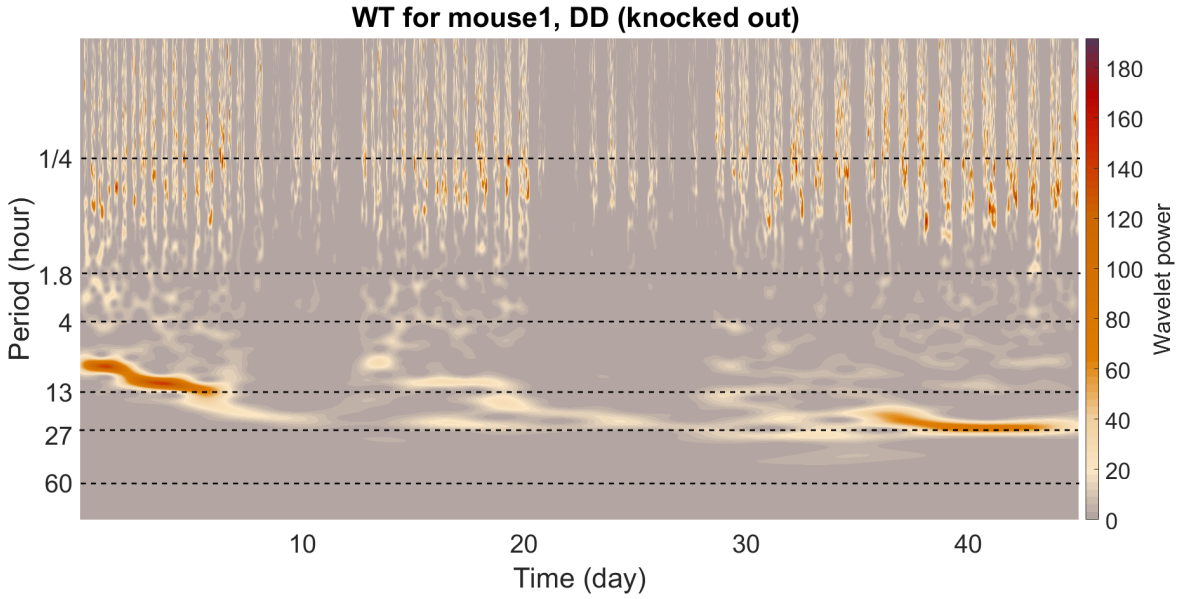

Figure 4.12: Time-frequency representation obtained via the wavelet transform of behavioural data from mouse 1 in constant darkness over 45 days. The wavelet transform is applied using the lognormal wavelet and a frequency resolution parameter of 1.8.

4.3 Study 3: Evaluating the effect of MA administration utilising longer recording

As previously mentioned in Study 1, the timeframe was insufficient to thoroughly evaluate the effects of a rhythm falling within the period when the MA was administered. We analyzed data both with the administration of MA, as illustrated in figure 4.14, and without its effect as illustrated in figure 4.13. Time-average power calculations were performed for specifically focusing on the DD condition. We selected and processed data from a total of 65 days to compute the overall power for this condition. There are noticeable peaks for both groups, with the red line (Meth group) showing higher peaks than the blue line (No Meth group), suggesting

stronger or more pronounced oscillatory activity at those periods. The group treated with methamphetamine generally exhibits higher average power across several periods, which could indicate that methamphetamine affects the intensity and regularity of the oscillatory behaviors being measured.

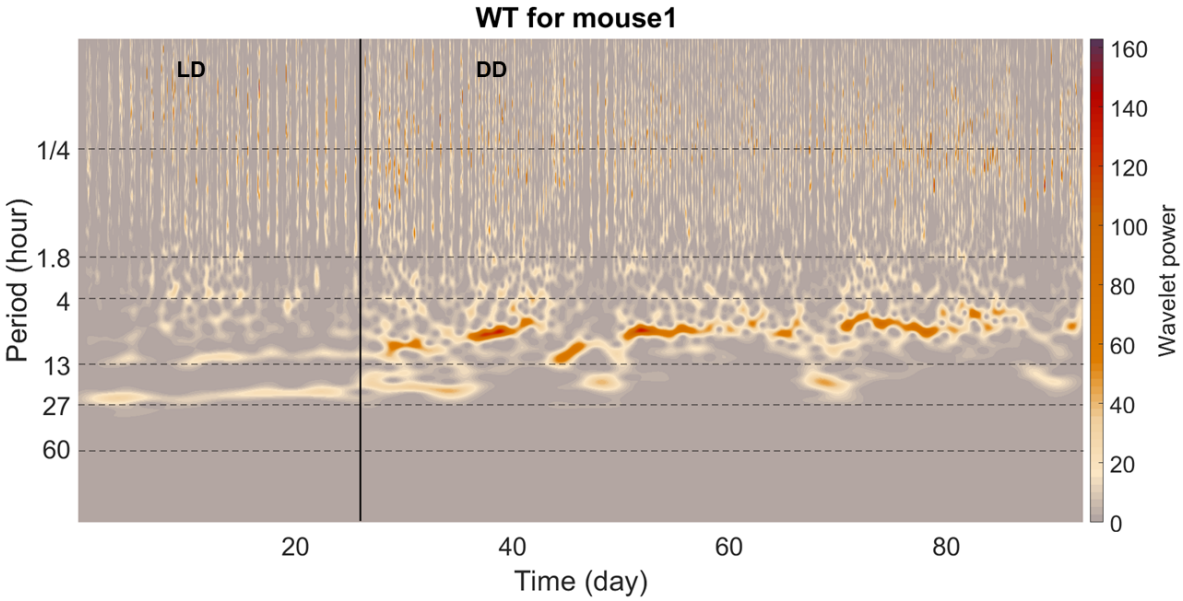

Figure 4.13: Time-frequency representation obtained via the wavelet transform of behavioural data from mouse 1 (NO MA). The vertical black line indicates the start/end of a given condition, where the horizontal dashed black lines indicate the frequency band of interest. The wavelet transform is applied using the lognormal wavelet and a frequency resolution parameter of 1.8.

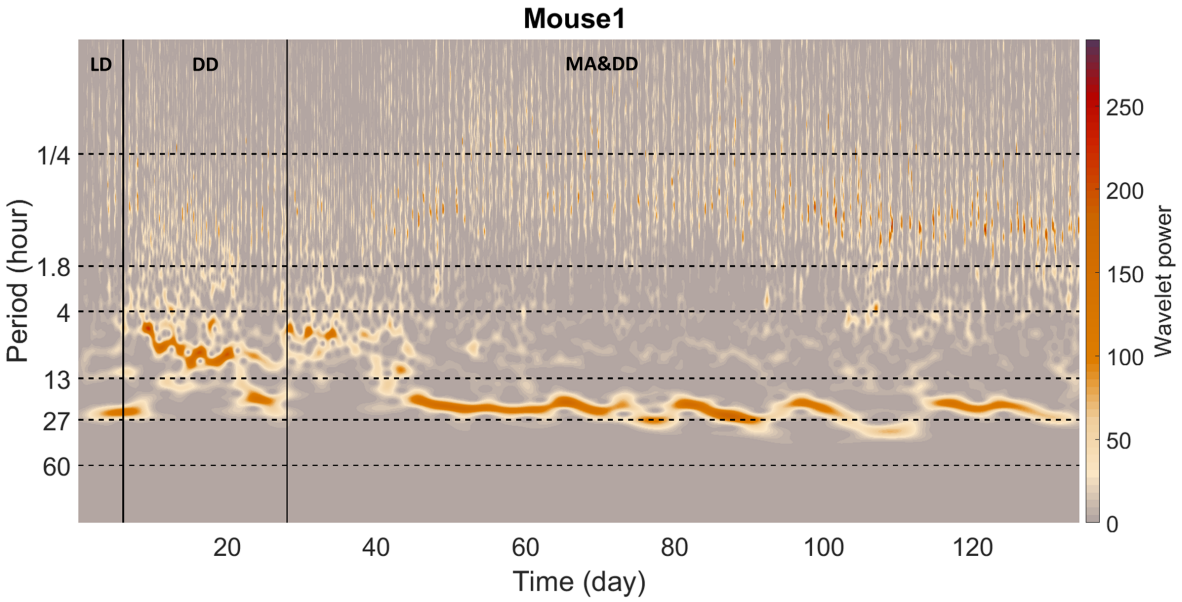

Figure 4.14: Time-frequency representation obtained via the wavelet transform of behavioural data from mouse 1(with MA). The vertical black line indicates the start/end of a given condition, where the horizontal dashed black lines indicate the frequency band of interest. The wavelet transform is applied using the lognormal wavelet and a frequency resolution parameter of 1.8.

It is obvious that in the absence of methamphetamine, the circadian rhythm is attenuated but still recognisable; on the other hand, once methamphetamine is administered, the circadian rhythm becomes quite prominent. In addition, MA has significantly enhanced the emergence of a new rhythm, with a pronounced effect observed around the 40 hour This is a period of time in which the signals are largely unpredictable when there is no exposure to methamphetamine 4.15.

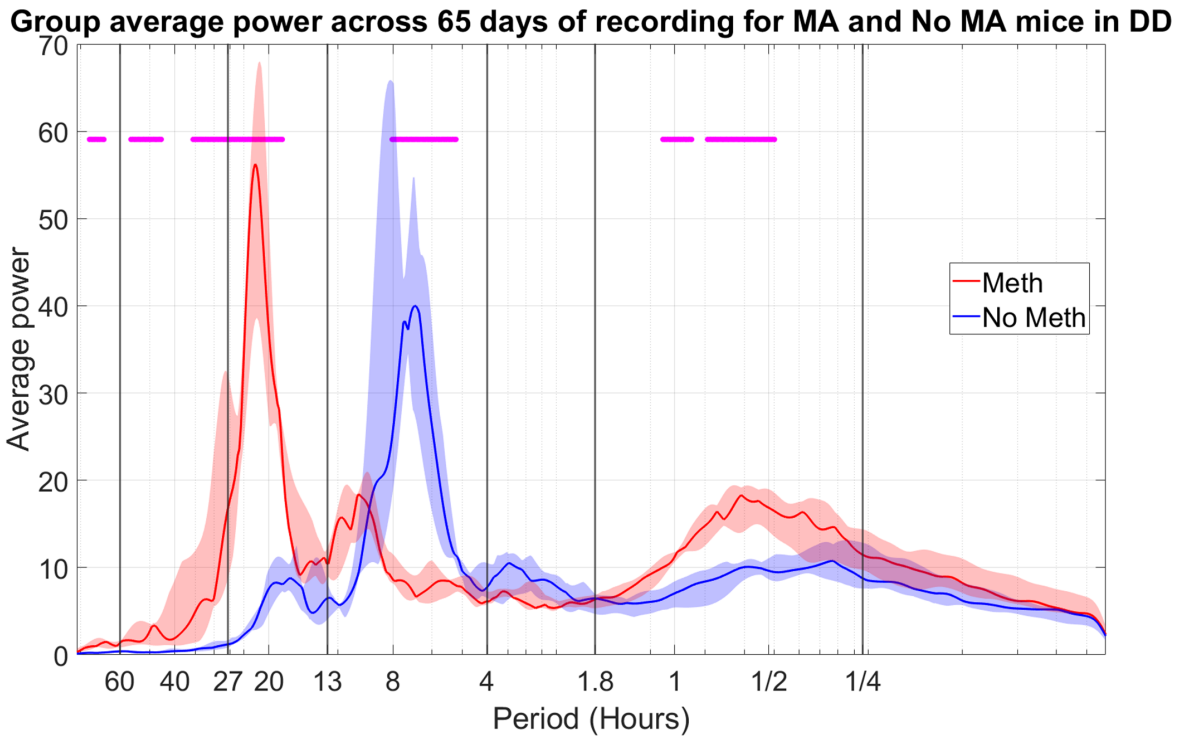

Figure 4.15: Group average power across 65 days of recording for two groups of mice in DD condition. One group have been administered MA, indicated by the red line, and the other group have not received methamphetamine (No MA), shown by the blue line. The pink horizontal lines indicate periods where significant differences were observed between the two groups with (p-value <0.05). while the shading indicated the 25th/ 75th percentile.

4.3.1 High harmonics components

By applying the harmonic finder algorithm to both methamphetamine-treated and untreated mice in constant darkness, the algorithm effectively identifies the oscillatory components that make up the harmonic connections. This approach helps to reveal the underlying rhythmic patterns in both conditions. This analysis encompasses a complete range of frequencies, thoroughly encompassing all relevant oscillatory components, specifically oscillations 1, 2, 3, 4, and 5. This method allows for a clear comparison of the impact of methamphetamine on the harmonic structures in these oscillatory elements.

Figure 4.16 displays a representative MA-treated mouse, while Figure 4.17 illustrates a MA-untreated mouse (additional harmonic results for other mice are presented in the Appendix). The dashed lines in the figure trace the frequency limits for each detected oscillation (labeled as oscillation 1 through 5) in the time-frequency analysis. All potential oscillation pairings have been examined, with the dashed outlines superimposed on the harmonic findings. When the overlap of combinations occurs in regions with higher values, it indicates an increased likelihood of a harmonic connection between the paired oscillations.

For all mice which treated with MA, there appears to be minimal or possibly no discernible evidence indicating harmonic relationships. This implies that in the spectral analysis of the data from the MA-treated group, the expected phase coupling or frequency correlations that typically signify harmonic interactions were either absent or too slight to be reliably identified. Additionally, the analysis shows no evidence of the low-frequency band being in a harmonic relationship with any of the higher-frequency bands.. This implies that the low-frequency oscillations observed in the MA group are likely functioning as an independent mode of activity. The group not exposed to MA exhibits clear signs of harmonic interaction, indicating a likely harmonic connection between approximately 7 and 3.5 hours in most of the mice. This indicates that, within

the spectral analysis of this control group, there is a detectable phase coupling or frequency correlation within these time frames. Such harmonic relations are typically indicative of regular, stable oscillatory activity, which in this case, were maintained or undisturbed in the absence of methamphetamine treatment.

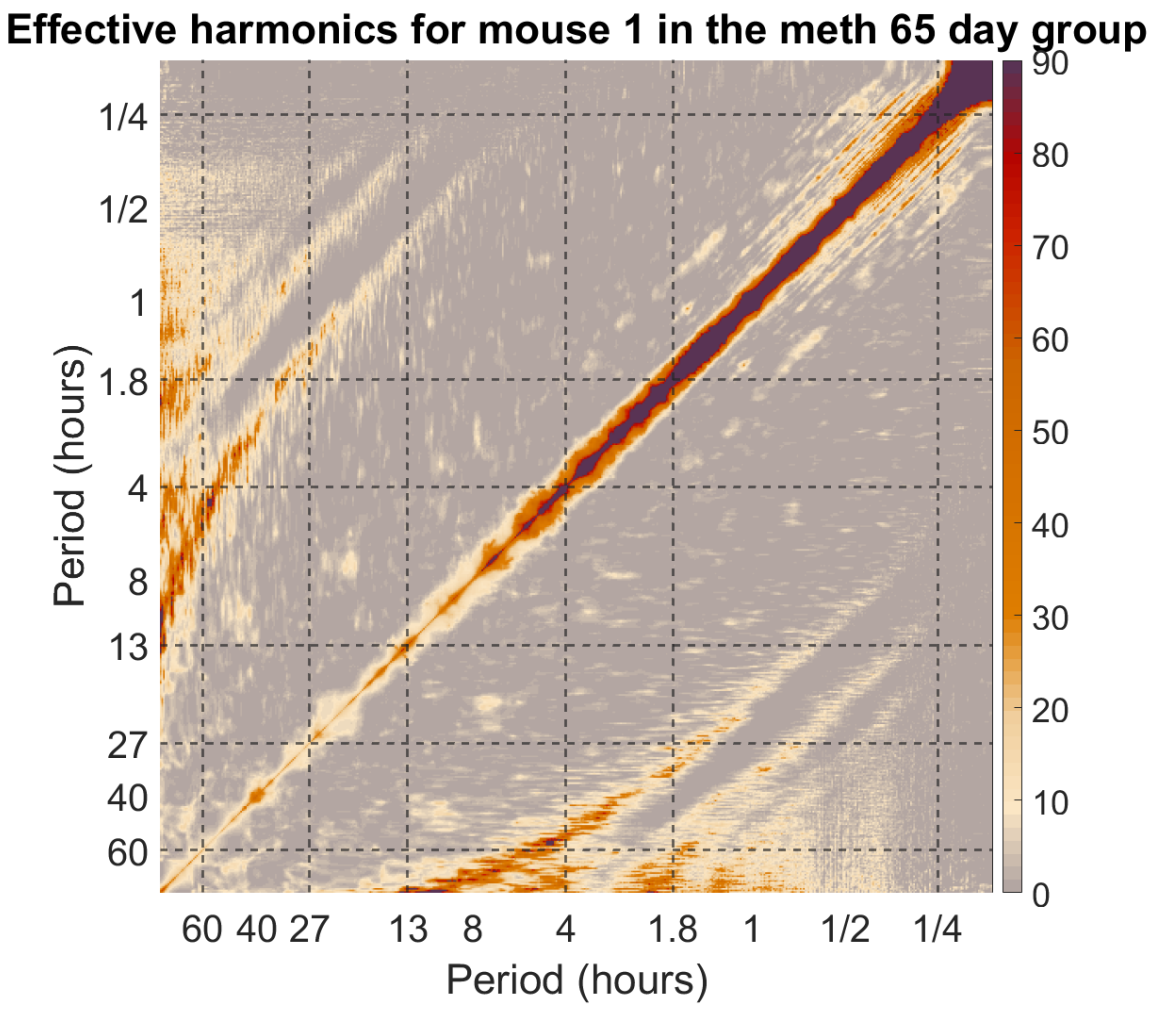

Figure 4.16: The detected harmonics within the behavioral data of mouse 1 under effectiveness of MA. The plot is a frequency-frequency representation showing what oscillations are in harmonic relationships. The image is symmetric over the diagonal; therefore, only half of the figure is considered. All the different combinations of frequencies are investigated, and the dashed lines are plotted over the harmonic results. The color code shows a dimensionless quantity obtained from the actual value, minus the mean of the surrogate distribution, divided by the standard deviation of the surrogate distribution. Negative values correspond to results with values lower than the surrogate mean; therefore, significant results are those above 0. For oscillation combinations which overlap with higher valued areas, the two frequencies are more likely in a harmonic relationship.

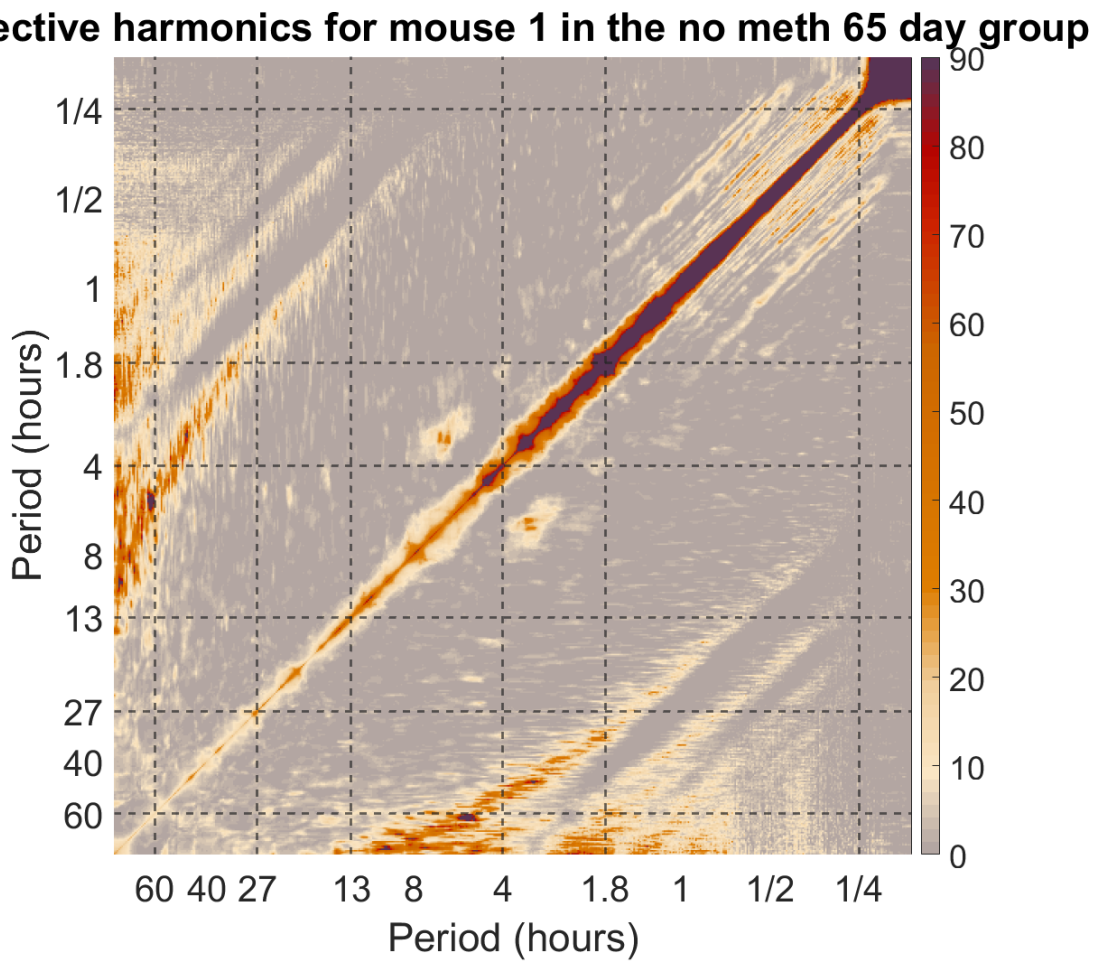

Figure 4.17: The detected harmonics within the behavioral data of mouse 1 with no effectiveness of MA. The plot is a frequency-frequency representation showing what oscillations are in harmonic relationships. The image is symmetric over the diagonal; therefore, only half of the figure is considered. All the different combinations of frequencies are investigated, and the dashed lines are plotted over the harmonic results. The color code shows a dimensionless quantity obtained from the actual value, minus the mean of the surrogate distribution, divided by the standard deviation of the surrogate distribution. Negative values correspond to results with values lower than the surrogate mean; therefore, significant results are those above 0. For oscillation combinations which overlap with higher valued areas, the two frequencies are more likely in a harmonic relationship.

4.3.2 Bispectral analysis and coupling

Bispectral analysis has been employed for both groups of mice, those treated with methamphetamine and those left untreated, under conditions of constant darkness. This analytical approach enables the differentiation between harmonic and non-harmonic components within the biological signals of the mice. To calculate the biamplitude value, which is the modulus of the time-averaged instantaneous wavelet bispectrum, at each point in frequency-frequency space, a process is followed that includes the application of a statistical significance test. This test is used to identify points in the frequency-frequency space where the biamplitude value is deemed "significant." In more detail, at each specific point within this space, the process involves subtracting a critical threshold from the wavelet biamplitude value. This critical threshold is determined at a 95% significance level and is derived from the bispectra of the iterative amplitude adjusted Fourier transform (IAAFT2) surrogates. The wavelet bispectra are calculated using a lognormal wavelet with frequency resolution 1.8. Through this method, significant biamplitude values are effectively isolated and identified across the frequency-frequency space. Therefore, in these bispectra plots, the strictly positive values (i.e., those that are not grey) indicate the regions where the bispectrum value is deemed "significant." This means that the non-grey areas represent points in the bispectra where the calculated values exceed the threshold of significance.

In the study involving mice treated with methamphetamine, as referenced in the figure 4.18, there are indications of a possible interaction between the circadian frequencies, which usually function on an approximate 24-hour cycle, and the high-frequency bands that oscillate at a more rapid pace. This finding is significant as it suggests that methamphetamine treatment may influence or alter the normal coupling patterns in the circadian system of the mice.

In contrast, for the control group of mice that did not receive methamphetamine 4.19, a different pattern of coupling is observed. The coupling in this group appears to

occur between the 7-hour mode, which is a shorter cycle compared to the circadian rhythm, and the high-frequency oscillations. This contrast in coupling patterns between the methamphetamine-treated group and the control group highlights the potential impact of methamphetamine on the synchronization and interaction of different frequency bands within the circadian system.

The bispectral analysis presented utilizes a time-averaged method to emphasize potential couplings within the data. To delve deeper into the characteristics of these couplings, such as their directionality, strength, and duration, dynamic Bayesian inference (DBI) methods were employed. For each individual mouse, under both conditions—with and without MA, DBI was applied to every possible pairing of oscillations (labeled as oscillation 1, 2, 3,4 and 5), which were identified from the time-frequency data through ridge extraction. Through DBI, the coupling strength between pairs of oscillations was quantified over time, and this was done for both possible directions of coupling. In alignment with the bispectral analysis, for mice administered with MA, the coupling from circadian oscillation to high frequency oscillation emerged as the most substantial and enduring over time. Conversely, in the absence of MA, the coupling from ultradian oscillation to high frequency oscillation proved to be the most consistent over time, thus supporting the findings of the bispectral analysis. Although at a cursory look the coupling from oscillation 2 to oscillation 5 appears to be the strongest, it is important to note that this prominence is observed only for a relatively brief period within the overall time frame of the analysis.

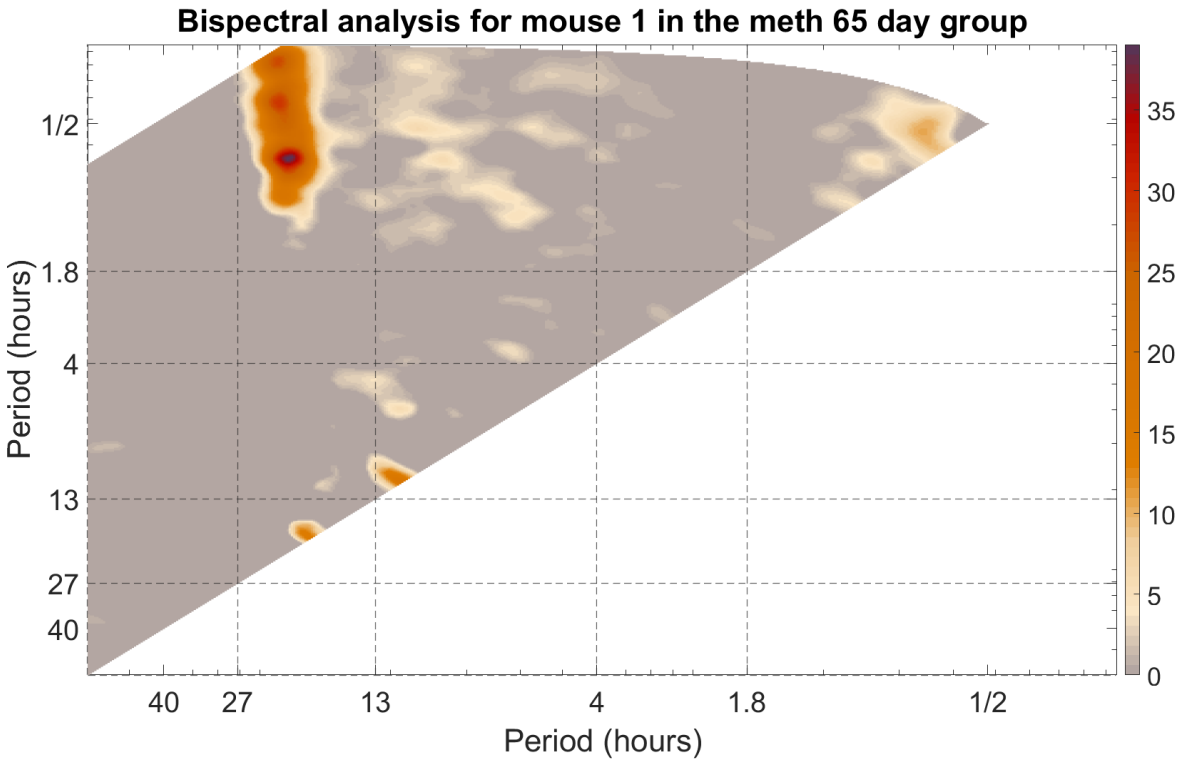

Figure 4.18: Wavelet bispectra of behavioural data from mouse 1 with MA, which illustrate the wavelet biamplitude associated with each point in frequency-frequency space. This representation is achieved after subtracting the 95% significance critical threshold, as determined by a surrogate test. This test involves 19 numerically generated IAAFT2 surrogate signals. The calculation of the wavelet bispectra is performed using a lognormal wavelet, characterized by a frequency resolution of 1.8.

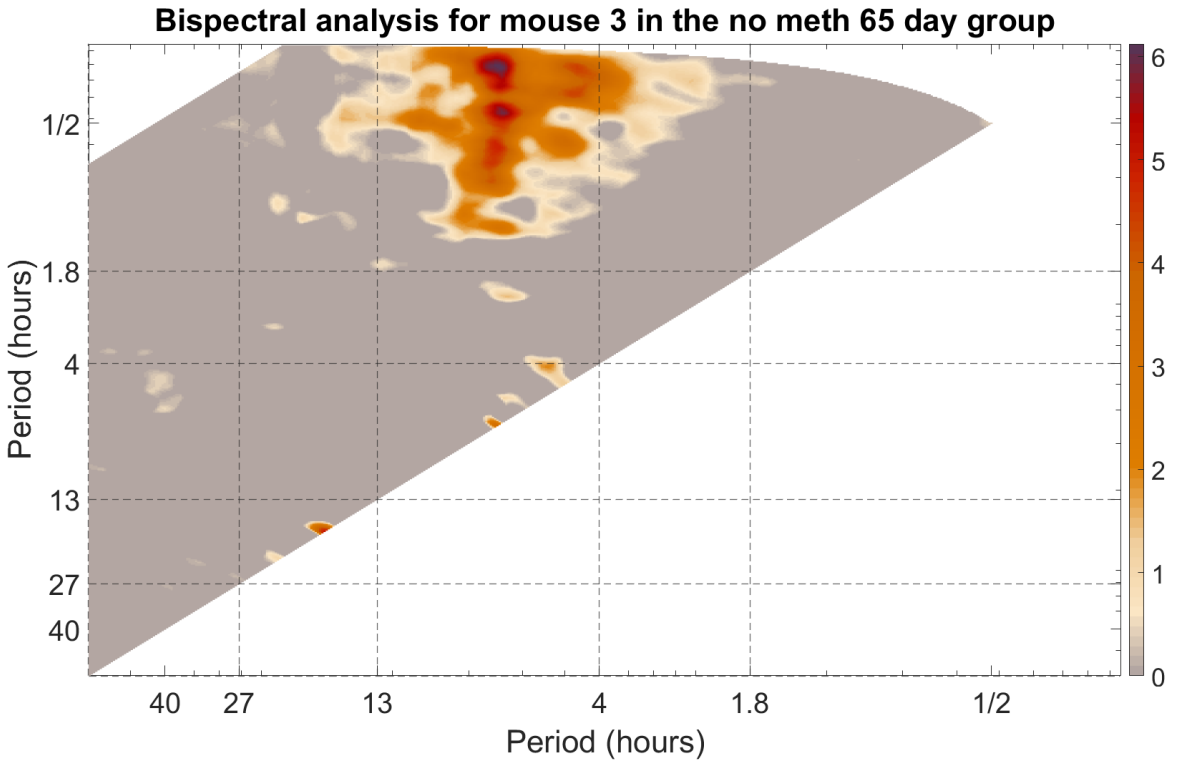

Figure 4.19: Wavelet bispectra of behavioural data from mouse 3 with no MA, which illustrate the wavelet biamplitude associated with each point in frequency-frequency space. This representation is achieved after subtracting the 95% significance critical threshold, as determined by a surrogate test. This test involves 19 numerically generated IAAFT2 surrogate signals. The calculation of the wavelet bispectra is performed using a lognormal wavelet, characterized by a frequency resolution of 1.8.

a)

From \ To	osc.2	osc.3	osc.4	osc.5
osc. 2	0	25	5	50
osc.3	15	0	5	25
osc.4	5	5	0	10
osc.5	5	5	0	0

c)

From \ To	osc. 2	osc. 3	osc. 4	osc. 5
osc. 2	0	7.5	0	2.5
osc. 3	12.5	0	30	50
osc. 4	5	30	0	35
osc. 5	2.5	2.5	2.5	0

b)

From \ To	osc.2	osc.3	osc.4	osc.5
osc. 2	0	17.6	25.1	161
osc.3	11.5	0	25.2	105
osc.4	12.4	11.1	0	79.8
osc.5	5.84	8.34	17.7	0

d)

From \ To	osc. 2	osc. 3	osc. 4	osc. 5
osc. 2	0	12.9	23.2	174
osc. 3	9.14	0	29.1	153
osc. 4	11.7	14.3	0	156
osc. 5	7.28	62	18.3	0

Figure 4.20: (a,c) Group median values for the percentage of time the coupling results between oscillations within murine behavioral data from all mice with MA (a) and without MA in (c) is above the surrogate threshold, as a heatmap (color scale from 0 to 100). (b,d) Group median values for coupling strength ($\times 10^{-4}$) within murine behavioral data from all mice with MA (b) and without MA in (d) when the coupling results are above the surrogate threshold, as a heatmap (color scale from 0 to 161).

5. Model

Coupled phase oscillators were employed to represent the oscillatory modes and their interactions as observed in the behavioral data. This approach allows for the creation of a baseline with known parameters, which serves as a reference point for evaluating and validating the outcomes of the experimental investigation. By establishing this ground truth, it can better understand the accuracy and reliability of experimental findings, as well as refine modeling techniques for future studies [134].

For the *Per1/2/3* mice model, whether subjected to methamphetamine or not, the structure included three principal oscillators: a high-frequency one, another oscillating around seven hours, and a third oscillator approximating a circadian rhythm. To align with the real data, the model used a 1-minute time step over a 65-day time series. The coupling parameters were selected to accurately represent the observed dynamics. The equations defining the coupled phases for the *Per1/2/3* KO DD mice are as follows [134].

$$\begin{aligned} \dot{\phi_1} &= \omega_1 \\ \dot{\phi_2} &= \omega_2, \\ \dot{\phi_3} &= \omega_3 + E_1 \cos\left(\phi_1 + \pi/2.5\right) + E_2 \cos\left(\phi_2 + \pi/2.5\right), \end{aligned} \tag{5.1}$$

Where, ϕ_i are the phases of each oscillator, which are subsequently added together to produce a time series,

$$X(t) = A_1 \cos(\phi_1(t)) + A_2 \cos(\phi_2(t)) + A_3 \cos(\phi_3(t)). \tag{5.2}$$

The amplitudes, A, were selected to be the best recreation of the observed power spectra. The natural frequencies changed over time to allow us to represent the time-variability witnessed in the experimental results,

$$\omega_i(t) = \omega_{i0} + A_i S(\omega_{ivar} t), \tag{5.3}$$

where ω_{i0} is the natural frequency, S represents a square wave, A_i is the amplitude of the frequency variation, and ω_{ivar} represents the frequency of the square wave modulation applied to the natural frequency $\omega_i(t)$.

For the wild-type mice, there seemed to be several coupled modes present, with the circadian clearly the most dominant. As such, multiple phase oscillators were used [134]

$$\begin{aligned}
\dot{\phi_1} &= \omega_1 + E_1 \cos\left(\phi_6 + \pi/2.5\right), \\
\dot{\phi_2} &= \omega_2, \\
\dot{\phi_3} &= \omega_3 + E_2 \cos\left(\phi_2 + \pi/2.5\right), \\
\dot{\phi_4} &= \omega_4 + E_3 \cos\left(\phi_3 + \pi/2.5\right), \\
\dot{\phi_5} &= \omega_5 + E_4 \cos\left(\phi_4 + \pi/2.5\right), \\
\dot{\phi_6} &= \omega_6 + E_5 \cos\left(\phi_4 + \pi/2.5\right) + E_6 \cos\left(\phi_1 + \pi/2.5\right),
\end{aligned} \tag{5.4}$$

The parameters for each of these configurations are as follows

Parameters	**Wild-type**	**DD**	**MDD**
ω_{10} (Hz)	24	20	24
ω_{20} (Hz)	7.2	7.5	8
ω_{30} (Hz)	6	0.5	0.5
ω_{40} (Hz)	3	NA	NA
ω_{50} (Hz)	1.25	NA	NA
ω_{60} (Hz)	0.75	NA	NA
ϵ_1	0.1	0.05	0.2
ϵ_2	0.1	0.2	0.05
ϵ_3	0.1	NA	NA
ϵ_4	0.1	NA	NA
ϵ_5	0.1	NA	NA
ϵ_6	0.1	NA	NA
A_1	1.5	0.8	0.85
A_2	0.25	0.3	0.3
A_3	0.25	0.85	0.8
A_4	0.5	NA	NA
A_5	0.65	NA	NA
A_6	0.3	NA	NA

Parameters	**Wild-type**	**DD**	**MDD**
ω_{1var} (Hz)	0.0000025	0.00025	0.00025
ω_{2var} (Hz)	0.0005	0.0003	0.0003
ω_{3var} (Hz)	0.001	0.1	0.1
ω_{4var} (Hz)	0.0025	NA	NA
ω_{5var} (Hz)	0.05	NA	NA
ω_{6var} (Hz)	0.015	NA	NA
Amp_1	0.000000000001	0.0005	0.0005
Amp_2	0.00001	0.0015	0.0015
Amp_3	0.0005	0.125	0.125
Amp_4	0.000001	NA	NA
Amp_5	0.0001	NA	NA
Amp_6	15	NA	NA

5.1 Wild-type model

The model for wild-type mice demonstrated a clear and stable circadian rhythm with an average frequency of approximately 24 hours. This indicates that the canonical circadian clock, regulated by the *Per1/2/3*, is functioning effectively in these mice. The time-frequency representation for wild-type mice, figure 5.1(B), generated through wavelet transforms, which shows a consistent frequency pattern over time, with minimal fluctuations. This stability suggests that the circadian clock is resilient to external perturbations, maintaining a regular rhythm. The time-averaged power analysis showed a single sharp peak centered around 24 hours, reflecting the robustness of the circadian oscillator in wild-type mice, figure 5.1(C). The ridge extraction clearly capture the strong, consistent 24-hour period seen in the wavelet power spectrum. The ridge at 24 hours is likely the most prominent and stable feature across the entire 30-day period

[134], figure 5.1(D).

Harmonic analysis revealed significant evidence for harmonics centered on the circadian oscillation in wild-type mice. This means that the observed peaks in activity were not independent modes but rather related to the primary circadian rhythm. The presence of harmonics indicates that the oscillatory behavior is tightly regulated and exhibits predictable patterns, which is characteristic of a well-functioning circadian system, figure 5.1(E). In terms of coupling, the bispectral analysis shows some weak phase couplings, primarily between circadian and higher frequency oscillations, although no strong patterns of coupling were found due to the short recording window for these mice, figure 5.1(F).

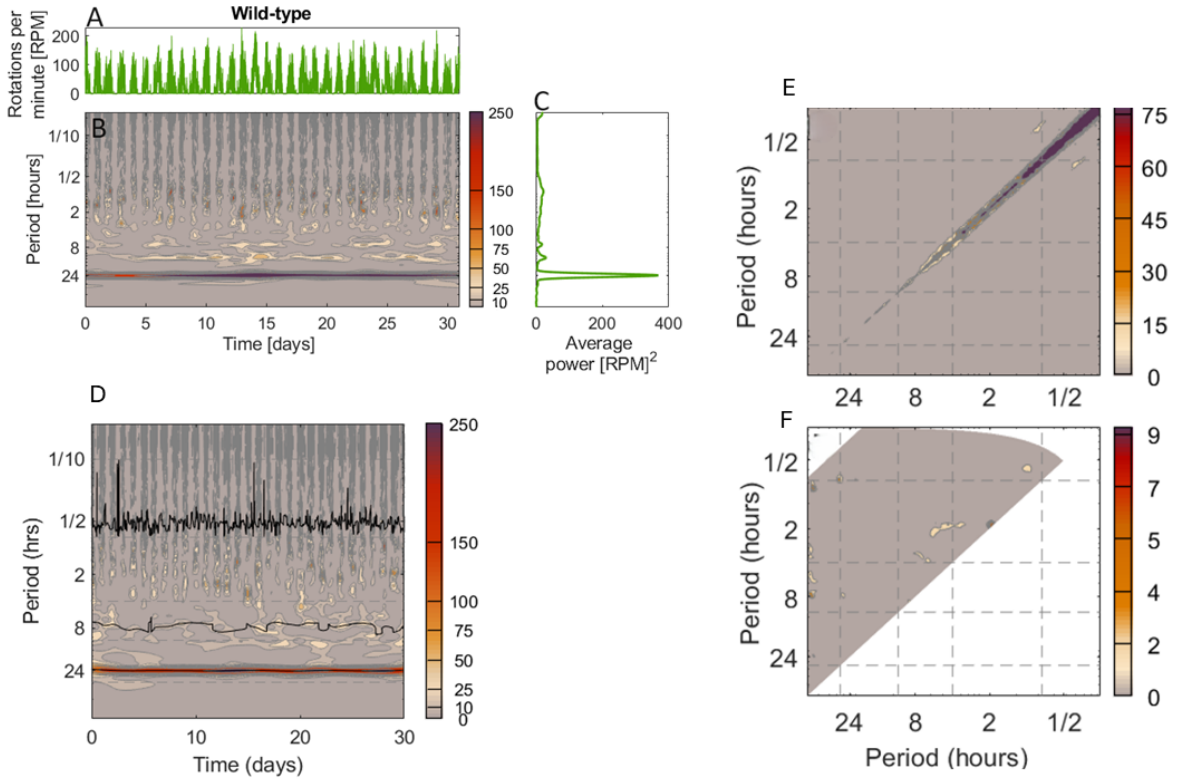

Figure 5.1: Multiscale oscillatory activity in wild-type. (A) Time-series of wheel rotations per minute. (B) Time/frequency representations. (C) Time-averaged power. (E) Harmonic analysis demonstrates pronounced harmonics, arising from circadian oscillations. The colourful peaks indicate the detection of these harmonics. The diagonal line, representing the comparison of the same oscillation to itself, shows high mutual information, while off-diagonal peaks signify the presence of harmonics, such as those observed between 24 and 12 hours. (F) Bispectral analysis highlights couplings between oscillatory modes at different frequencies. Similar to harmonics, contoured peaks indicate regions of significant coupling between these modes.

5.2 *Per1/2/3* knockout DD model

The Per1/2/3 KO mice show disrupted circadian rhythms, and their activity becomes

more fragmented, with multiple lower-frequency oscillations (e.g., around 7 hours). The absence of a strong 24-hour rhythm is evident. Wavelet analyses indicate significantly different power distributions, with reduced circadian power and enhanced ultradian rhythms, figure5.2(B). The ridge extraction shows a weakened or nearly absent 24-hour ridge, indicating the disruption of the dominant circadian rhythm. The ridge for the 24-hour period may be fragmented, signifying irregular or non-continuous circadian activity. It focuses on an 8-hour period, where a more prominent ridge is visible, figure 5.2(D).

In *Per1/2/3* knockout mice, the harmonic structure is notably altered. While some harmonics exist (particularly between oscillations at 7 and 3.5 hours), the dominant circadian-driven harmonics (like those at 12 and 8 hours) are absent or significantly reduced. This indicates that the loss of Per genes disrupts the hierarchical organization of oscillations, figure 5.2(E). In terms of coupling, Bispectral analysis of KO mice reveals strong coupling between a 7-hour oscillator and high-frequency components. The circadian to high-frequency coupling is weak, indicating a shift in the primary driver of activity from circadian to ultradian rhythms [134],figure 5.2(F).

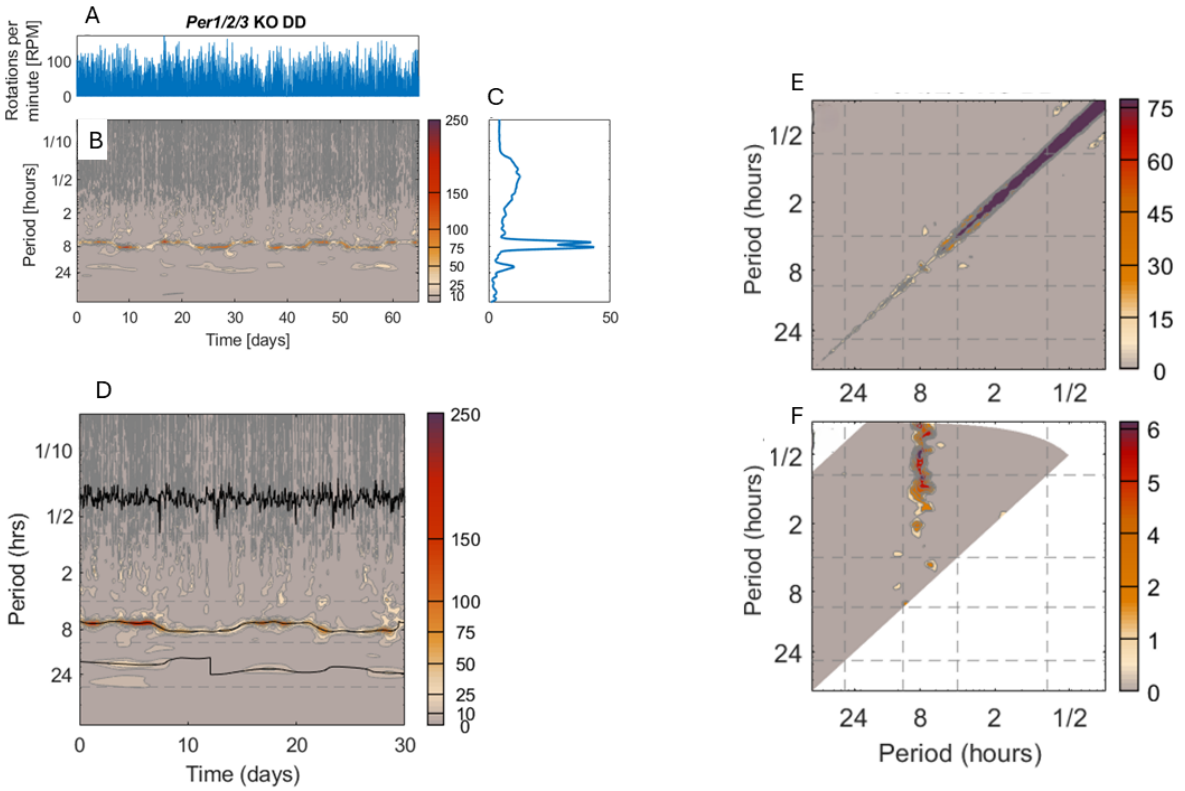

Figure 5.2: Multiscale oscillatory activity in *Per1/2/3* KO DD mice. (A) Time-series of wheel rotations per minute. (B) Time/frequency representations. (C) Time-averaged power. (E) Harmonic analysis demonstrates pronounced harmonics, arising from circadian oscillations. The colourful peaks indicate the detection of these harmonics. The diagonal line, representing the comparison of the same oscillation to itself, shows high mutual information, while off-diagonal peaks signify the presence of harmonics, such as those observed between 24 and 12 hours. (F) Bispectral analysis highlights couplings between oscillatory modes at different frequencies. Similar to harmonics, contoured peaks indicate regions of significant coupling between these modes.

5.3 *Per1/2/3* Knockout DD with MA model

The Per1/2/3 KO mice exposed to methamphetamine exhibit further disruptions in

their oscillatory behavior. High-frequency oscillations become more pronounced, and coupling between these high frequencies and ultradian rhythms is more dominant. Power in the high-frequency range increases significantly after methamphetamine exposure, figure 5.3(B). Time-averaged power data shows a distinct shift in activity patterns compared to both the KO DD and wild type groups. Ridge extraction captures chaotic high-frequency oscillations, with both circadian and ultradian rhythms disrupted, and no clear, continuous ridges for either rhythm [134], figure 5.3(D).

In the methamphetamine-exposed knockout mice, there is a lack of consistent harmonic relationships between oscillatory modes. The methamphetamine disrupts the normally harmonic nature of oscillations, particularly between the circadian and ultradian frequencies. No clear harmonic structure, such as those seen in wild type or unexposed knockout mice, is observed, figure 5.3(E). In terms of coupling, Bispectral analysis reveals strong phase coupling between MASCO and high-frequency components. This shows that methamphetamine amplifies specific coupling dynamics that are absent in the unexposed KO mice, figure 5.3(F).

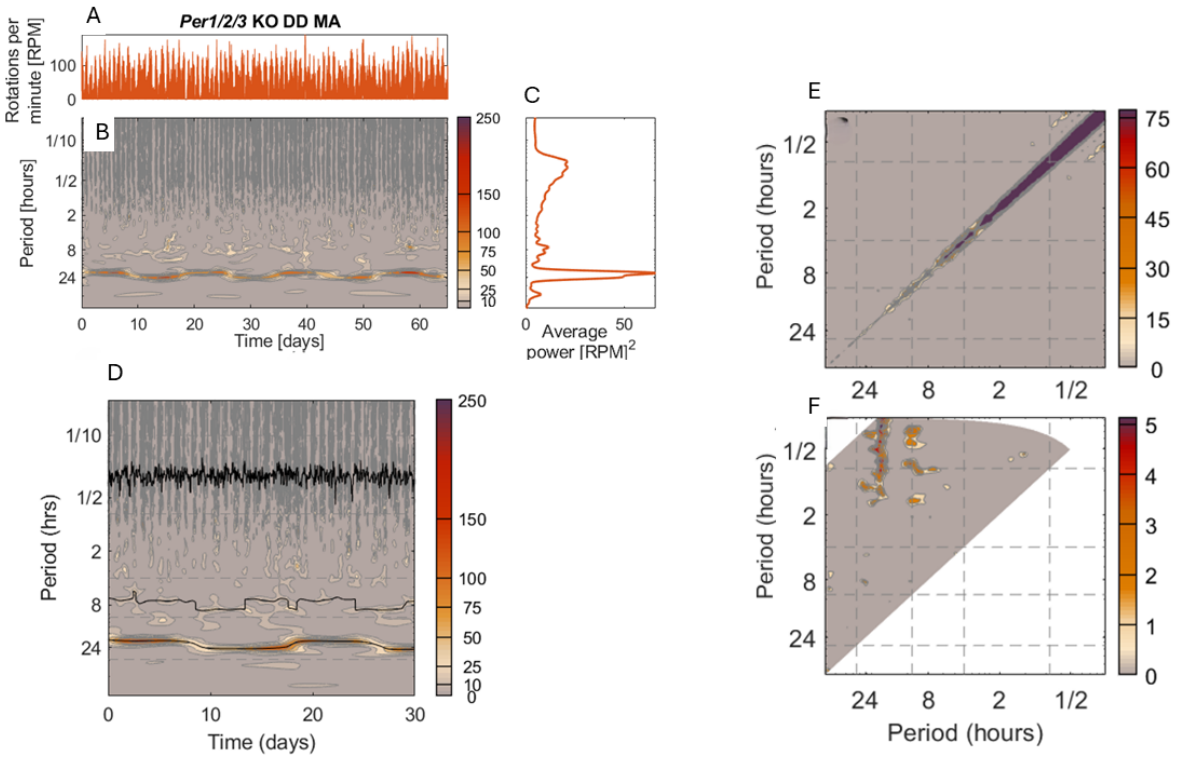

Figure 5.3: Multiscale oscillatory activity in *Per1/2/3* KO DD MA mice. (A) Time-series of wheel rotations per minute. (B) Time/frequency representations. (C) Time-averaged power. (E) Harmonic analysis demonstrates pronounced harmonics, arising from circadian oscillations. The colourful peaks indicate the detection of these harmonics. The diagonal line, representing the comparison of the same oscillation to itself, shows high mutual information, while off-diagonal peaks signify the presence of harmonics, such as those observed between 24 and 12 hours. (F) Bispectral analysis highlights couplings between oscillatory modes at different frequencies. Similar to harmonics, contoured peaks indicate regions of significant coupling between these modes.

6. Discussion and summary

In this chapter, we delve into a detailed examination and interpretation of the experimental outcomes as outlined in Chapter 4. Our objective is to offer a coherent and plausible explanation for the results obtained from our data collection and subsequent analysis. To this end, we will provide a concise summary of these findings, setting the stage for a thorough discussion. This will include an assessment of the significance of the results, their alignment with existing literature, and the potential implications for the field.

We explore the outcomes derived from the application of wavelet transform to our dataset. Notably, the *per1/2/3* triple knockout mice, when exposed to a variety of conditions, exhibited a consistent response following the administration of methamphetamine while the rhythms in wild-type mice are more stable and consistent. This response was observed uniformly across the cohort of mice, as evidenced by the time-frequency representations that were generated. Each mouse being evaluated using the same wavelet transform technique, the results were remarkably similar, indicating a robust effect of the drug on the circadian regulatory mechanisms of these genetically modified organisms. This finding prompts a deeper inquiry into the influence of methamphetamine on the circadian system, particularly in the absence of the per1/2/3 genes, which are traditionally associated with the regulation of these rhythms. The uniformity in response across the experimental subjects underscores the potential utility of wavelet transform as a reliable method for capturing drug effects in chronobiological studies.

6.1 Does circadian rhythm persist when clock genes are knocked out?

We delve into the intriguing findings from the wavelet transform analysis of the behavioral data. Remarkably, the analysis suggests that the 24-hour circadian rhythm persists even in the absence of clock genes. This conclusion comes from the meticulous examination of the data through wavelet transform techniques. The time-frequency representation of Mouse 4 and mouse 1 behavioral data, as depicted in Figure 4.5 and 4.6, allows for the clear observation of the circadian rhythm under light-dark (LD) conditions. O'Neill et al. [135] in their study about circadian rhythms in eukaryotes, particularly focusing on the unicellular green alga Ostreococcus tauri, involved examining both transcriptional and non-transcriptional mechanisms in circadian timekeeping. They have found that circadian cycles in eukaryotes can persist under constant darkness even when transcription is inhibited, indicating that the mechanisms underlying circadian clocks are resilient to disruptions in cellular transcription and cytosolic translation. This finding underscores the robust and adaptable nature of the circadian system, capable of maintaining its rhythmic periodicity even in scenarios where key genetic elements, typically involved in rhythm generation, are impaired or inactive. This research highlights the intricate and resilient design of circadian systems, capable of sustaining essential biological rhythms against a backdrop of genetic alterations. However, circadian rhythms can persist in *Per1/2/3* knockout mice under constant darkness, but these rhythms may be less stable and exhibit different characteristics compared to those in wild-type mice.

6.2 Does methamphetamine administration cause a disruption in the rhythm of the mice?

The tests conducted on the impact of methamphetamine on the circadian rhythms of mice offered valuable new insights into how this substance can affect biological rhythms.. Methamphetamine, a potent psychostimulant, has been shown to significantly alter circadian patterns, as evident in the altered activity and sleep cycles observed in the test subjects. Upon detailed examination, the impact of methamphetamine administration on the rhythmicity in mice is evident, particularly in the conditions of methamphetamine under dark-dark (MA & DD(1)) and methamphetamine under light-light (MA & LL) cycles. The figure 4.8 effectively illustrates the total power within the frequency band that spans from 60 to 27 hours. Notably, there is a discernible deceleration of the rhythm post the initiation of methamphetamine treatment, highlighting the drug's influence in altering the circadian patterns. This observation highlights the profound impact of methamphetamine on the subjects' internal biological clocks, as evidenced by the emergence of a clearly enhanced new rhythm.

Moreover, the effects of methamphetamine on the circadian rhythms of mice, it's notable that administration of the drug appeared to restore the 24-hour rhythm in the MA & DD conditions. Following methamphetamine administration, there was a significant increase in the total power within the 27 - 13 hour frequency band, as shown in figure 4.9. This suggests that methamphetamine not only alters the circadian rhythm but can also intensify specific frequency bands within the rhythm. These changes underline the profound impact that substances like methamphetamine can have on the biological clocks of organisms, potentially altering their natural rhythms in significant ways. Logan et al. [136] have mentioned in their study that exposure to drugs of abuse can alter circadian rhythms and lead to the exacerbation or progression of certain symptoms related to brain disorders . For example, studies have shown that chronic

exposure to drugs such as cocaine, methamphetamine, and alcohol can disrupt circadian rhythms and lead to sleep disturbances and other symptoms.

Ogeil et al. [137] has been demonstrated that methamphetamine significantly disrupts circadian rhythms. Research suggests that amphetamine-type stimulants, particularly MA, influence various circadian-regulated functions, including body temperature, appetite, mood, and alertness. These substances have been found to affect not only the direct outputs of the circadian clock but also the fundamental mechanisms that control its operation. Furthermore, methamphetamine is known to directly disrupt the circadian clock by altering the regulation of core clock genes, crucial for the establishment and preservation of circadian rhythmicity. This evidence underscores the profound and multifaceted impact of methamphetamine on the body's natural time-keeping systems. Brown et al. [23] also has studied of MASCO in rodents. It was observed that when rodents are subjected to chronic administration of low-dose methamphetamine, a distinct behavioral rhythm associated with MASCO emerges. Intriguingly, both the food-entrainable oscillator (FEO) and MASCO operate independently of the canonical circadian genes that are typically involved in timekeeping. This independence was further elucidated through experiments measuring the phases of luminescence rhythms in ex vivo tissues, which demonstrated that both FEO and MASCO could function effectively in a system where the SCN acts as the conductor, and the peripheral oscillators as the musicians. These findings suggest that the SCN, while a primary circadian pacemaker, is not the sole entity capable of orchestrating these biological rhythms. This insight points to a more complex and versatile circadian system than previously understood, with multiple potential pacemakers like the FEO and MASCO contributing to the overall temporal regulation in organisms.

Applying the harmonic finder algorithm to both methamphetamine-treated and untreated mice in constant darkness has yielded insightful results regarding oscillatory behavior. In the methamphetamine-treated group, figure 4.16, the algorithm did not

detect significant harmonic relationships, suggesting an absence or minimal presence of expected phase coupling or frequency correlations. This lack of harmonic interaction, especially in the low-frequency band, implies that these oscillations might be functioning independently in the MA-treated mice. Conversely, the control group, which was not exposed to methamphetamine, figure 4.17, showed substantial signs of harmonic interaction, particularly between the 7-hour and 3.5-hour frequencies. Morris et al. [138] has studied about the presence of noncanonical circadian pacemakers in mice, the study used a harmonic finder algorithm to detect high harmonics in time-varying systems and found that the 8-hour and 4-hour rhythms, as well as the 8-hour and 20-minute rhythms, were in a harmonic relationship. This observation in the spectral analysis indicates a detectable phase coupling or frequency correlation, suggesting a more structured and interconnected oscillatory activity in the untreated group. The observed results underscore methamphetamine's capacity to disrupt the harmonic and rhythmic dynamics within biological systems. This disruption manifests in the alteration of typical frequency interactions and phase couplings, indicating that methamphetamine can significantly affect the intricate balance of oscillatory activities that are essential for normal physiological functioning. This insight sheds light on the broader implications of methamphetamine use, particularly in terms of its potential to disturb the natural rhythmic patterns inherent in biological systems.

Employing bispectral analysis and DBI, offer profound insights into the impact of methamphetamine on the circadian system of mice. The time-averaged bispectral analysis initially highlighted potential couplings within the data, but it was the application of DBI that brought depth to our understanding, revealing the nuances of these couplings in terms of their directionality, strength, and duration. In MA-treated mice, a significant coupling between specific oscillations was observed, but notably, this coupling was prominent only for a brief period. This transient nature of the coupling suggests that MA might induce temporary but significant alterations in the oscillatory patterns of the circadian system. In contrast, the control group displayed a different,

more consistent coupling pattern, indicating a probable harmonic connection in the absence of MA. Our analysis reveals a robust and stable coupling from longer rhythms (hours) to shorter ones (minutes). In mammalian cell biology, transcription typically occurs over a timescale of approximately 10 minutes, as noted by Shamir et al. [139]. This suggests that Oscillation 4 might be linked to essential cellular processes governed by the metabolic cycle. Additionally, Yamazaki et al. [140] reported 14-minute neural activity rhythms within and outside the hamster's suprachiasmatic nucleus (SCN) under constant darkness. This might indicate a broader biological significance of these shorter rhythmic patterns, possibly extending beyond the scope of circadian rhythms.

6.3 Does the system retain a memory of past disturbances under varying conditions?

Upon applying wavelet transform analysis to behavioral data affected by methamphetamine figure 4.1, and then observing the system post-removal of the drug's effect, it became evident that the system exhibits a form of memory as it obviously clear as it illustrated in figure 4.8. The analysis revealed a tendency for the rhythmic patterns to attempt a return to their pre-methamphetamine state. This observation suggests that despite the significant impact of methamphetamine on circadian rhythms, the underlying biological system retains a memory of its original state, striving to re-establish the prior rhythm once the influence of the drug is diminished. This finding highlights the resilience and adaptability of the circadian system, even in the face of substantial external disturbances like drug administration. The research conducted by Mahoney et al. [141] suggests that the effects of methamphetamine can vary significantly based on dosage. Specifically, they found that administering methamphetamine in low doses acutely can enhance certain cognitive functions. In

individuals who are dependent on methamphetamine and show baseline cognitive impairments, such as reduced attention, slowed information processing speed, and diminished working memory, a low dose of the drug appeared to improve these cognitive parameters. This finding introduces a nuanced perspective on the impact of methamphetamine, indicating that its effects are not uniformly detrimental and can be dose-dependent.

7. Concluding remarks

7.1 Summary

To summarise, the following constitute the primary components of this thesis:

- The background of biological rhythms, encompassing circadian, ultradian, and infradian rhythms, has been reviewed.
- The techniques for analyzing the behavioral data are explored and discussed.
- Nonlinear dynamical systems and the techniques for investigating them using time series data are introduced.
- Behavioral data from various mice subjected to different conditions, including those involving the administration of MA, are examined and discussed.

The primary objective of this thesis is to explore the persistence of behavioral rhythms in biological systems when the standard circadian timekeeping mechanisms are inactivated and administrate the MA to the mice and see the effect of it to them under different conditions. Modeling such systems presents significant challenges, as oversimplifications can obscure their most fascinating features. Within these systems, oscillators display varying frequencies, phases, amplitudes, and interactive behaviors. To decipher these complex dynamics, the study employs sophisticated numerical techniques. The gathered time series data, representing behavioral observations over

time, are subjected to specialized analytical methods. These methods are specifically designed for time-resolved analysis of multi-oscillatory dynamics, thereby capturing the detailed and dynamic nature of biological rhythms and their interactions. The analytical algorithms applied to biological systems take into account both the phases and amplitudes of signals, rather than just amplitudes which are more prone to noise and distortions. Crucially, these algorithms operate without presuming constancy in phases or frequencies. Such a methodology enables a more precise and detailed comprehension of the dynamic, often variable characteristics of biological oscillators. It effectively captures the inherent real-time variability and complexity present in living systems.

7.2 Original contributions

The following summarizes the original contributions of this study:

- Time frequency representation of the data indicated the rhythms across various conditions which is revealed that the 24-hour circadian rhythm is maintained even without the presence of the clock gene.
- The finding that administering MA to the mice restored the 24 rhythm for MADD(1).
- MA caused an increase in total power compared to the other conditions.
- In the final DD condition, circadian activity appears to persist even in the absence of MA exposure.
- The harmonic analysis revealed that, in all mice not exposed to MA, there is a harmonic relationship between 7-8 hours and 3.5-4 hours cycles.

- The characteristic frequency of the circadian rhythm in wild-type mice is almost constant in time, contrary to the characteristic frequency of the circadian rhythm restored by MA, which is highly variable.

- Bispectral analysis and DBI revealed a strong coupling between circadian oscillation and the high-frequency ultradian rhythms in behavioral data of mice exposed to MA. In contrast, mice not exposed to MA showed a strong coupling between ultradian oscillation and the high-frequency band.

7.3 Future work

This project is anticipated to gain from the following upcoming endeavors:

- **Long-term behavioral analysis:** Extending the research to look at long-term behavioral alterations in mice. Examining whether and how the effects of methamphetamine exposure evolve or endure over time, potentially beyond 140 days.

- **Recovery and reversibility studies:** Study how the mice recover and if the effects of the drug can be reversed after stopping exposure. This might include gradually stopping methamphetamine use and watching how the mouse's body functions, and how its behavior changes back.

- **Behavioral conditioning and cognitive assessments:** Explore the cognitive and behavioral conditioning aspects, assessing learning, memory, and adaptation skills in mice-models over time.

Appendix

A. Data arrangements and approvals

In following agreement to use the data as well as ethics approval is provided as background of this work.

Shin Yamazaki, Ph.D.
Professor, Department of Neuroscience
Director, Neuroscience Microscopy Facility
Director, O'Donnell Brain Institute NeuroMicroscopy Core

UT Southwestern
Medical Center

Peter O'Donnell Jr. Brain Institute
Department of Neuroscience

January 3, 2024

RE: collaboration agreement

In accordance with our prior correspondence via email, I hereby confirm my consent for the sharing of data collected by my group with Mansour Alanazi, under Aneta Stefanovska's supervision. It is understood that the outcomes derived from this collaboration are presented in Mansour Alanazi's Ph.D. Thesis, that will be submitted to Lancaster University in January 2024. It is already agreed that a joint journal publication by the Lancaster University and UT Southwestern team will follow.

Sincerely,

Shin Yamazaki, Ph.D.
Director of the Neuroscience Imaging Laboratory
Director of the O'Donnell Brain Institute NeuroMicroscopy Core
Professor in the Department of Neuroscience
UT Southwestern Medical Center
6000 Harry Hines Blvd.
Dallas, Texas 75390-9111
U.S.A.

Email: shin.yamazaki@utsouthwestern.edu
Phone: 214-648-1830

Figure A.1: Agreement letter

Shin Yamazaki

From: Topaz
Sent: Monday, July 5, 2021 2:39 PM
To: TOPAZ1; Mathieu Keck; Shin Yamazaki; Alexandra Brown
Subject: Animal Protocol 2016-101376-G is Approved

The IACUC office is pleased to inform you that the animal protocol indicated below has been approved.

Investigator: Yamazaki, Shin
Protocol Title: Revealing the Palatable Meal-Inducible Circadian Oscillator
Protocol Number: 2016-101376-G
Approval Date: 7/5/2021
Expiration Date: 7/5/2024

Please note that this documents approval of animal use only. Any proposed use of hazardous biological material or chemicals with your animals may not commence until you have obtained approval from the Institutional Biosafety Committee or Chemical Safety Committee and have discussed the implementation of that plan with the ARC Supervisor in your animal use facility. Similarly, the use of radioactive materials or radiation-producing devices with animals must first be authorized by the Office of Safety and Business Continuity (SBC) and discussed with the ARC Supervisor in your animal use facility. Additional training for study personnel and animal care staff may also be required.

Please contact the IACUC office at IACUC@UTSouthwestern.edu if you have any questions. Please do not reply directly to this email.

University of Texas Southwestern Medical Center IACUC Office
5323 Harry Hines Boulevard
Dallas, Texas 75390-9107
phone: 214-648-0456
fax: 214-648-2109

UT Southwestern

Medical Center

The future of medicine, today.

Figure A.2: IACUC protocol approval email

B. Time-frequency representation

For time-frequency representations of the behavioural data, the signals are first detrended. Then, the wavelet transform is applied using the lognormal wavelet and a frequency resolution parameter of 1.8. A cone of influence is not applied. Figs. B1–B4 show the time-frequency representations of behavioural data from mice 1–6. The y-axis is in logarithmic scale. Five oscillatory components emerge for all mice. The wavelet power is the squared amplitude of the wavelet, and has, along with the average power, units (wheel revolutions/min)^2.

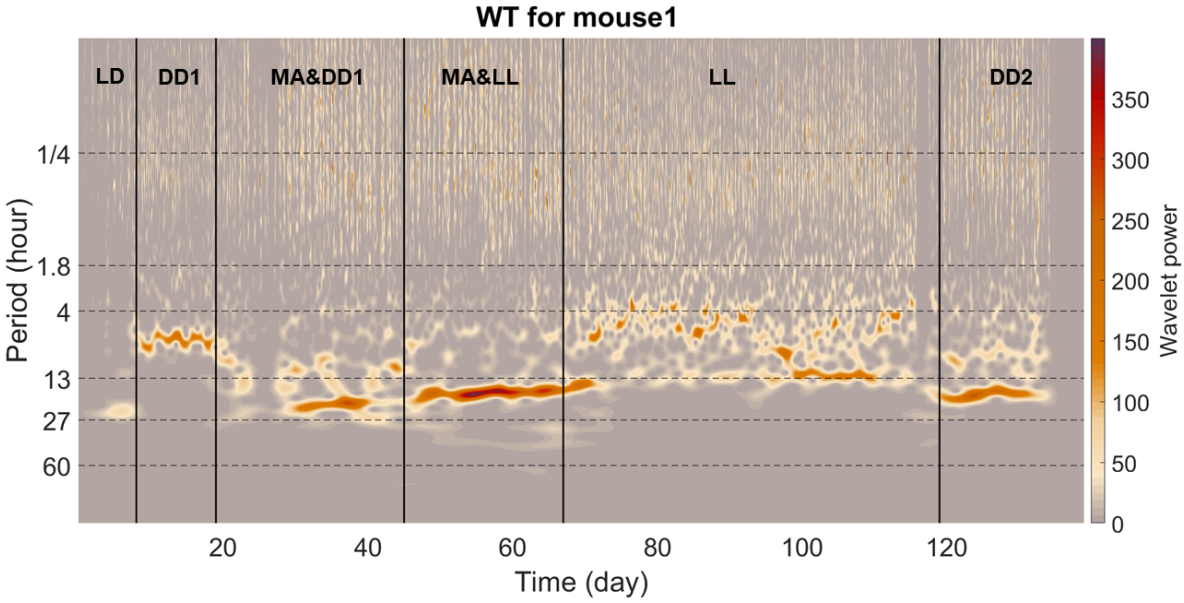

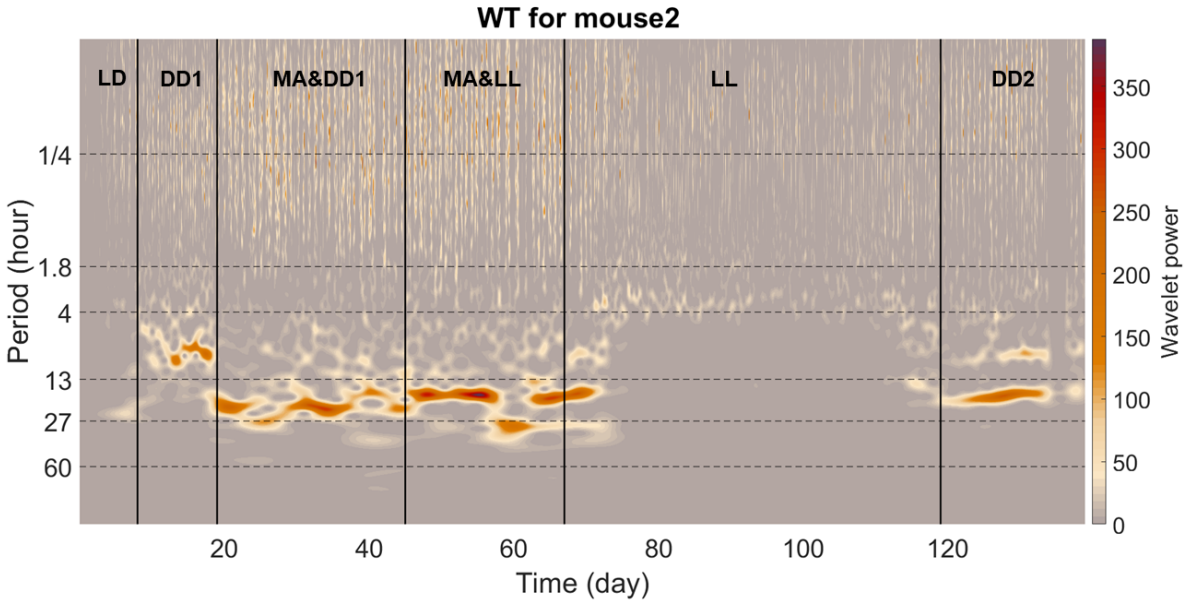

Figure B.1: Time-frequency representation obtained via the wavelet transform of behavioural data from mouse 1 and mouse 2 from study 1. The vertical black lines indicate the start/end of a given condition, where the horizontal dashed black lines indicate the frequency band of interest.

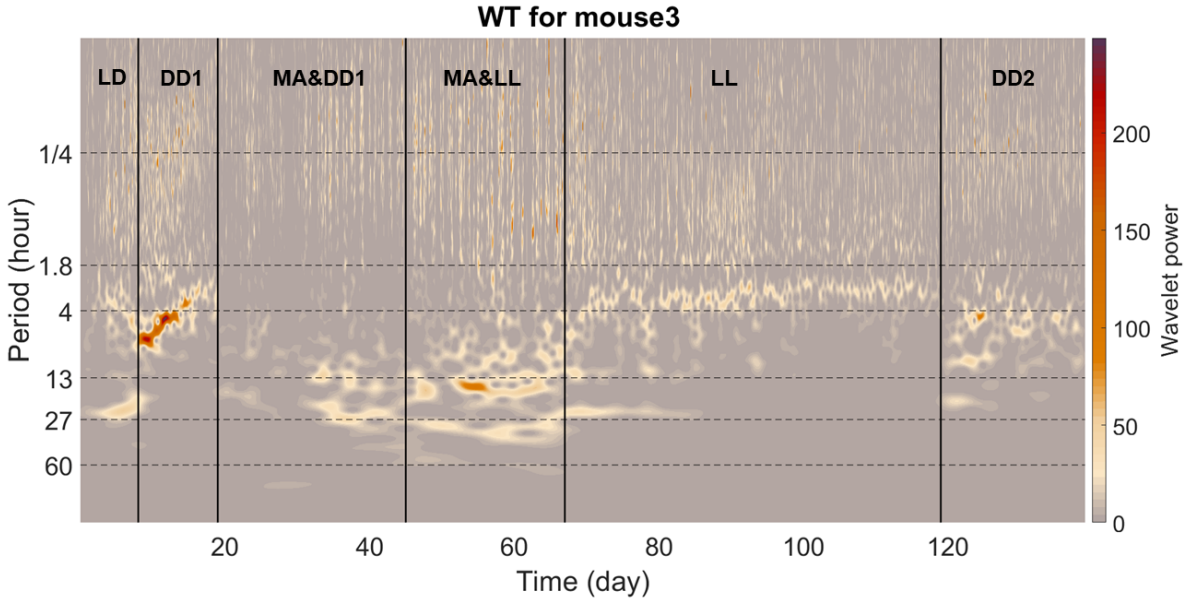

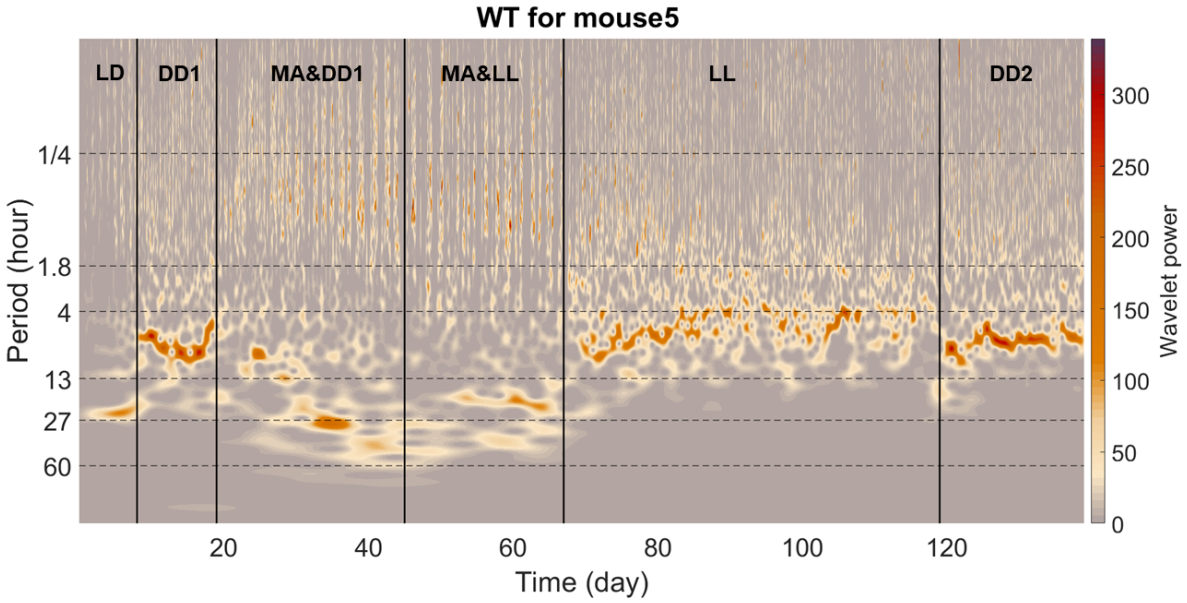

Figure B.2: Time-frequency representation obtained via the wavelet transform of behavioural data from mouse 3 and mouse 5 from study 1. The vertical black lines indicate the start/end of a given condition,where the horizontal dashed black lines indicate the frequency band of interest.

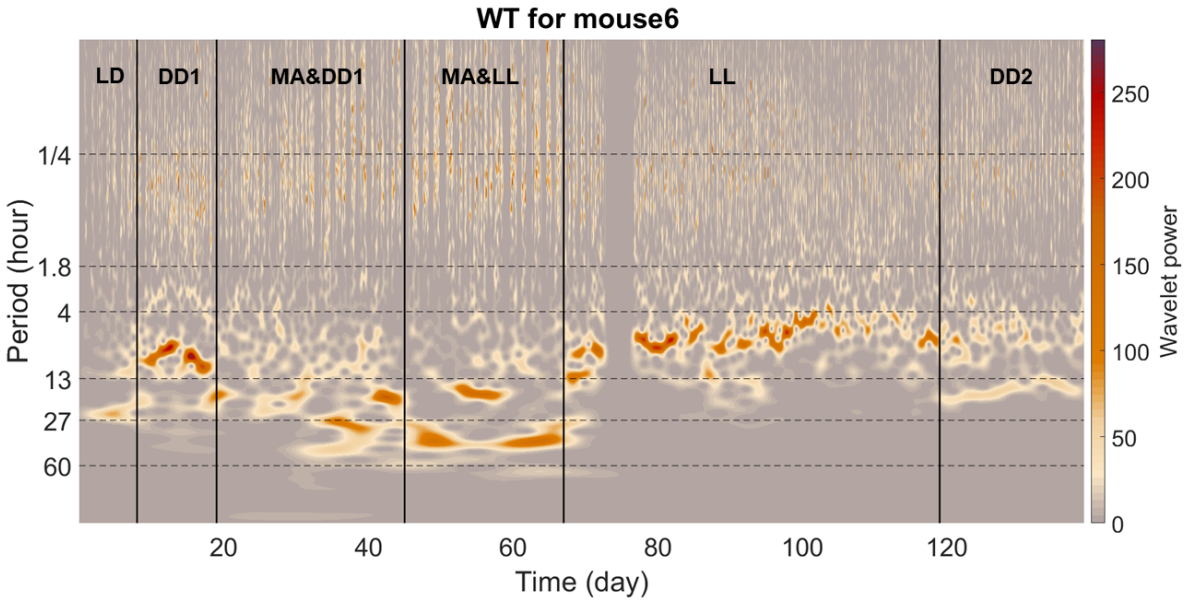

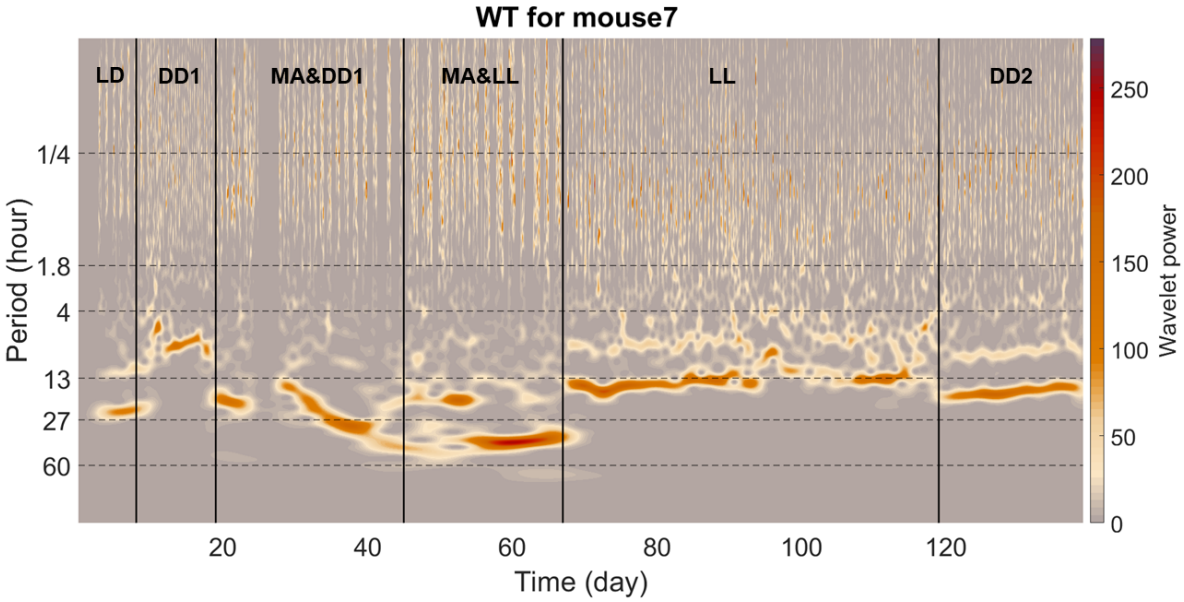

Figure B.3: Time-frequency representation obtained via the wavelet transform of behavioural data from mouse 6 and mouse 7 from study 1. The vertical black lines indicate the start/end of a given condition,where the horizontal dashed black lines indicate the frequency band of interest.

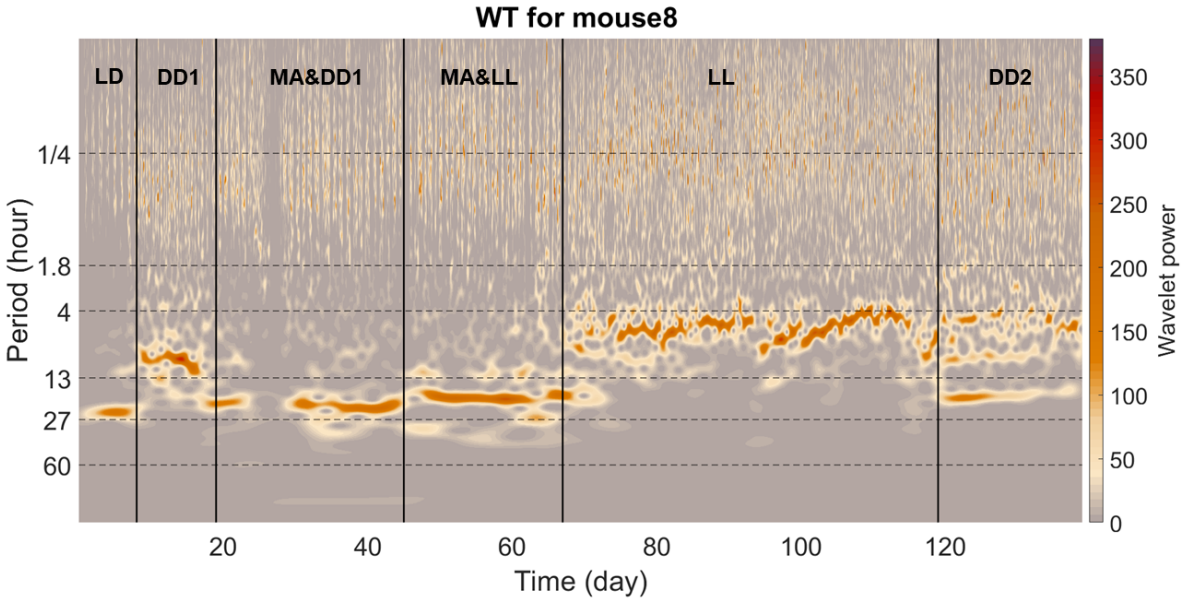

Figure B.4: Time-frequency representation obtained via the wavelet transform of behavioural data from mouse 8 from study 1. The vertical black lines indicate the start/end of a given condition, where the horizontal dashed black lines indicate the frequency band of interest.

For the extra data that we have analysed, time-frequency representations of the behavioural data, the signals are first detrended. Then, the wavelet transform is applied using the lognormal wavelet and a frequency resolution parameter of 1.8. A cone of influence is not applied. Figs. (B.5- B.7) show the time-frequency representations of behavioural data from mice 1–7 which have only two conditions where Figs. (B.8-B.9) show the time-frequency representations of behavioural data from mice 1–7 which have the condition of administration of MA. The y-axis is in logarithmic scale. Five oscillatory components emerge for all mice. The wavelet power is the squared amplitude of the wavelet, and has, along with the average power, units (wheel revolutions/min)^2.

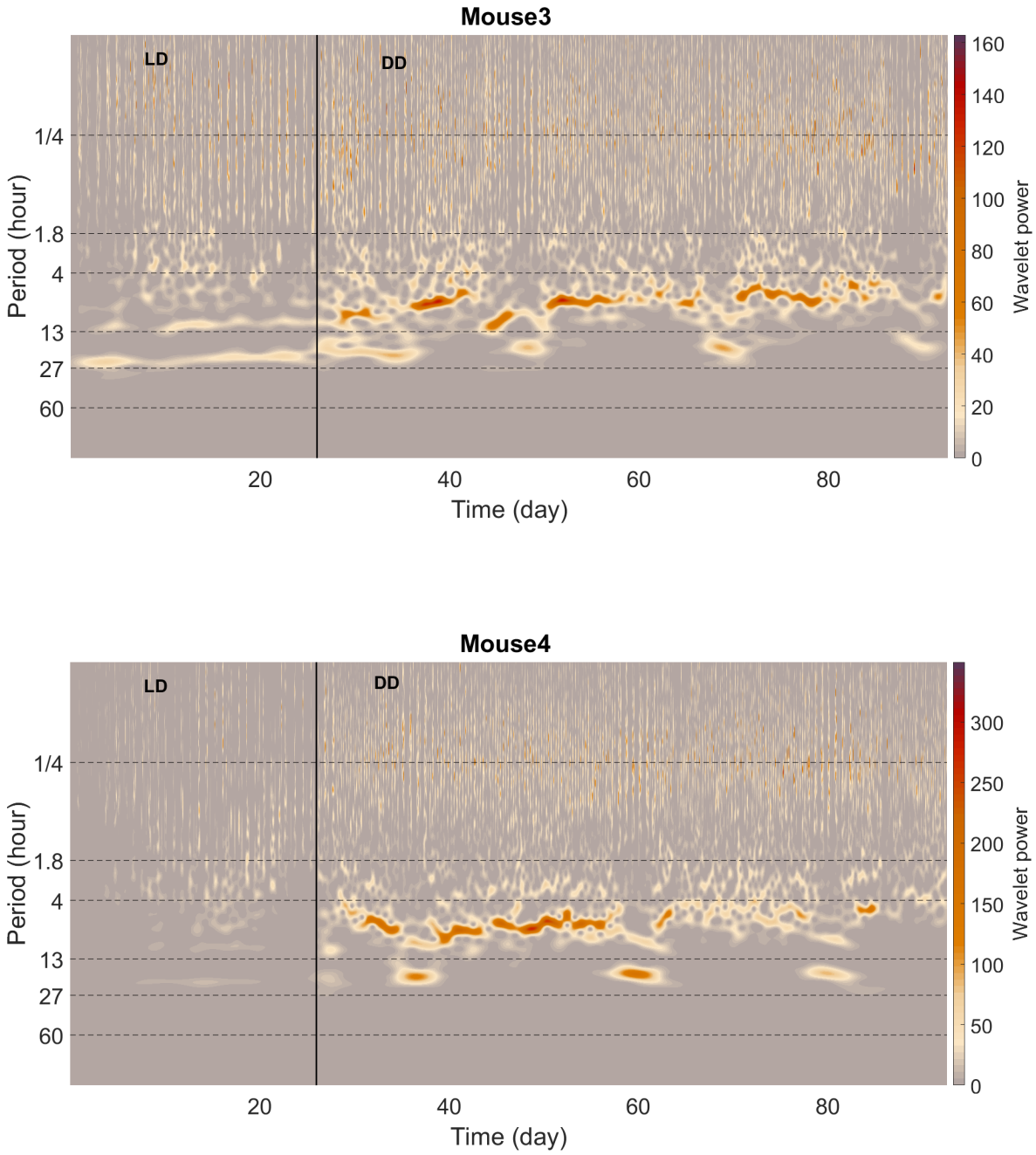

Figure B.5: Time-frequency representation obtained via the wavelet transform of behavioural data from mouse 3 and mouse 4 from study 2. The vertical black lines indicate the start/end of a given condition,where the horizontal dashed black lines indicate the frequency band of interest.

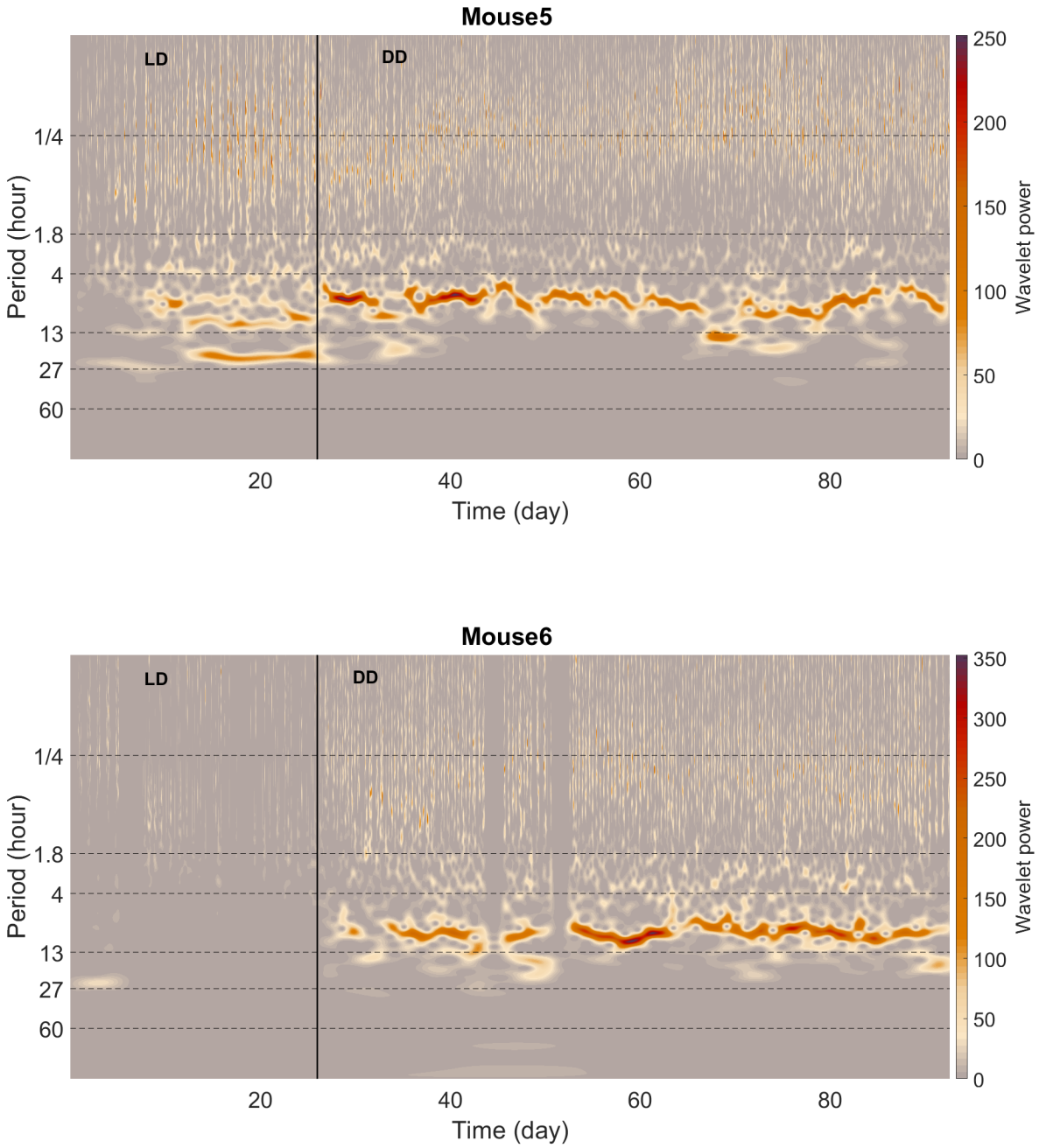

Figure B.6: Time-frequency representation obtained via the wavelet transform of behavioural data from mouse 5 and mouse 6 from study 2. The vertical black lines indicate the start/end of a given condition,where the horizontal dashed black lines indicate the frequency band of interest.

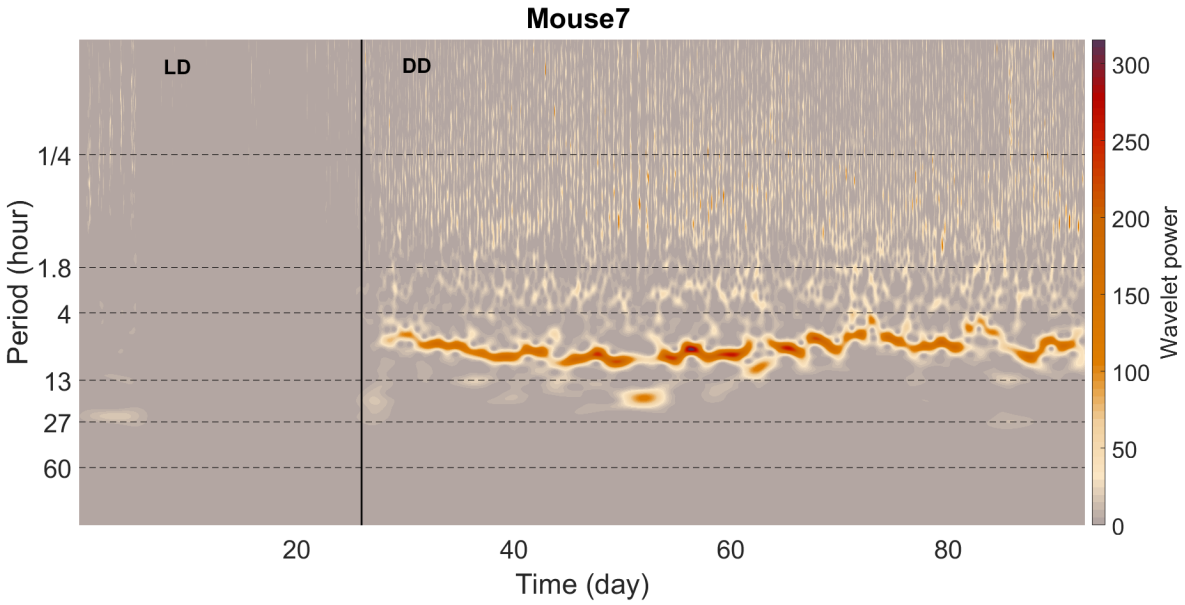

Figure B.7: Time-frequency representation obtained via the wavelet transform of behavioural data from mouse 7 from study 2. The vertical black lines indicate the start/end of a given condition,where the horizontal dashed black lines indicate the frequency band of interest.

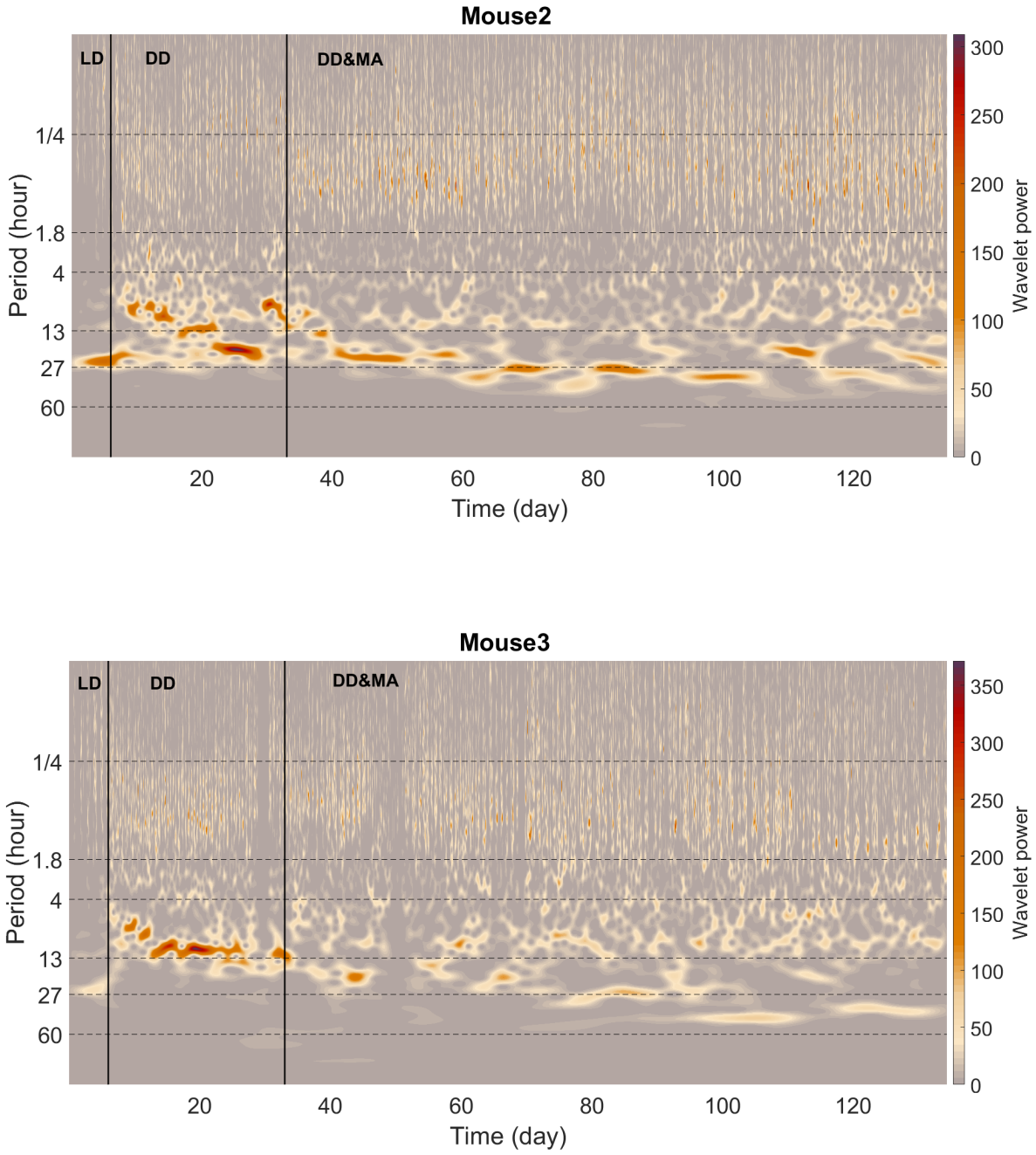

Figure B.8: Time-frequency representation obtained via the wavelet transform of behavioural data from mouse 2 and mouse 3 from study 3. The vertical black lines indicate the start/end of a given condition,where the horizontal dashed black lines indicate the frequency band of interest.

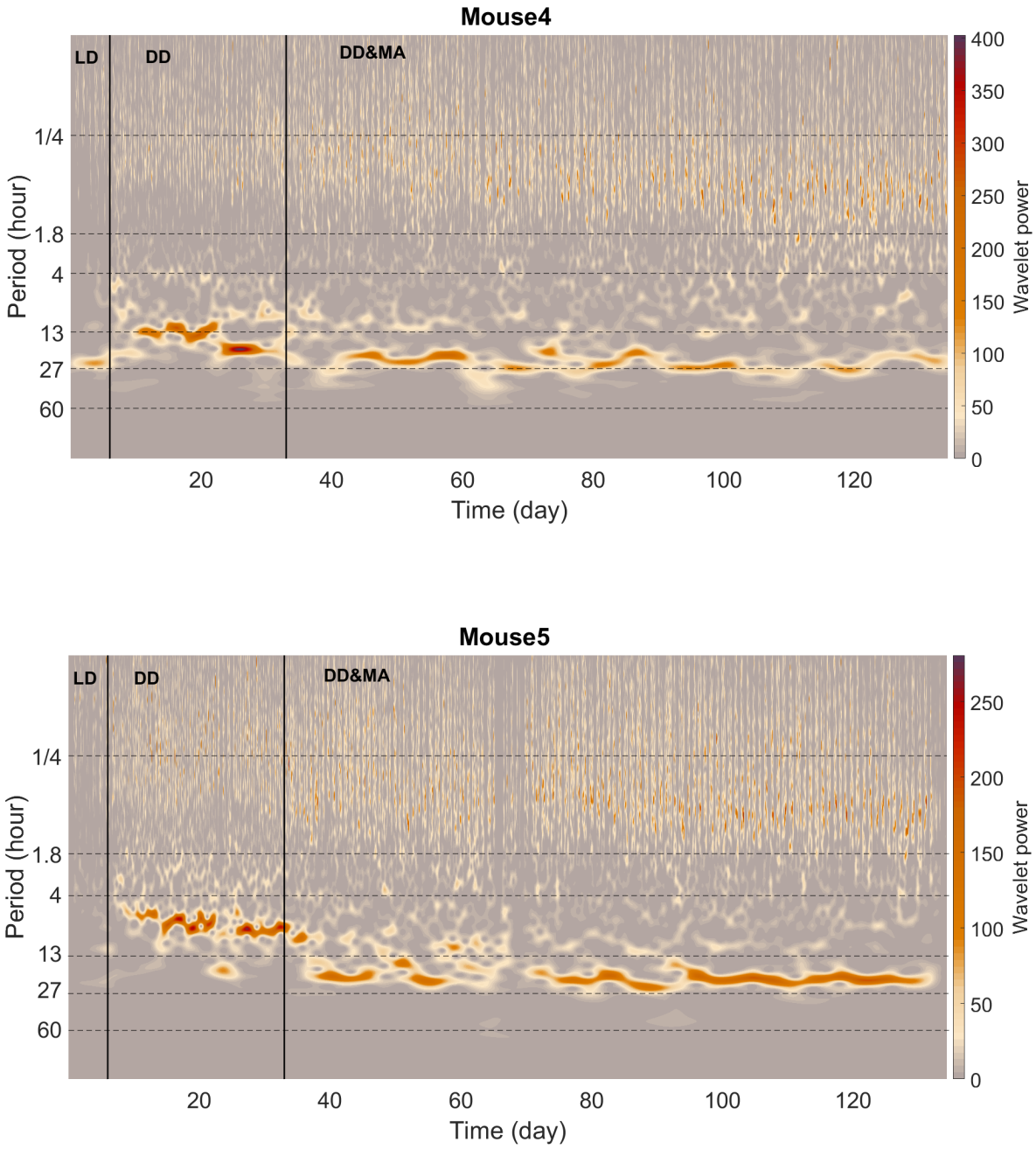

Figure B.9: Time-frequency representation obtained via the wavelet transform of behavioural data from mouse 4 and mouse 5 from study 3. The vertical black lines indicate the start/end of a given condition,where the horizontal dashed black lines indicate the frequency band of interest.

C. Ridges

The technique employed for ridge extraction from a time-frequency representation is applied in this study. The wavelet transform is executed on the behavioral data gathered from all mice.

In the process of ridge extraction, it is imperative that the chosen boundaries encapsulate the entire oscillatory component under investigation, and no more. To ascertain accurate boundaries, both the time-frequency representation and the average power spectrum are utilized. This comprehensive approach ensures the precision of ridge extraction.

It is noteworthy that the units for wavelet power and the average power are expressed in (wheel revolutions/min)^2, aligning with the specific characteristics of the behavioral data and the oscillatory patterns being analyzed.

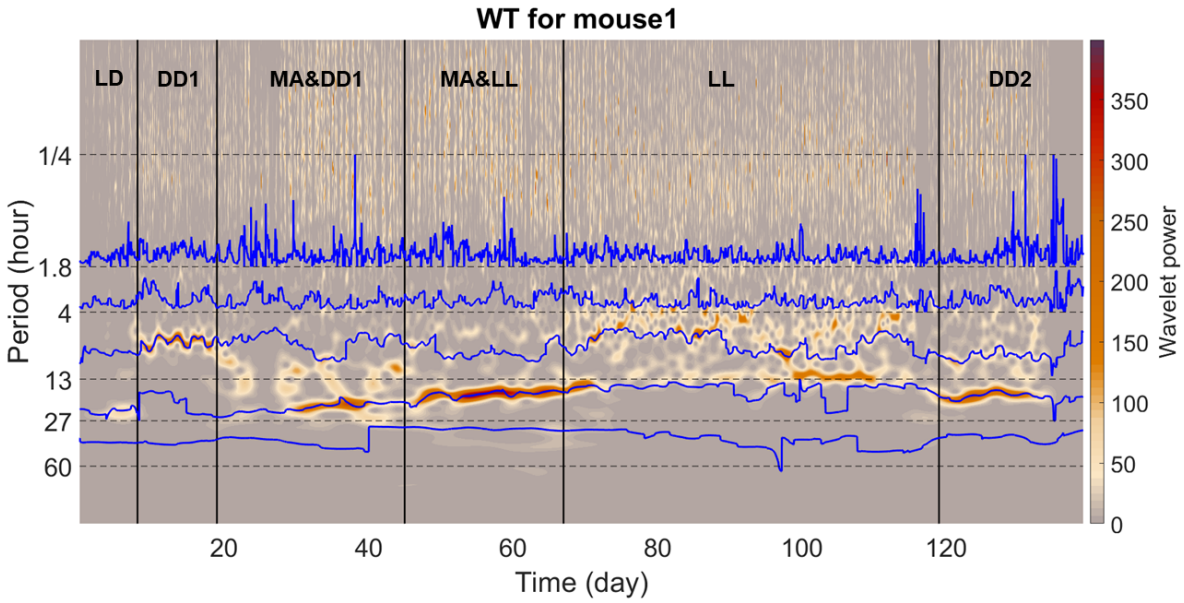

Figure C.1: The method for extracting ridges from a time-frequency representation, and the extracted ridges. The wavelet transform is performed on the behavioral data of mouse 1.

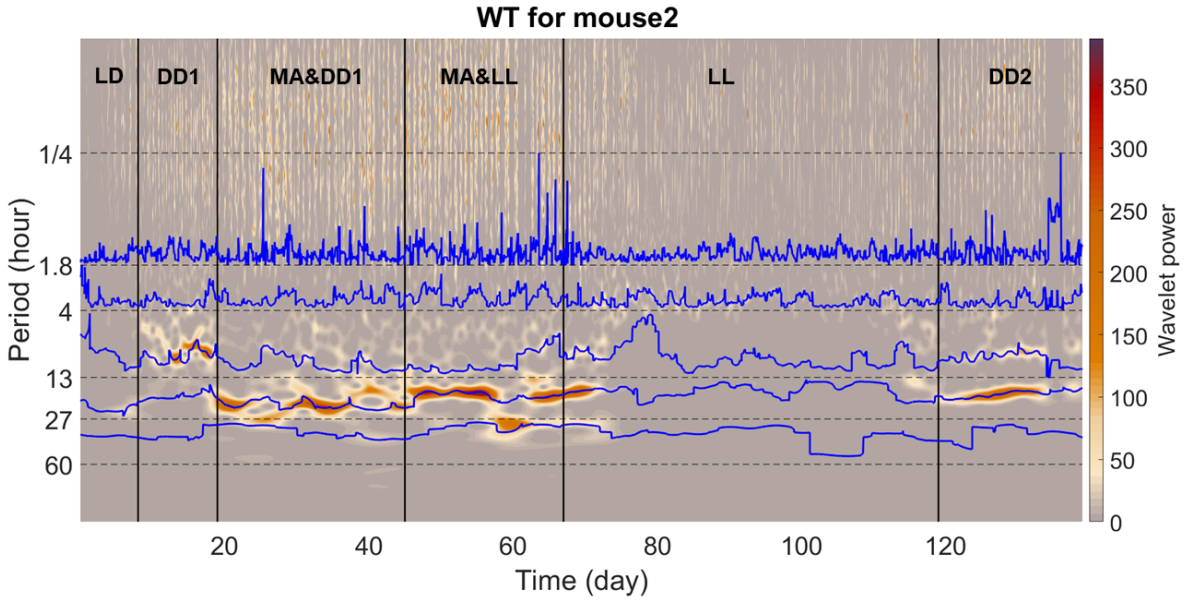

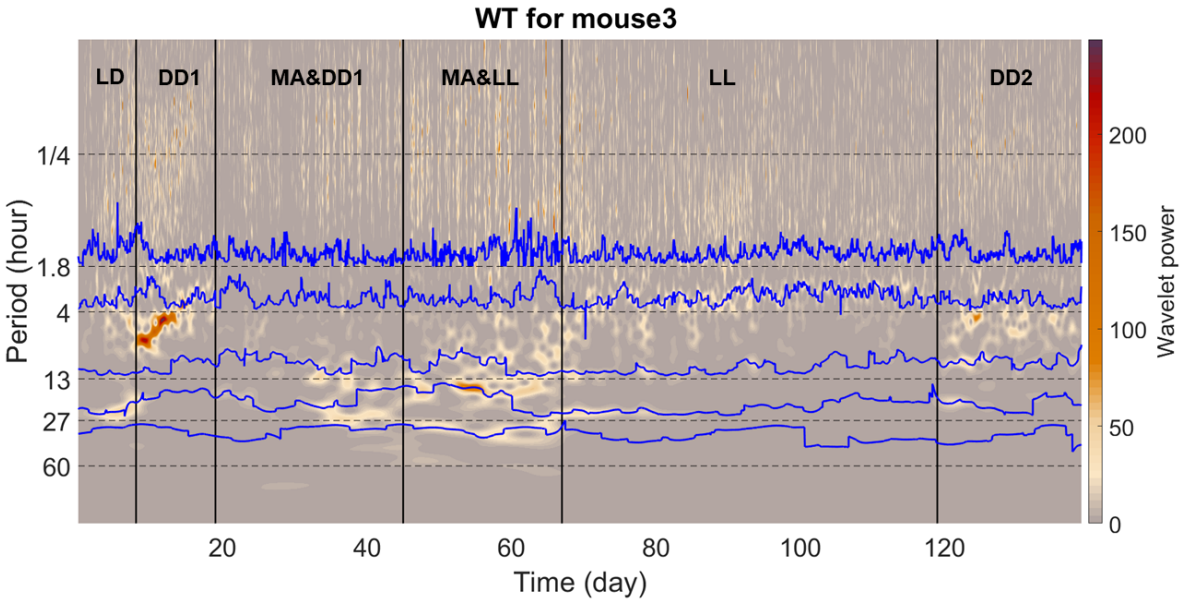

Figure C.2: The method for extracting ridges from a time-frequency representation, and the extracted ridges. The wavelet transform is performed on the behavioral data of mouse 2 and mouse 3.

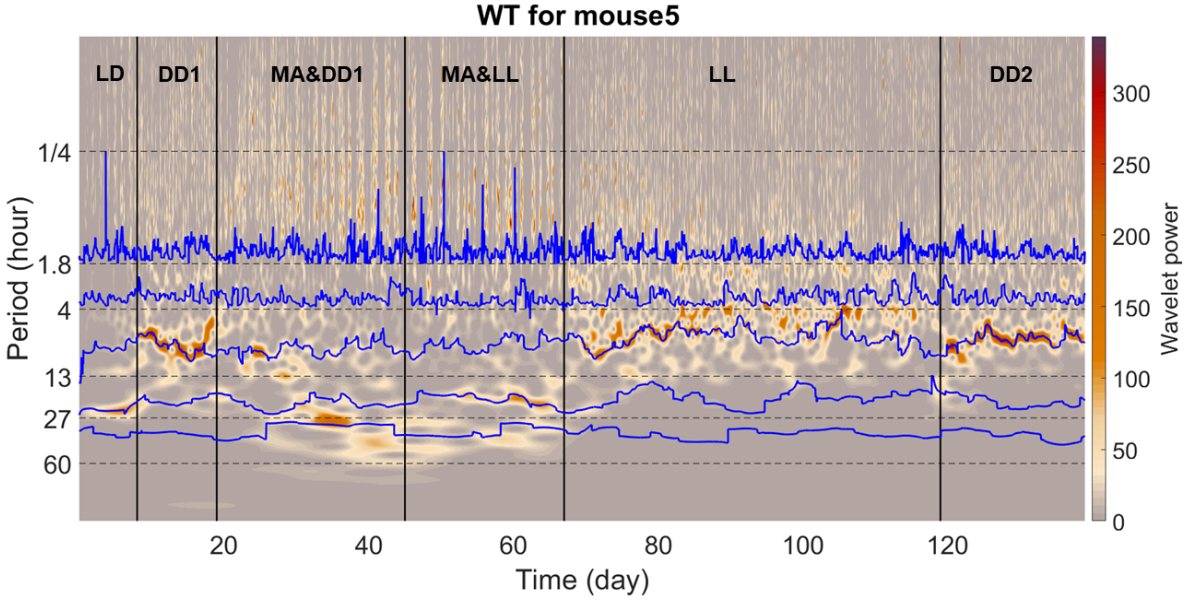

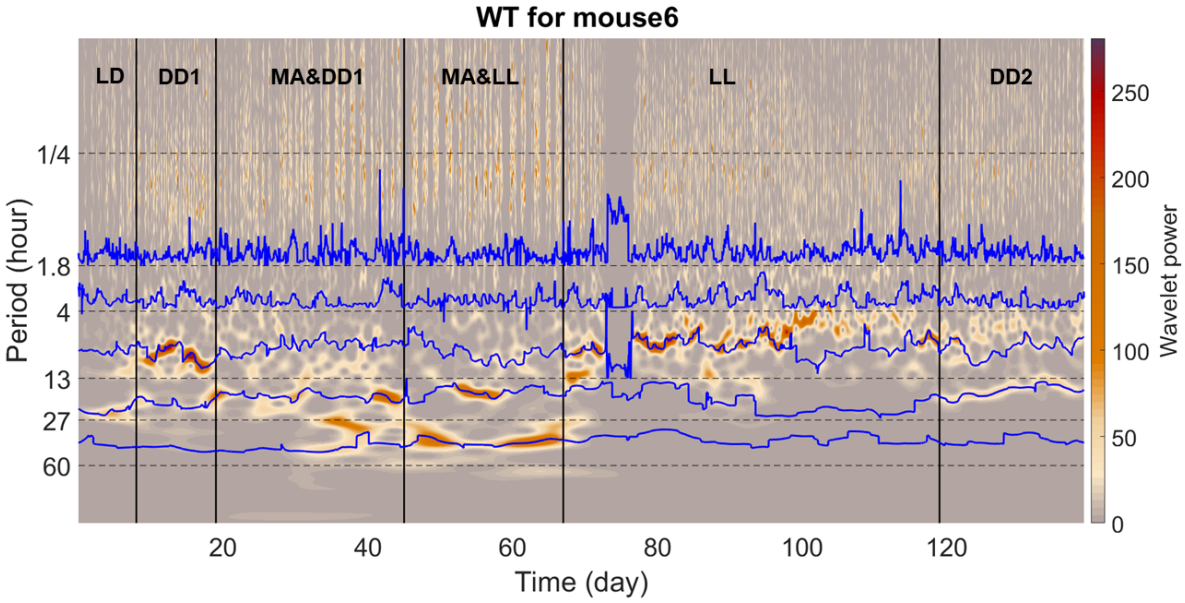

Figure C.3: The method for extracting ridges from a time-frequency representation, and the extracted ridges. The wavelet transform is performed on the behavioral data of mouse 5 and mouse 6.

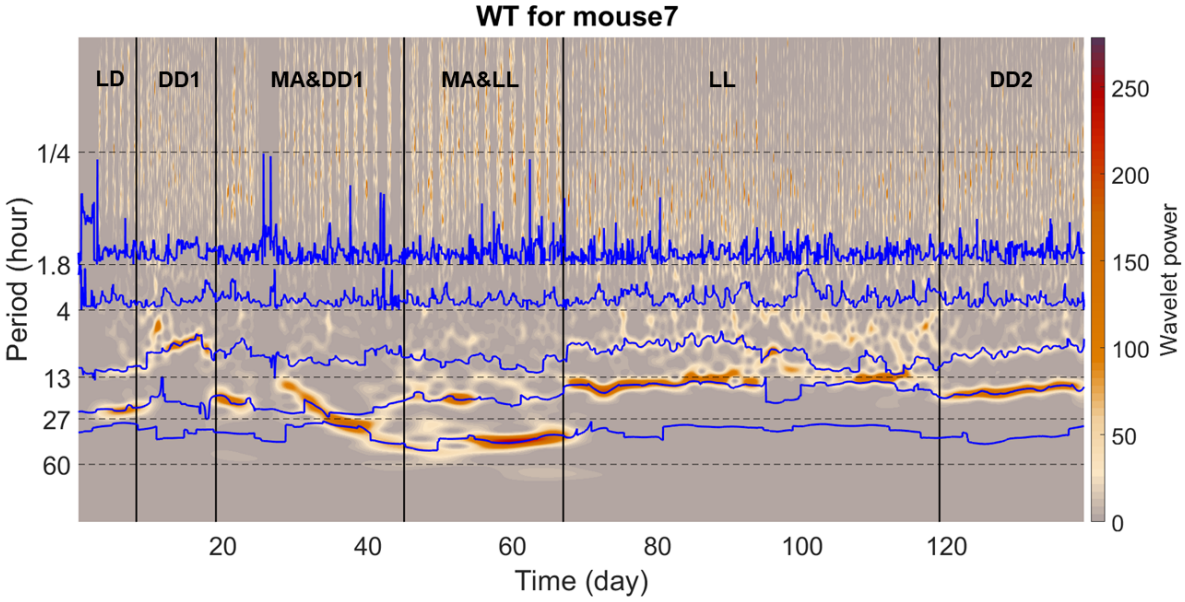

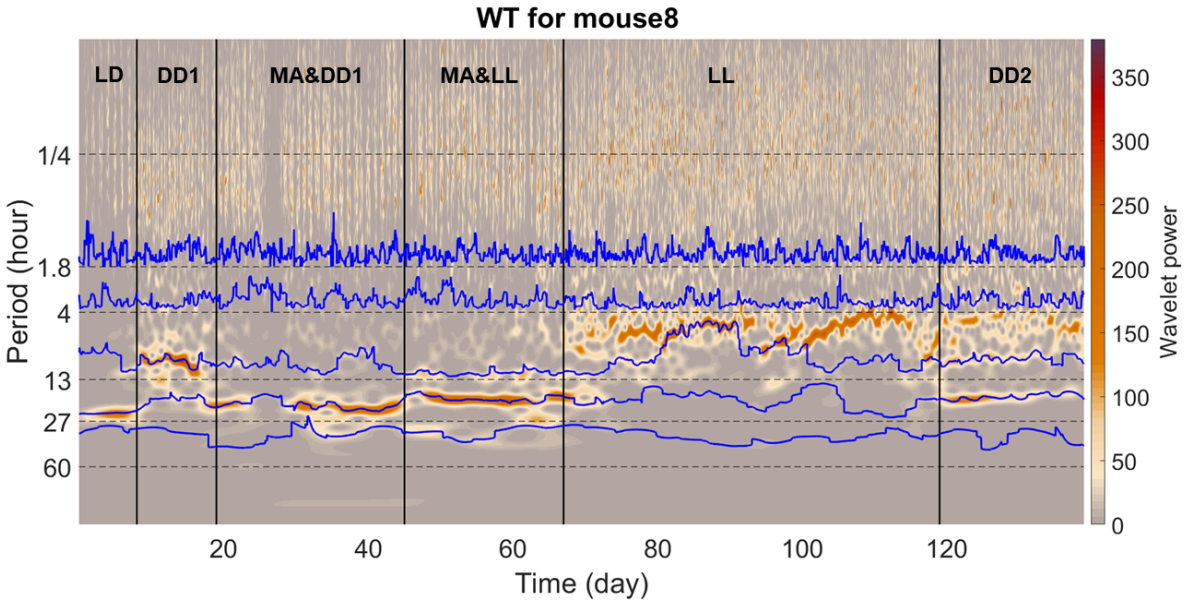

Figure C.4: The method for extracting ridges from a time-frequency representation, and the extracted ridges. The wavelet transform is performed on the behavioral data of mouse 7 and mouse 8.

D. Alternative method to detect interactions between oscillations

Phase coherence and phase difference

The wavelet phase coherence approach is utilised to assess the temporal relationship between phases of two signals at certain frequencies of interest [142, 143, 144, 145, 146]. If oscillations are seen at identical frequencies in two distinct time series, and if the difference between the instantaneous phases $\phi_{1k,n}$ and $\phi_{2k,n}$ remains constant, then we can conclude that it might be stated that the oscillations exhibit coherence at the specified frequency. The calculation of wavelet phase coherence (WPC) between the signals $x_1(t)$ and $x_2(t)$ is achieved by performing wavelet transforms on each signal, as described in Equation 3.17. The wavelet transform of signal $f(t)$ is denoted as W_{si}. The calculation of WPC between the two signals [143] is provided as

$$WPC_{x_1;x_2}(f) = \frac{1}{L}\int_o^L e^{iarg[W_{x_1}(s,t)W^*_{x_2}(s,t)]}dt|, \tag{D.1}$$

where the scale s is related to the frequency f by $s = 1/(2\pi f)$. The phase coherence function $C_\theta(fk)$ is obtained by computing and averaging over time the sine and cosine components of the phase differences for the whole signal, effectively defining the time-averaged WPC as

$$C_\theta(\omega_k) = \sqrt{\langle\cos\Delta\theta_{kn}\rangle^2 + \langle\sin\Delta\theta_{kn}\rangle^2}. \tag{D.2}$$

The phase coherence function $C_\theta(fk)$ as defined in equation D.2 is exactly the discrete version of the phase coherence formula in equation D.1. In addition, we can also calculate the phase difference $\Delta\theta_{kn}$ between two signals according to

$$\Delta\theta_{kn} = \theta_{2k,n} - \theta_{1k,n}. \tag{D.3}$$

The value of $\Delta\theta_{kn}$ lies within 180° and gives information about the phase of one oscillator relative to the other.

Connections can be identified between two signals or components as a result of their interactions or shared external factors on both. The reliability of the computed coherence between processes is contingent upon the ability to replicate the computation in the absence of interaction or common impact. One method for assessing the importance coherence involves the utilisation of surrogate signals [147]. The surrogate employed for all signals is the iterative amplitude adjusted Fourier transform (IAAFT), as discussed in next Section. The null hypothesis posits that the phase relationship between the signals is not influenced by frequency. This implies that surrogates can be generated by the randomization of temporal phase information [20].

E. High harmonic components

The phase time-series for each frequency component is meticulously extracted through the application of the wavelet transform, enabling a pairwise comparison. This comparative analysis serves as the basis for determining the presence of harmonic relationships. The algorithm computes the mutual information between each pair, providing insights into the intricate connections between frequency components.

To ensure a comprehensive exploration of harmonic relationships within the frequency interval of interest, specific parameters are set for the harmonic algorithm. These parameters guarantee the inclusion of all previously identified oscillatory components in the investigative process, contributing to a holistic understanding of the harmonic landscape.

The wavelet transform, characterized by a time resolution of 1.8, is employed to extract the phase time-series for each frequency component. This meticulous approach adds precision to the analysis. Additionally, the use of 19 amplitude-adjusted Fourier transform (AAFT) surrogates further enhances the robustness of the examination, contributing to the reliability of the findings. Figures D.1–D.4 visually represent the detected harmonics present in the behavioral data collected from all mice. The plots exhibit a frequency-frequency representation, illuminating the intricate harmonic relationships among different oscillations. Notably, the symmetry observed over the diagonal in the image implies that only half of the figure needs to be considered for a comprehensive understanding of the harmonic patterns. This graphical representation aids in visualizing the harmonic interplay within the dataset, offering insights into

the complex dynamics of the observed oscillations. The colour code employed in this representation indicates a dimensionless quantity derived by subtracting the mean of the surrogate distribution from the actual value and then dividing it by the standard deviation of the surrogate distribution. Negative values on the color scale signify results lower than the surrogate mean, and, consequently, significant results are represented by values above 0.

E.1 No MA case

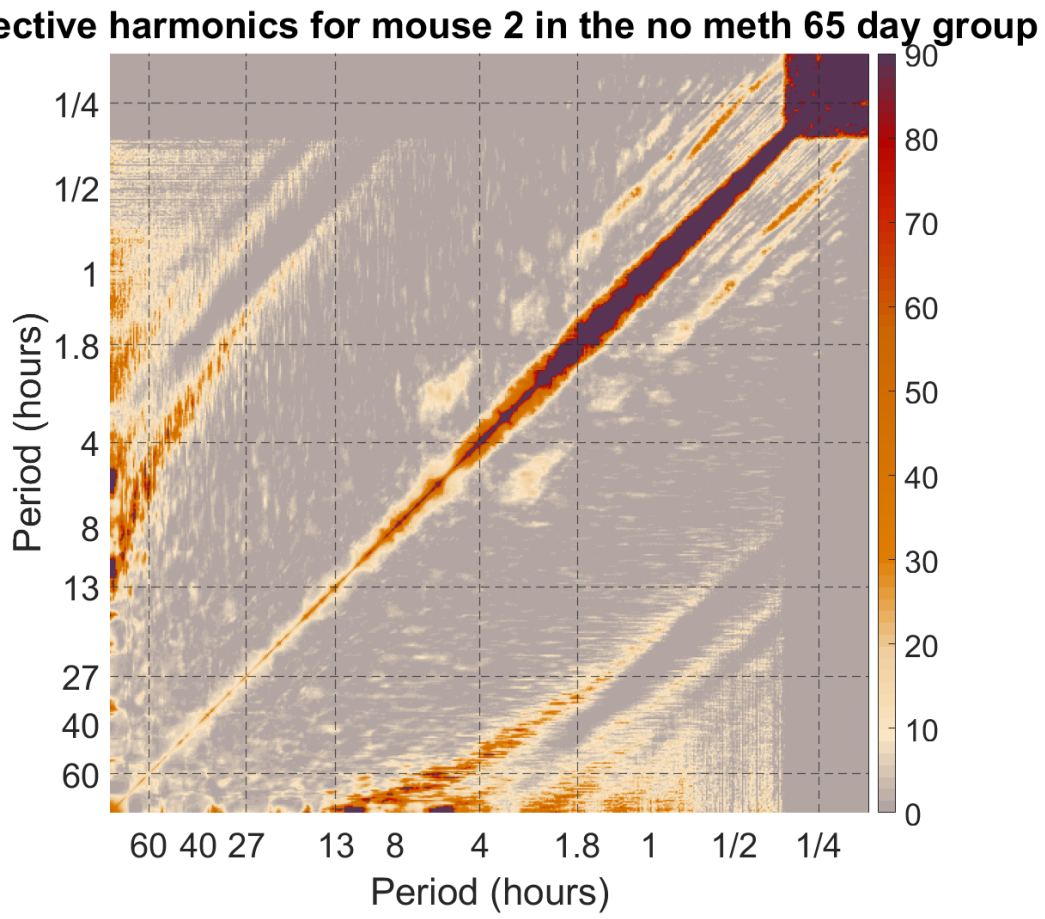

Figure E.1: The detected harmonics within the behavioral data of mouse 2 with no effectiveness of MA.

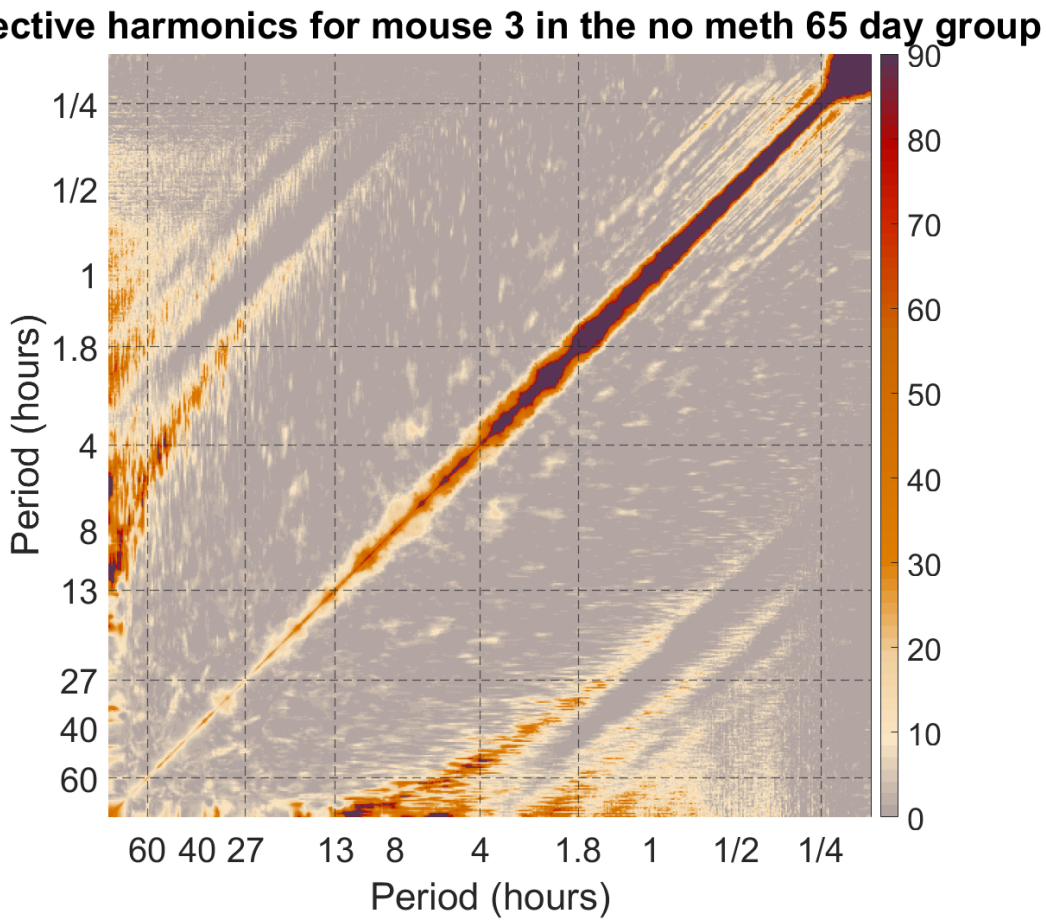

Figure E.2: The detected harmonics within the behavioral data of mouse 3 with no effectiveness of MA

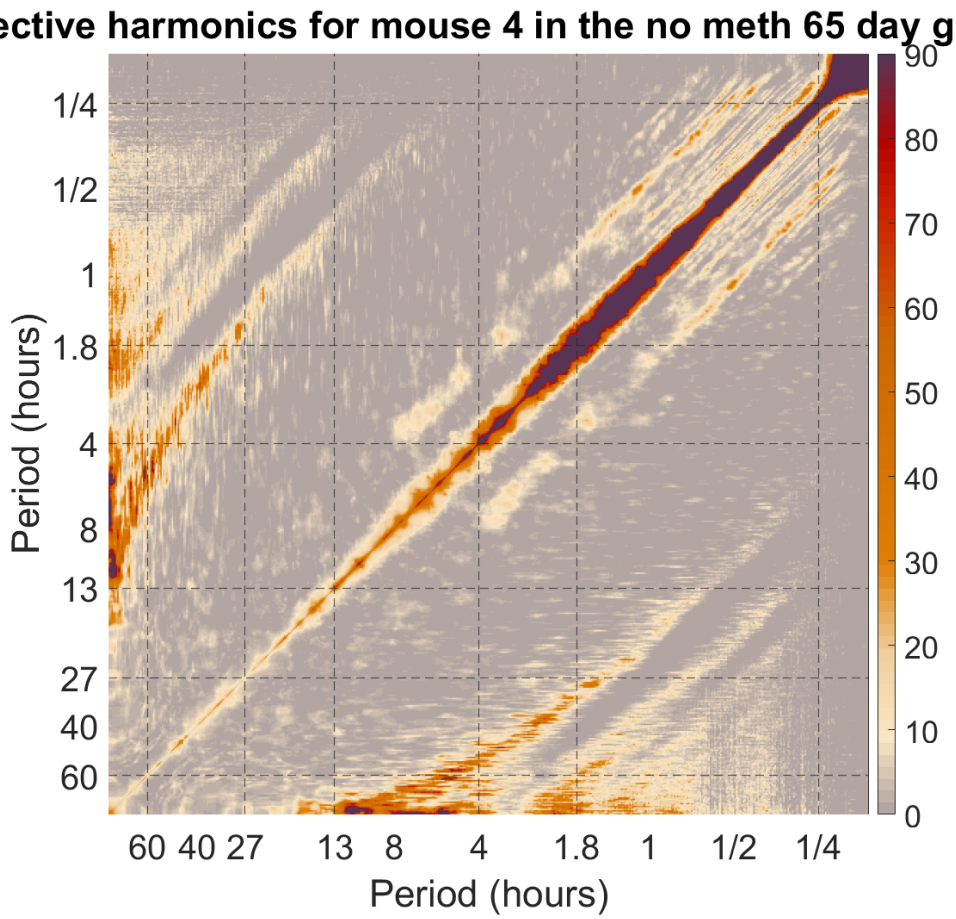

Figure E.3: The detected harmonics within the behavioral data of mouse 4 with no effectiveness of MA

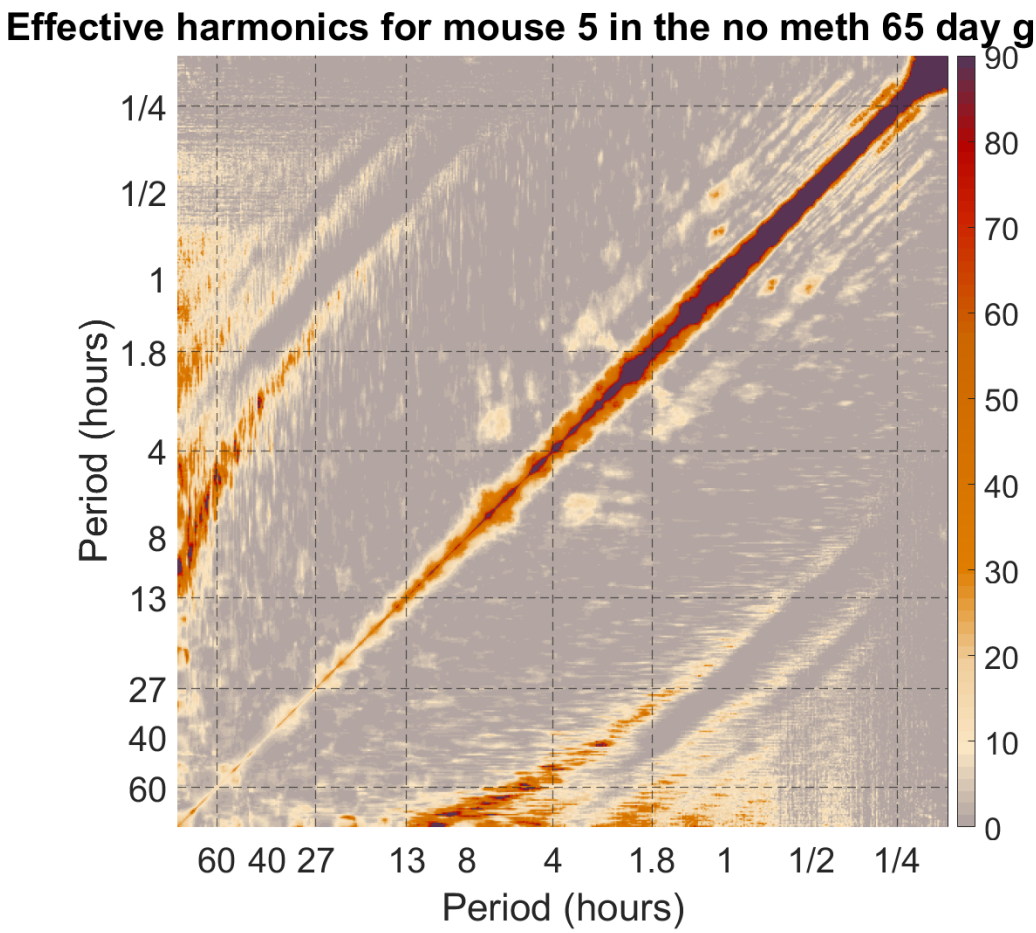

Figure E.4: The detected harmonics within the behavioral data of mouse 5 with no effectiveness of MA.

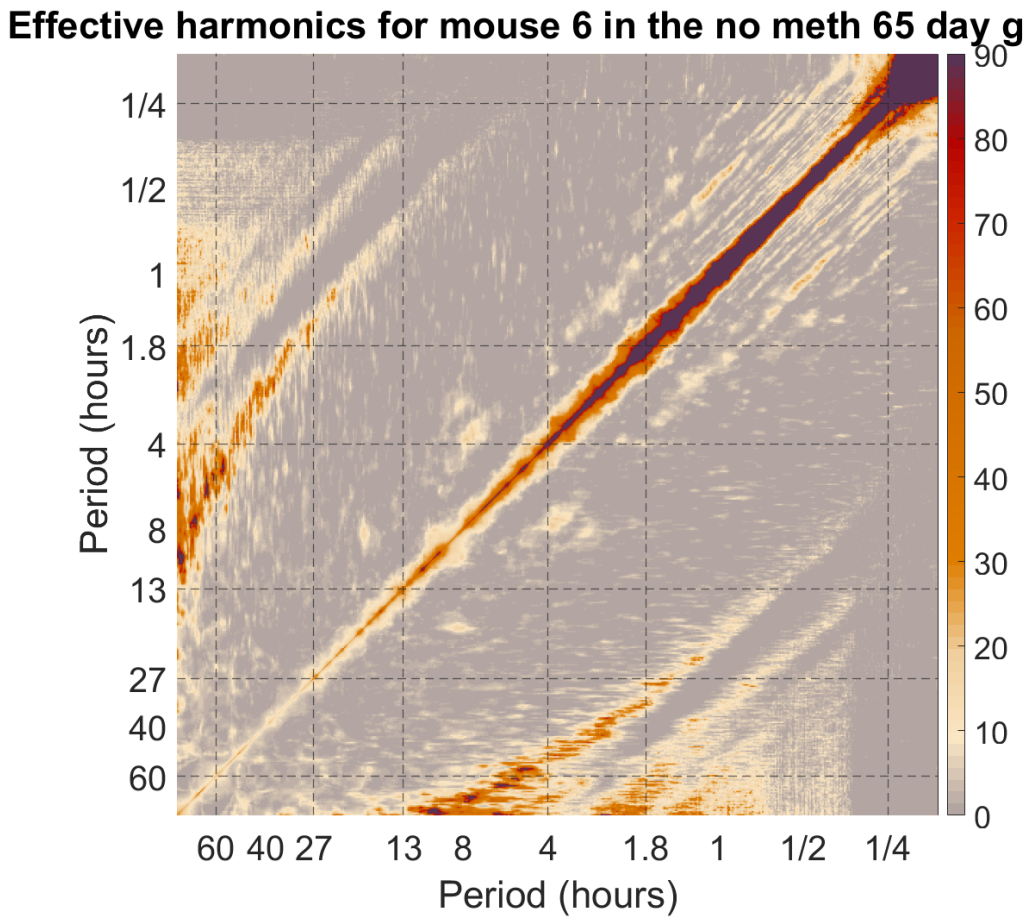

Figure E.5: The detected harmonics within the behavioral data of mouse 6 with no effectiveness of MA

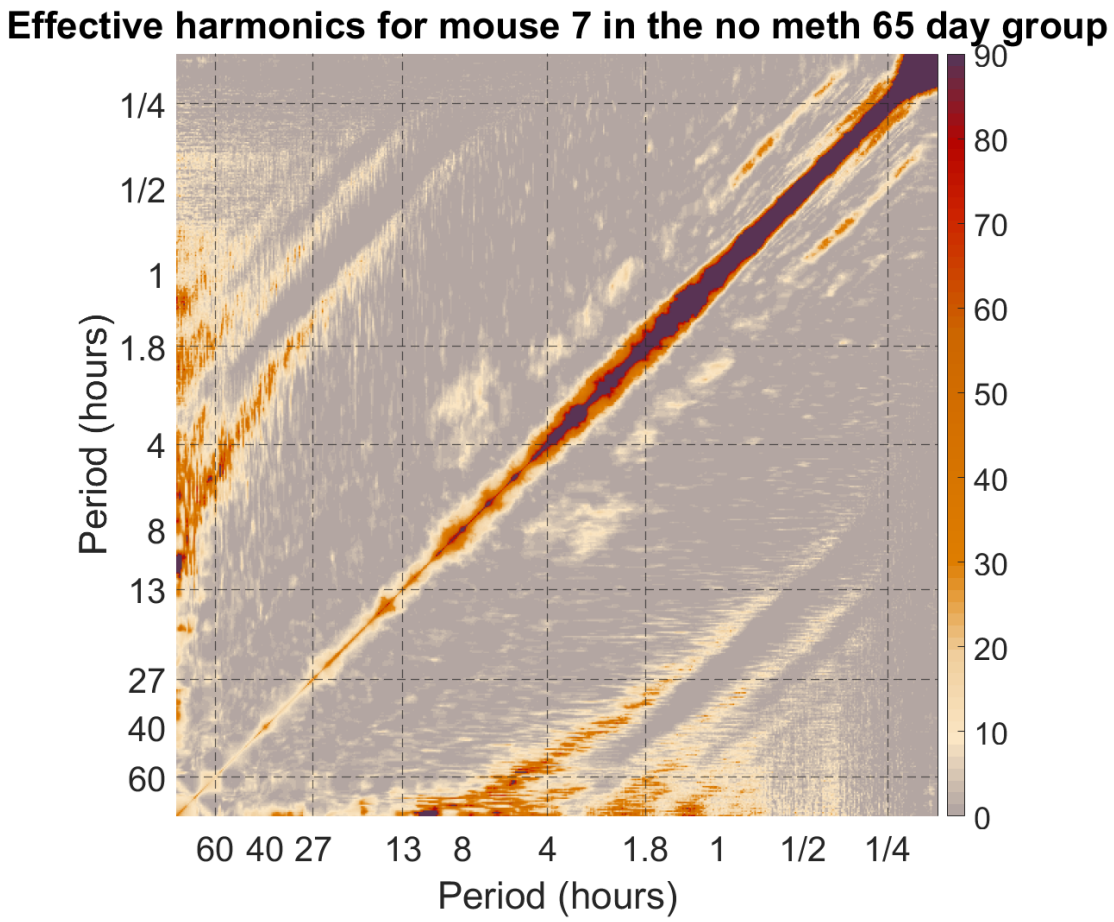

Figure E.6: The detected harmonics within the behavioral data of mouse 7 with no effectiveness of MA

E.2 MA case

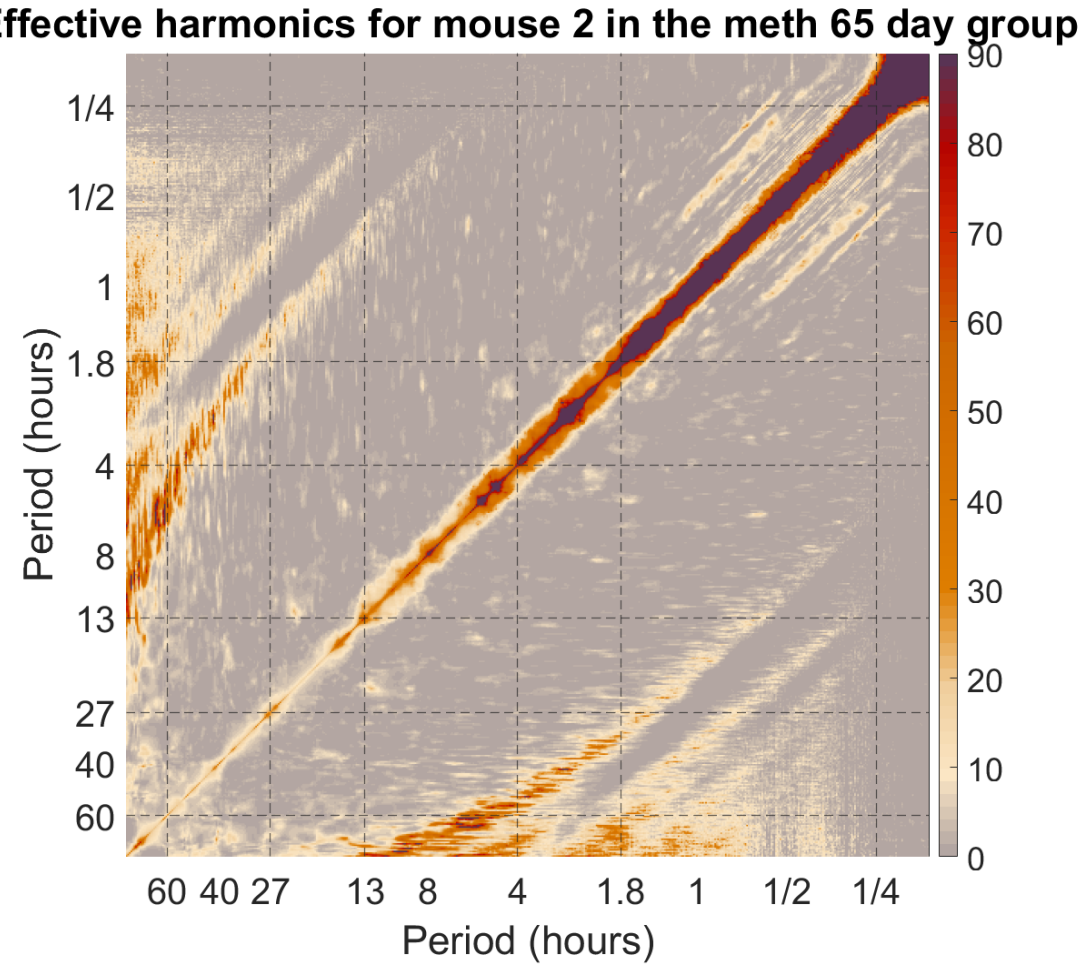

Figure E.7: The detected harmonics within the behavioral data of mouse 2 under effectiveness of MA.

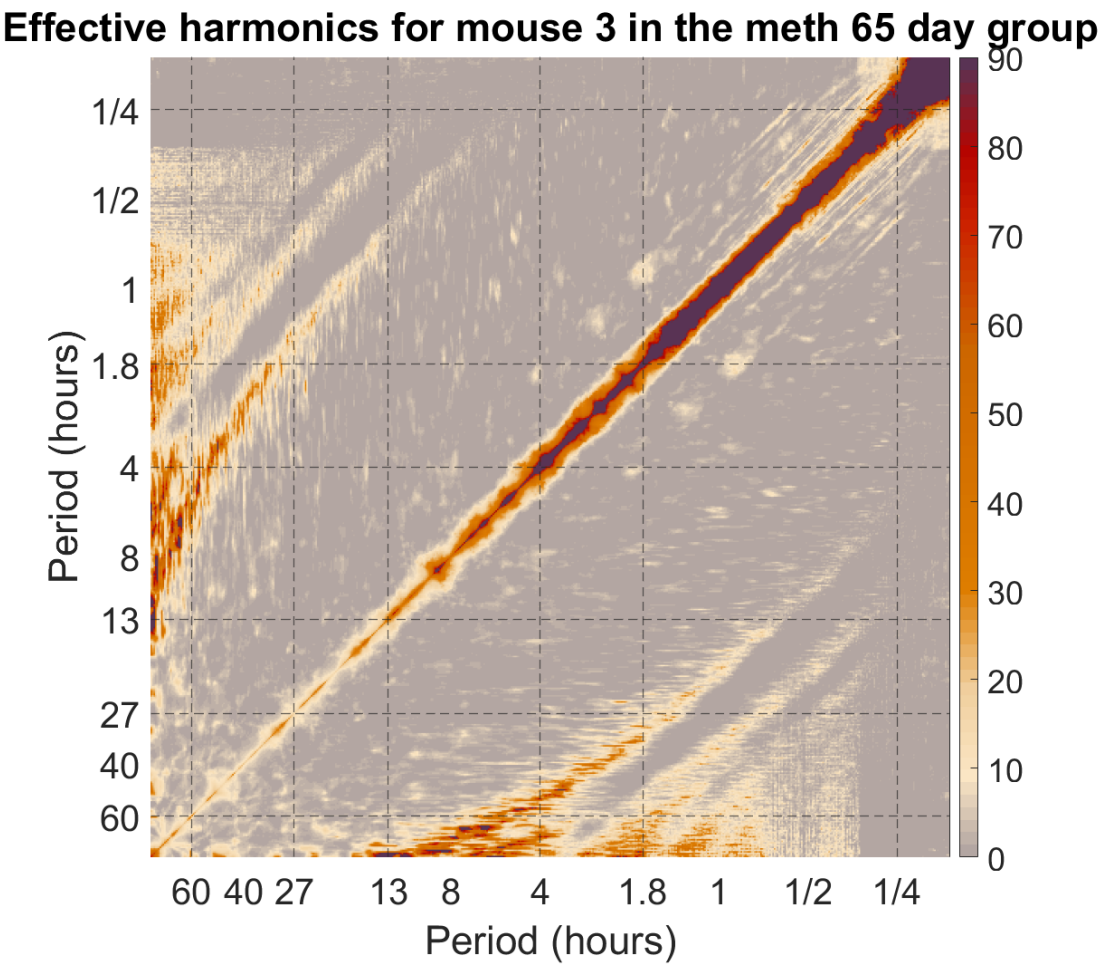

Figure E.8: The detected harmonics within the behavioral data of mouse 3 under effectiveness of MA.

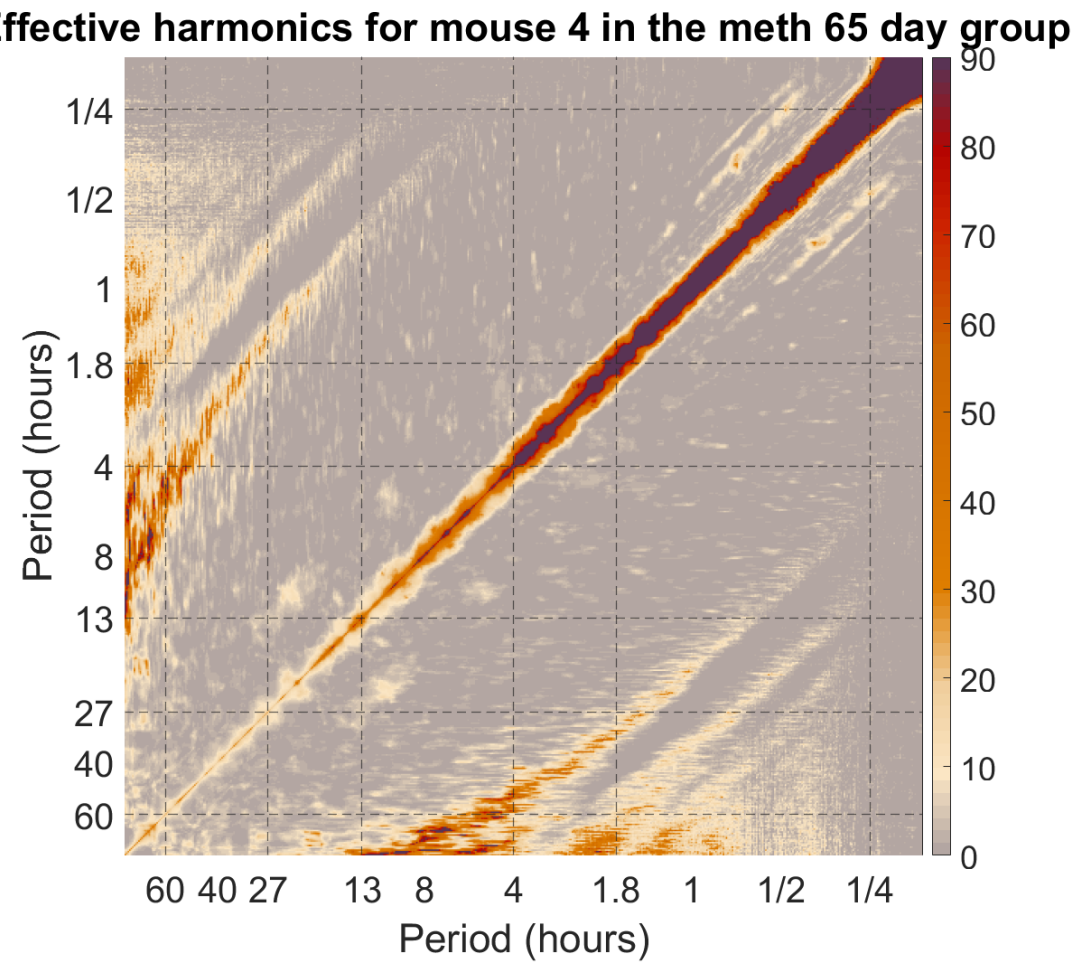

Figure E.9: The detected harmonics within the behavioral data of mouse 4 under effectiveness of MA.

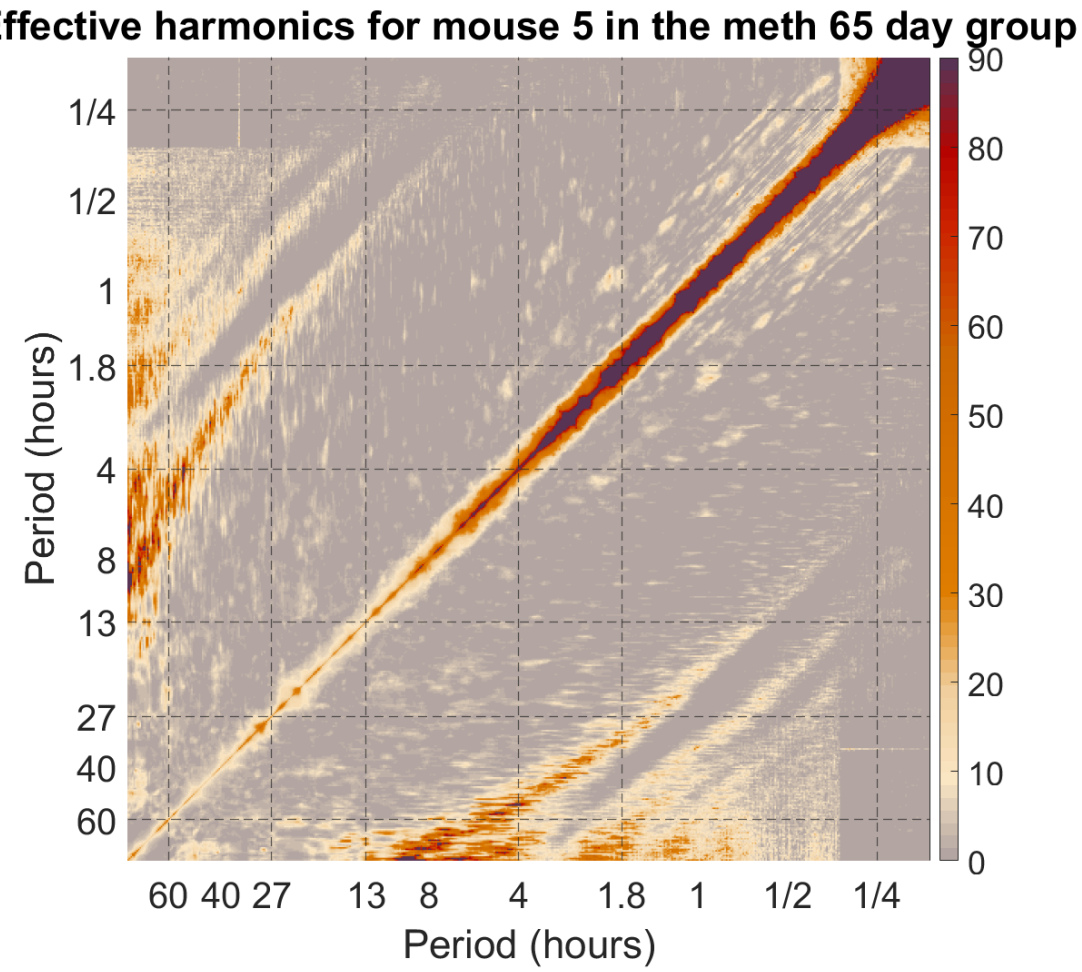

Figure E.10: The detected harmonics within the behavioral data of mouse 5 under effectiveness of MA.

F. Bispectral analysis

Bispectral analysis has been employed for both groups of mice, those treated with methamphetamine and those left untreated, under conditions of constant darkness. This analytical approach enables the differentiation between harmonic and non-harmonic components within the biological signals of the mice. To calculate the biamplitude value, which is the modulus of the time-averaged instantaneous wavelet bispectrum, at each point in frequency-frequency space, a process is followed that includes the application of a statistical significance test. This test is used to identify points in the frequency-frequency space where the biamplitude value is deemed "significant." In more detail, at each specific point within this space, the process involves subtracting a critical threshold from the wavelet biamplitude value. This critical threshold is determined at a 95% significance level and is derived from the bispectra of the iterative amplitude adjusted Fourier transform (IAAFT2) surrogates. The wavelet bispectra are calculated using a lognormal wavelet with frequency resolution 1.8. Through this method, significant biamplitude values are effectively isolated and identified across the frequency-frequency space. Therefore, in these bispectra plots, the strictly positive values (i.e., those that are not grey) indicate the regions where the bispectrum value is deemed "significant." This means that the non-grey areas represent points in the bispectra where the calculated values exceed the threshold of significance.

F.1 No MA case

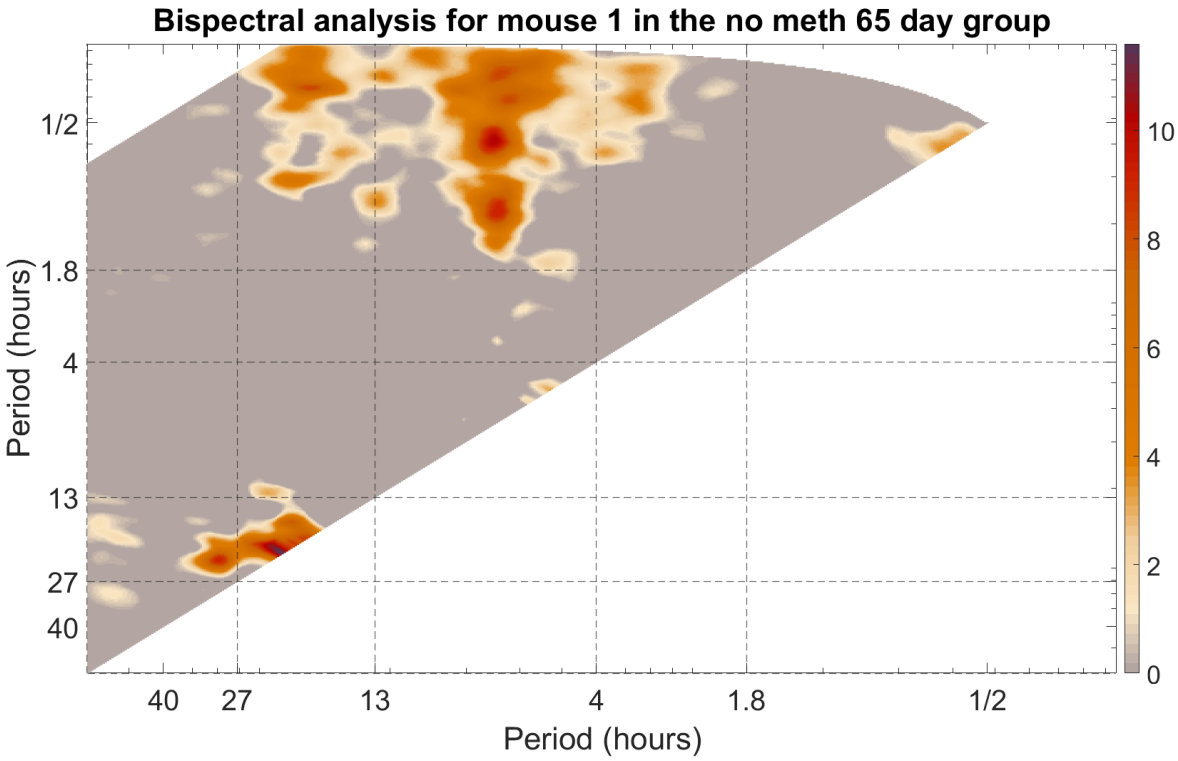

Figure F.1: Wavelet bispectra of behavioural data from mouse 1.

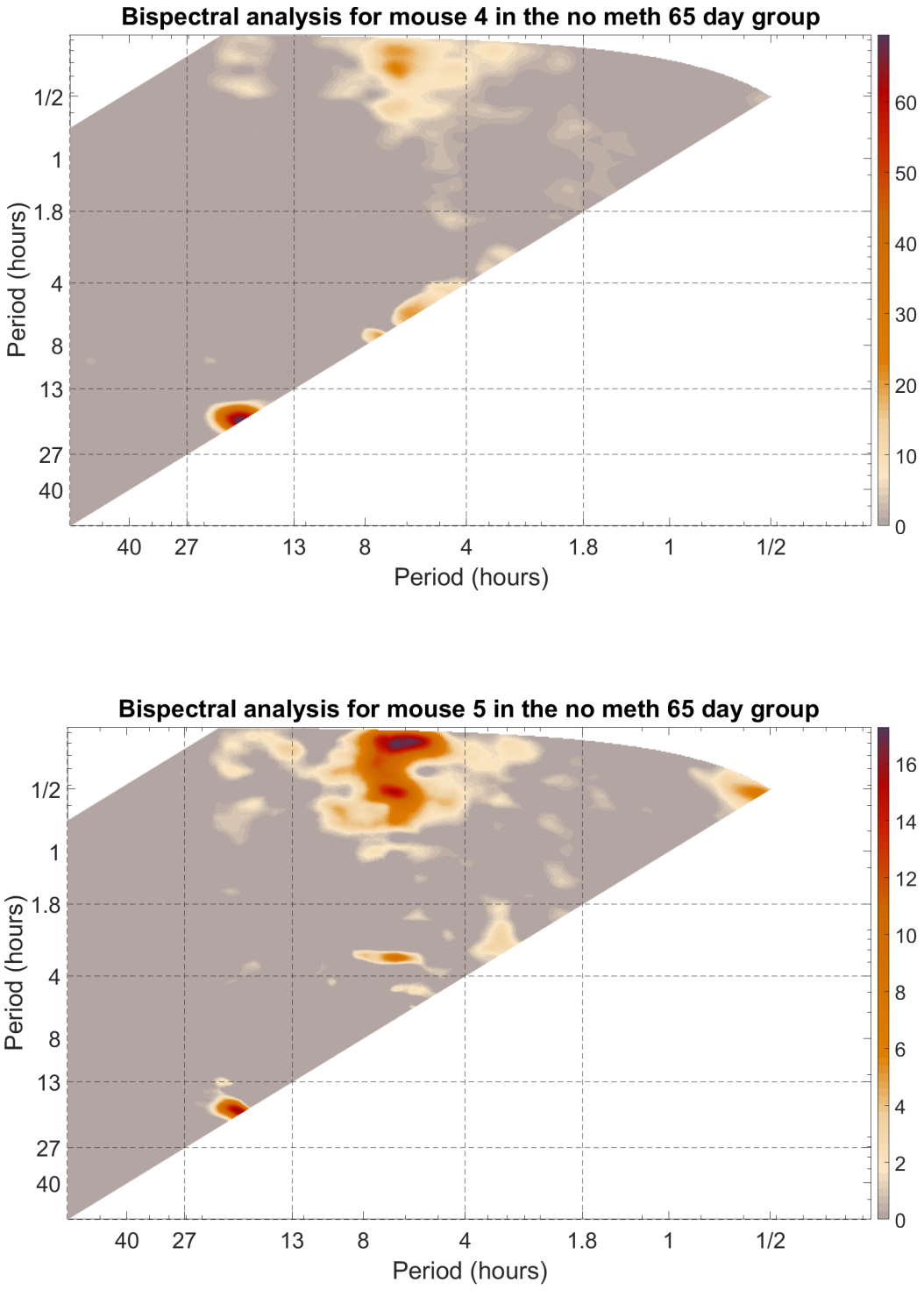

Figure F.2: Wavelet bispectra of behavioural data from mouse 4 and mouse 5.

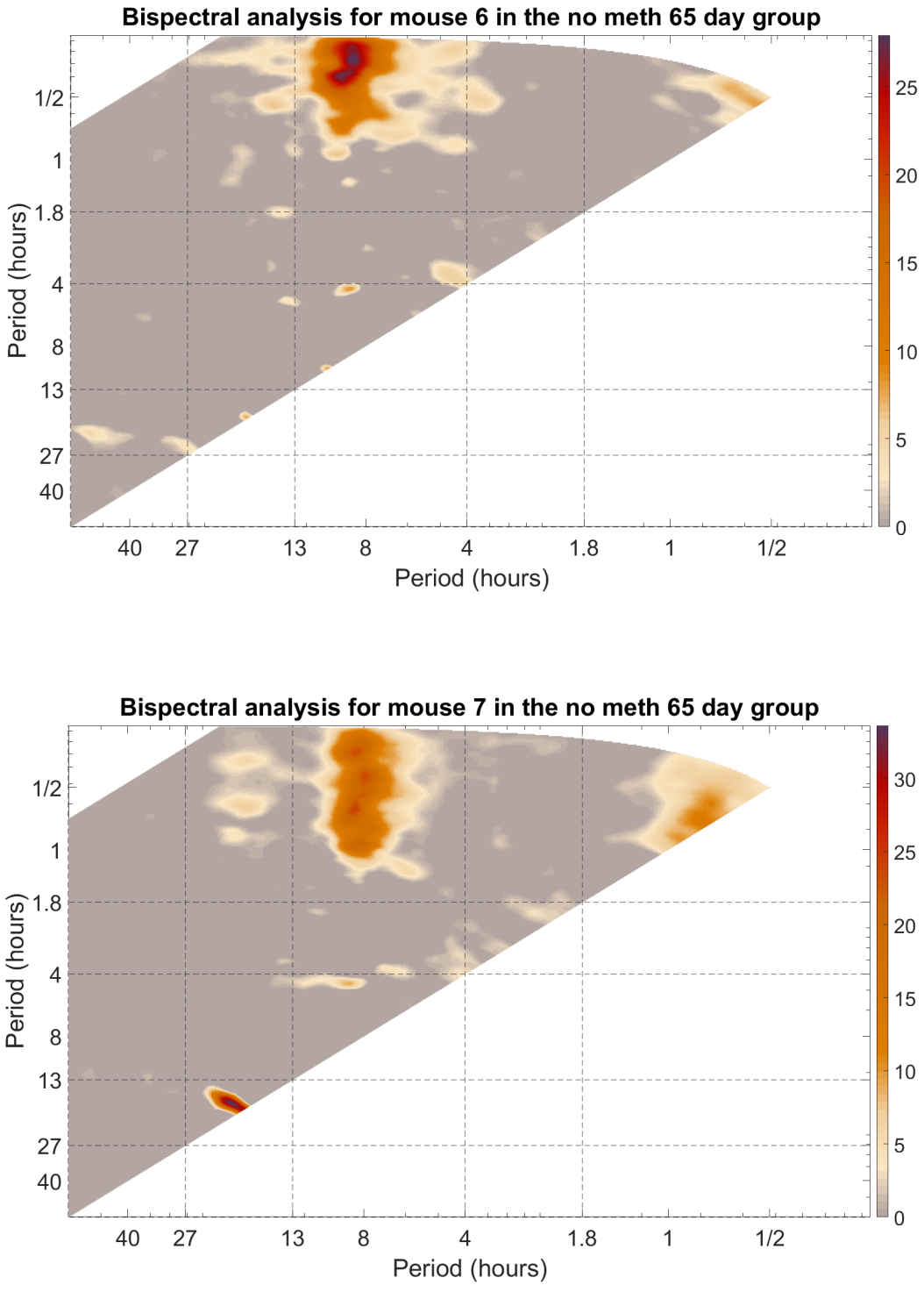

Figure F.3: Wavelet bispectra of behavioural data from mouse 6 and mouse 7.

F.2 MA case

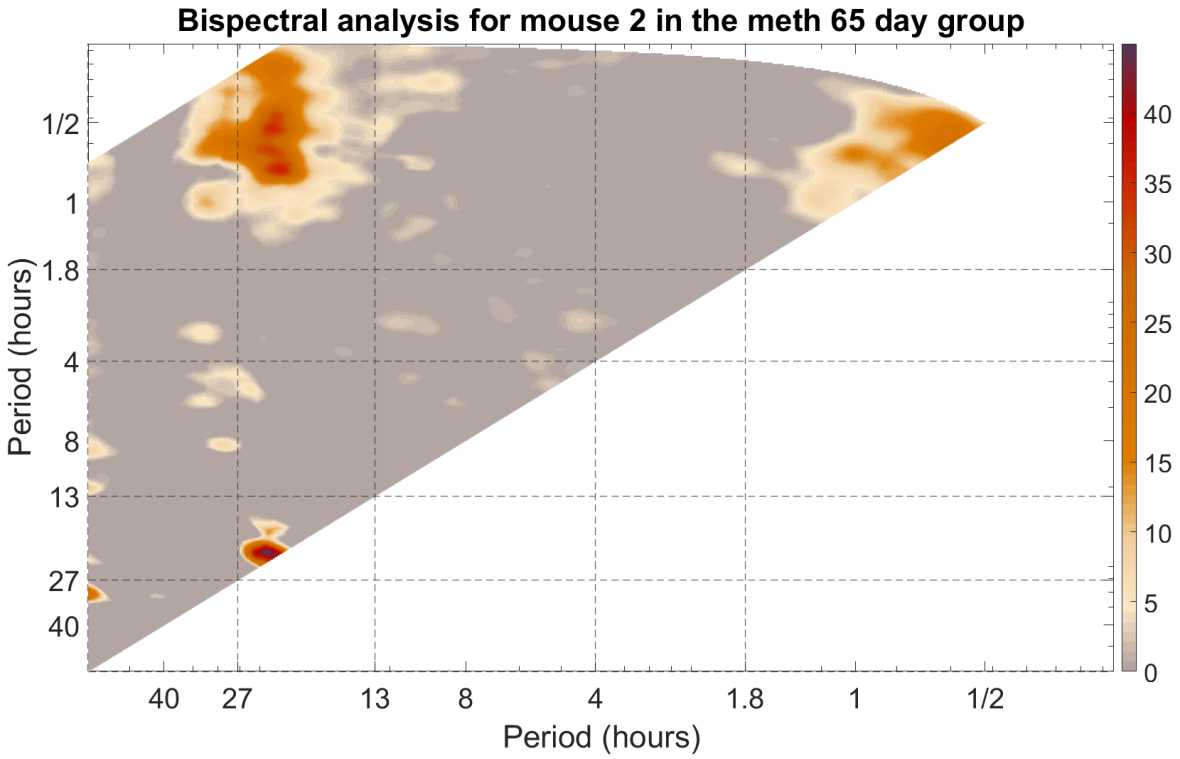

Figure F.4: Wavelet bispectra of behavioural data from mouse 2.

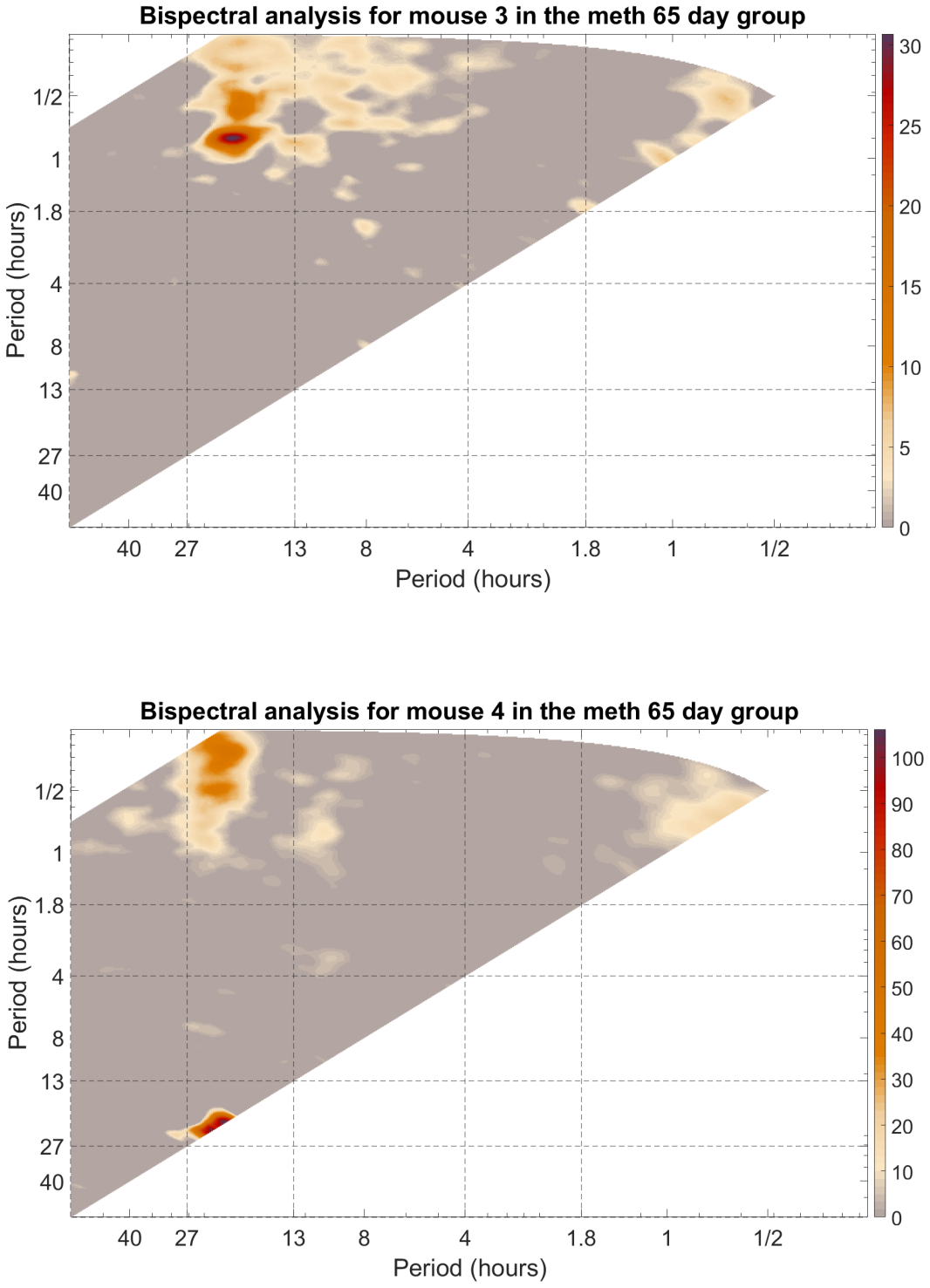

Figure F.5: Wavelet bispectra of behavioural data from mouse 3 and mouse 4.

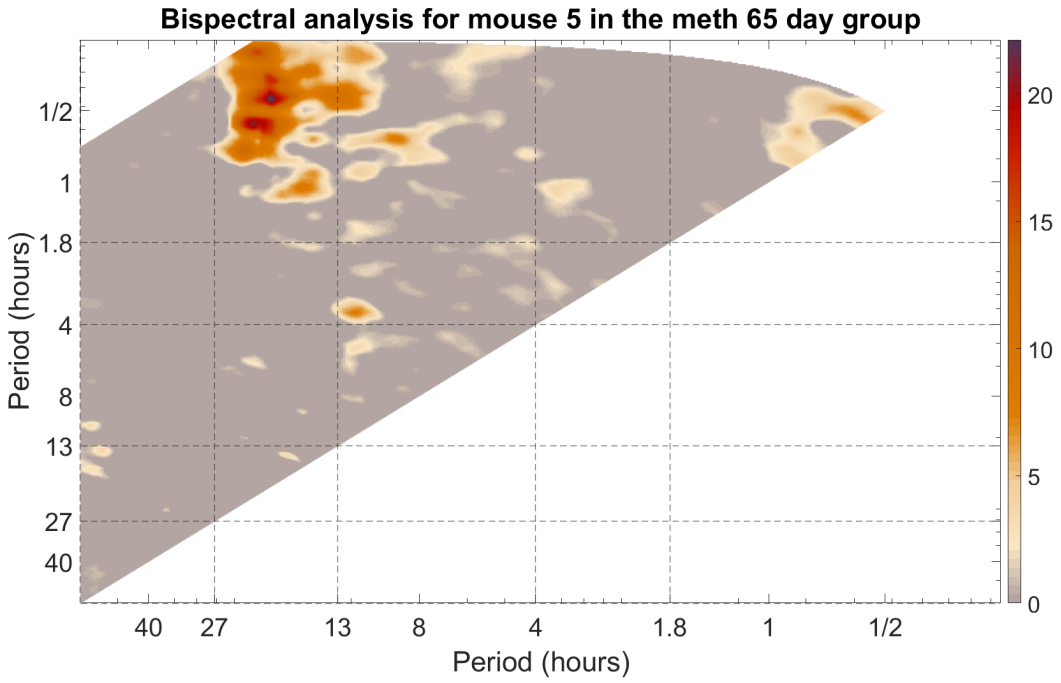

Figure F.6: Wavelet bispectra of behavioural data from mouse 5.

References

[1] J. Evans and R. Silver, "The suprachiasmatic nucleus and the circadian timekeeping system of the body," *Neuroscience in the 21st Century*, p. 1–49, 2015.

[2] A. Katharine and H. Julia, "How do our cells tell time?," *Frontiers for Young Minds*, Feb 2019.

[3] A. Charrier, B. Olliac, P. Roubertoux, and S. Tordjman, "Clock genes and altered sleep–wake rhythms: Their role in the development of psychiatric disorders," *International Journal of Molecular Sciences*, vol. 18, p. 938, Apr 2017.

[4] D. Zumpe and R. P. Michael, *Notes on the elements of behavioral science*. Springer Science & Business Media, 2001.

[5] S. Tordjman, S. Chokron, R. Delorme, A. Charrier, E. Bellissant, N. Jaafari, and C. Fougerou, "Melatonin: Pharmacology, functions and therapeutic benefits," *Current Neuropharmacology*, vol. 15, p. 434–443, Feb 2017.

[6] M. A. B. Oliveira, A. C. O. V. de Abreu, D. B. Constantino, A. C. Tonon, A. Díez-Noguera, F. G. Amaral, and M. P. Hidalgo, "Taking biological rhythms into account: From study design to results reporting," *Physiology & Behavior*, vol. 273, p. 114387, 2024.

[7] M. Littner, C. A. Kushida, W. M. Anderson, D. Bailey, R. B. Berry, D. G. Davila,

M. Hirshkowitz, S. Kapen, M. Kramer, D. Loube, *et al.*, "Practice parameters for the role of actigraphy in the study of sleep and circadian rhythms: an update for 2002," *Sleep*, vol. 26, no. 3, pp. 337–341, 2003.

[8] V. Natale, G. Plazzi, and M. Martoni, "Actigraphy in the assessment of insomnia: a quantitative approach," *Sleep*, vol. 32, no. 6, pp. 767–771, 2009.

[9] K. L. Lichstein, K. C. Stone, J. Donaldson, S. D. Nau, J. P. Soeffing, D. Murray, K. W. Lester, and R. N. Aguillard, "Actigraphy validation with insomnia," *Sleep*, vol. 29, no. 2, pp. 232–239, 2006.

[10] A. Sadeh, "The role and validity of actigraphy in sleep medicine: an update," *Sleep Medicine Reviews*, vol. 15, no. 4, pp. 259–267, 2011.

[11] F. Halberg, Y. L. Tong, and E. Johnson, "Circadian system phase—an aspect of temporal morphology; procedures and illustrative examples," in *The Cellular Aspects of Biorhythms: Symposium on Rhythmic Research Sponsored by the VIIIth International Congress of Anatomy Wiesbaden 8.–14. August 1965*, pp. 20–48, Springer, 1967.

[12] G. Cornelissen, "Cosinor-based rhythmometry," *Theoretical Biology and Medical Modelling*, vol. 11, no. 1, pp. 1–24, 2014.

[13] R. Refinetti, G. Cornélissen, and F. Halberg, "Procedures for numerical analysis of circadian rhythms," *Biological Rhythm Research*, vol. 38, no. 4, pp. 275–325, 2007.

[14] T. L. Leise, "Wavelet analysis of circadian and ultradian behavioral rhythms," *Journal of Circadian Rhythms*, vol. 11, no. 1, pp. 1–9, 2013.

[15] B. Krishnan, J. D. Levine, M. K. S. Lynch, H. B. Dowse, P. Funes, J. C. Hall, P. E. Hardin, and S. E. Dryer, "A new role for cryptochrome in a drosophila circadian oscillator," *Nature*, vol. 411, no. 6835, pp. 313–317, 2001.

[16] J. D. Levine, P. Funes, H. B. Dowse, and J. C. Hall, "Advanced analysis of a cryptochrome mutation's effects on the robustness and phase of molecular cycles in isolated peripheral tissues of drosophila," *BMC Neuroscience*, vol. 3, no. 1, pp. 1–17, 2002.

[17] W. Yu and P. E. Hardin, "Use of firefly luciferase activity assays to monitor circadian molecular rhythms in vivo and in vitro," *Circadian Rhythms: Methods and Protocols*, pp. 465–480, 2007.

[18] R. Fossion, A. L. Rivera, J. C. Toledo-Roy, M. Angelova, and M. El-Esawi, "Quantification of irregular rhythms in chrono-biology: A time-series perspective," in *Circadian Rhythm: Cellular and Molecular Mechanisms*, pp. 33–58, InTech, 2018.

[19] P. T. Clemson and A. Stefanovska, "Discerning non-autonomous dynamics," *Physics Reports*, vol. 542, no. 4, pp. 297–368, 2014.

[20] P. T. Clemson, G. Lancaster, and A. Stefanovska, "Reconstructing time-dependent dynamics," *IEEE Transactions on Signal Processing*, vol. 104, no. 2, pp. 223–241, 2016.

[21] C. A. Czeisler, J. F. Duffy, T. L. Shanahan, E. N. Brown, J. F. Mitchell, D. W. Rimmer, J. M. Ronda, E. J. Silva, J. S. Allan, J. S. Emens, D.-J. Dijk, and R. E. Kronauer, "Stability, precision, and near-24-hour period of the human circadian pacemaker," *Science*, vol. 284, p. 2177–2181, Jun 1999.

[22] J. E. Baggs and J. B. Hogenesch, "Genomics and systems approaches in the mammalian circadian clock," *Current Opinion in Genetics Development*, vol. 20, p. 581–587, Dec 2010.

[23] A. J. Brown, J. S. Pendergast, and S. Yamazaki, "Focus: Clocks and cycles:

Peripheral circadian oscillators," *PubMed Central (PMC)*, vol. 92(2), pp. 327–335, Jun 2019.

[24] M. Hastings, J. S. O'Neill, and E. S. Maywood, "Circadian clocks: regulators of endocrine and metabolic rhythms," *Journal of Endocrinology*, vol. 195, p. 187–198, Nov 2007.

[25] K. Krauchi, "How is the circadian rhythm of core body temperature regulated?," *Clinical Autonomic Research*, vol. 12, p. 147–149, Jun 2002.

[26] C. Wunderlich and J. Reeve, "The course of the temperature in diseases: a guide to clinical thermometry," *The American Journal of the Medical Sciences*, vol. 57, no. 425, p. 47, 1869.

[27] G. Kelly, "Body temperature variability (part 1): a review of the history of body temperature and its variability due to site selection, biological rhythms, fitness, and aging.," *Alternative Medicine Review*, vol. 11, no. 4, 2006.

[28] G. S. Kelly, "Body temperature variability (part 2): masking influences of body temperature variability and a review of body temperature variability in disease.," *Alternative Medicine Review*, vol. 12, no. 1, 2007.

[29] R. Hardeland, S. R. Pandi-Perumal, and D. P. Cardinali, "Melatonin," *The international Journal of Biochemistry & Cell Biology*, vol. 38, no. 3, pp. 313–316, 2006.

[30] B. Stankov and R. J. Reiter, "Melatonin receptors: current status, facts, and hypotheses," *Life Sciences*, vol. 46, no. 14, pp. 971–982, 1990.

[31] R. J. Reiter, H. Tamura, D. X. Tan, and X.-Y. Xu, "Melatonin and the circadian system: contributions to successful female reproduction," *Fertility and sterility*, vol. 102, no. 2, pp. 321–328, 2014.

[32] R. M. Slominski, R. J. Reiter, N. Schlabritz-Loutsevitch, R. S. Ostrom, and A. T. Slominski, "Melatonin membrane receptors in peripheral tissues: distribution and functions," *Molecular and Cellular Endocrinology*, vol. 351, no. 2, pp. 152–166, 2012.

[33] R. Hardeland, J. A. Madrid, D.-X. Tan, and R. J. Reiter, "Melatonin, the circadian multioscillator system and health: the need for detailed analyses of peripheral melatonin signaling," *Journal of Pineal Research*, vol. 52, no. 2, pp. 139–166, 2012.

[34] W. Anna and S. Basel, "How to measure circadian rhythms in humans," *Medicographia*, vol. 29, no. 1, pp. 84–90, 2007.

[35] R. J. Wurtman, J. Axelrod, and E. W. Chu, "Melatonin, a pineal substance: effect on the rat ovary," *Science*, vol. 141, no. 3577, pp. 277–278, 1963.

[36] R. J. Reiter, "The melatonin rhythm: both a clock and a calendar," *Experientia*, vol. 49, pp. 654–664, 1993.

[37] R. J. Gironda, J. Lloyd, M. E. Clark, and R. L. Walker, "Preliminary evaluation of reliability and criterion validity of actiwatch-score.," *Journal of Rehabilitation Research & Development*, vol. 44, no. 2, 2007.

[38] C. P. Pollak, W. W. Tryon, H. Nagaraja, and R. Dzwonczyk, "How accurately does wrist actigraphy identify the states of sleep and wakefulness?," *Sleep*, vol. 24, no. 8, pp. 957–965, 2001.

[39] D. Berson, "Strange vision: ganglion cells as circadian photoreceptors," *American Journal of Ophthalmology*, vol. 136, p. 1199, Dec 2003.

[40] E. D. Buhr and J. S. Takahashi, "Molecular components of the mammalian circadian clock," *Circadian Clocks*, pp. 3–27, 2013.

[41] D. K. Welsh, S.-H. Yoo, A. C. Liu, J. S. Takahashi, and S. A. Kay, "Bioluminescence imaging of individual fibroblasts reveals persistent, independently phased circadian rhythms of clock gene expression," *Current Biology*, vol. 14, p. 2289–2295, Dec 2004.

[42] D. K. Welsh, D. E. Logothetis, M. Meister, and S. M. Reppert, "Individual neurons dissociated from rat suprachiasmatic nucleus express independently phased circadian firing rhythms," *Neuron*, vol. 14, p. 697–706, Apr 1995.

[43] L. Morin and C. Allen, "The circadian visual system, 2005," *Brain Research Reviews*, vol. 51, p. 1–60, Jun 2006.

[44] S. J. Aton and E. D. Herzog, "Come together, right... now: Synchronization of rhythms in a mammalian circadian clock," *Neuron*, vol. 48, p. 531–534, Nov 2005.

[45] F. Gachon, E. Nagoshi, S. Brown, J. Ripperger, and U. Schibler, "The mammalian circadian timing system: from gene expression to physiology," *Chromosoma*, vol. 113, Aug 2004.

[46] M. H. Hastings, E. S. Maywood, and J. S. O'Neill, "Cellular circadian pacemaking and the role of cytosolic rhythms," *Current Biology*, vol. 18, p. R805–R815, Sep 2008.

[47] A. Kalsbeek, I. F. Palm, S. E. La Fleur, F. A. J. L. Scheer, S. Perreau-Lenz, M. Ruiter, F. Kreier, C. Cailotto, and R. M. Buijs, "Scn outputs and the hypothalamic balance of life," *Journal of Biological Rhythms*, vol. 21, p. 458–469, Dec 2006.

[48] H. Ohta, S. Yamazaki, and D. G. McMahon, "Constant light desynchronizes mammalian clock neurons," *Nature Neuroscience*, vol. 8, p. 267–269, Jan 2005.

[49] N. Inagaki, S. Honma, D. Ono, Y. Tanahashi, and K.-i. Honma, "Separate oscillating cell groups in mouse suprachiasmatic nucleus couple photoperiodically

to the onset and end of daily activity," *Proceedings of the National Academy of Sciences*, vol. 104, p. 7664–7669, May 2007.

[50] E. S. Maywood, A. B. Reddy, G. K. Wong, J. S. O'Neill, J. A. O'Brien, D. G. McMahon, A. J. Harmar, H. Okamura, and M. H. Hastings, "Synchronization and maintenance of timekeeping in suprachiasmatic circadian clock cells by neuropeptidergic signaling," *Current Biology*, vol. 16, p. 599–605, Mar 2006.

[51] E. D. Herzog, S. J. Aton, R. Numano, Y. Sakaki, and H. Tei, "Temporal precision in the mammalian circadian system: A reliable clock from less reliable neurons," *Journal of Biological Rhythms*, vol. 19, p. 35–46, Feb 2004.

[52] A. C. Liu, D. K. Welsh, C. H. Ko, H. G. Tran, E. E. Zhang, A. A. Priest, E. D. Buhr, O. Singer, K. Meeker, I. M. Verma, F. J. Doyle, J. S. Takahashi, and S. A. Kay, "Intercellular coupling confers robustness against mutations in the scn circadian clock network," *Cell*, vol. 129, p. 605–616, May 2007.

[53] D. K. Welsh, J. S. Takahashi, and S. A. Kay, "Suprachiasmatic nucleus: Cell autonomy and network properties," *Annual Review of Physiology*, vol. 72, p. 551–577, Mar 2010.

[54] R. J. Konopka and S. Benzer, "Clock mutants of drosophila melanogaster," *Proceedings of the National Academy of Sciences*, vol. 68, p. 2112–2116, Sep 1971.

[55] I. Edery, J. E. Rutila, and M. Rosbash, "Phase shifting of the circadian clock by induction of the drosophila period protein," *Science*, vol. 263, p. 237–240, Jan 1994.

[56] A. Sehgal, J. L. Price, B. Man, and M. W. Young, "Loss of circadian behavioral rhythms and per rna oscillations in the drosophila mutant timeless," *Science*, vol. 263, p. 1603–1606, Mar 1994.

[57] M. H. Vitaterna, D. P. King, A.-M. Chang, J. M. Kornhauser, P. L. Lowrey, J. D. McDonald, W. F. Dove, L. H. Pinto, F. W. Turek, and J. S. Takahashi, "Mutagenesis and mapping of a mouse gene, clock , essential for circadian behavior," *Science*, vol. 264, p. 719–725, Apr 1994.

[58] P. Pevet, B. Bothorel, H. Slotten, and M. Saboureau, "The chronobiotic properties of melatonin," *Cell and Tissue Research*, vol. 309, p. 183–191, Jul 2002.

[59] P. Pevet and E. Challet, "Melatonin: Both master clock output and internal time-giver in the circadian clocks network," *Journal of Physiology-Paris*, vol. 105, p. 170–182, Dec 2011.

[60] H. A. Slotten, S. Krekling, B. Sicard, and P. Pevet, "Daily infusion of melatonin entrains circadian activity rhythms in the diurnal rodent arvicanthis ansorgei," *Behavioural Brain Research*, vol. 133, p. 11–19, Jun 2002.

[61] H. A. Slotten, B. Pitrosky, S. Krekling, and P. Pevet, "Entrainment of circadian activity rhythms in rats to melatonin administered at t cycles different from 24 hours," *Neurosignals*, vol. 11, no. 2, p. 73–80, 2002.

[62] M. Zeman and I. Herichova, "Melatonin and clock genes expression in the cardiovascular system," *Frontiers In Bioscience*, vol. S5, no. 2, p. 743–753, 2013.

[63] J. D. Johnston, B. B. Tournier, H. Andersson, M. Masson-Pevet, G. A. Lincoln, and D. G. Hazlerigg, "Multiple effects of melatonin on rhythmic clock gene expression in the mammalian pars tuberalis," *Endocrinology*, vol. 147, p. 959–965, Feb 2006.

[64] T. D. Steeves, D. P. King, Y. Zhao, A. M. Sangoram, F. Du, A. M. Bowcock, R. Y. Moore, and J. S. Takahashi, "Molecular cloning and characterization of the humanclockgene: Expression in the suprachiasmatic nuclei," *Genomics*, p. 189–200, Apr 1999.

[65] J. S. Takahashi, "Transcriptional architecture of the mammalian circadian clock," *Nature Reviews Genetics*, vol. 18, p. 164–179, Dec 2016.

[66] S. Panda, M. P. Antoch, B. H. Miller, A. I. Su, A. B. Schook, M. Straume, P. G. Schultz, S. A. Kay, J. S. Takahashi, and J. B. Hogenesch, "Coordinated transcription of key pathways in the mouse by the circadian clock," *Cell*, vol. 109, p. 307–320, May 2002.

[67] J. C. Dunlap, "Molecular bases for circadian clocks," *Cell*, vol. 96, p. 271–290, Jan 1999.

[68] P. E. Hardin, "Activating inhibitors and inhibiting activators: a day in the life of a fly," *Current Opinion in Neurobiology*, vol. 8, p. 642–647, Oct 1998.

[69] P. L. Lowrey and J. S. Takahashi, "Genetics of circadian rhythms in mammalian model organisms," *The Genetics of Circadian Rhythms*, p. 175–230, 2011.

[70] C. Lee, J.-P. Etchegaray, F. R. Cagampang, A. S. Loudon, and S. M. Reppert, "Posttranslational mechanisms regulate the mammalian circadian clock," *Cell*, vol. 107, p. 855–867, Dec 2001.

[71] K. Kume, M. J. Zylka, S. Sriram, L. P. Shearman, D. R. Weaver, X. Jin, E. S. Maywood, M. H. Hastings, and S. M. Reppert, "mcry1 and mcry2 are essential components of the negative limb of the circadian clock feedback loop," *Cell*, vol. 98, p. 193–205, Jul 1999.

[72] L. P. Shearman, S. Sriram, D. R. Weaver, E. S. Maywood, I. Chaves, B. Zheng, K. Kume, C. C. Lee, G. T. J. van der, Horst, M. H. Hastings, and S. M. Reppert, "Interacting molecular loops in the mammalian circadian clock," *Science*, vol. 288, p. 1013–1019, May 2000.

[73] B. Marcheva, K. M. Ramsey, E. D. Buhr, Y. Kobayashi, H. Su, C. H. Ko, G. Ivanova, C. Omura, S. Mo, M. H. Vitaterna, J. P. Lopez, L. H. Philipson,

C. A. Bradfield, S. D. Crosby, L. JeBailey, X. Wang, J. S. Takahashi, and J. Bass, "Disruption of the clock components clock and bmal1 leads to hypoinsulinaemia and diabetes," *Nature*, vol. 466, p. 627–631, Jun 2010.

[74] P. Janich, G. Pascual, A. Merlos-Suárez, E. Batlle, J. Ripperger, U. Albrecht, H.-Y. M. Cheng, K. Obrietan, L. Di Croce, and S. A. Benitah, "The circadian molecular clock creates epidermal stem cell heterogeneity," *Nature*, vol. 480, p. 209–214, Nov 2011.

[75] G. K. Paschos, S. Ibrahim, W.-L. Song, T. Kunieda, G. Grant, T. M. Reyes, C. A. Bradfield, C. H. Vaughan, M. Eiden, M. Masoodi, J. L. Griffin, F. Wang, J. A. Lawson, and G. A. FitzGerald, "Obesity in mice with adipocyte-specific deletion of clock component arntl," *Nature Medicine*, vol. 18, p. 1768–1777, Nov 2012.

[76] J. S. Takahashi, H.-K. Hong, C. H. Ko, and E. L. McDearmon, "The genetics of mammalian circadian order and disorder: implications for physiology and disease," *Nature Reviews Genetics*, vol. 9, p. 764–775, Oct 2008.

[77] S. Yamazaki, R. Numano, M. Abe, A. Hida, R.-i. Takahashi, M. Ueda, G. D. Block, Y. Sakaki, M. Menaker, and H. Tei, "Resetting central and peripheral circadian oscillators in transgenic rats," *Science*, vol. 288, p. 682–685, Apr 2000.

[78] S.-H. Yoo, S. Yamazaki, P. L. Lowrey, K. Shimomura, C. H. Ko, E. D. Buhr, S. M. Siepka, H.-K. Hong, W. J. Oh, O. J. Yoo, M. Menaker, and J. S. Takahashi, "Period2::luciferase real-time reporting of circadian dynamics reveals persistent circadian oscillations in mouse peripheral tissues," *Proceedings of The National Academy of Sciences*, vol. 101, p. 5339–5346, Feb 2004.

[79] C. Dibner, U. Schibler, and U. Albrecht, "The mammalian circadian timing system: Organization and coordination of central and peripheral clocks," *Annual Review of Physiology*, vol. 72, p. 517–549, Mar 2010.

[80] H. Guo, J. M. Brewer, M. N. Lehman, and E. L. Bittman, "Suprachiasmatic regulation of circadian rhythms of gene expression in hamster peripheral organs: Effects of transplanting the pacemaker," *Journal of Neuroscience*, vol. 26, p. 6406–6412, Jun 2006.

[81] M. Stratmann and U. Schibler, "Properties, entrainment, and physiological functions of mammalian peripheral oscillators," *Journal of Biological Rhythms*, vol. 21, p. 494–506, Dec 2006.

[82] F. Damiola, N. Le Minh, N. Preitner, B. Kornmann, F. Fleury-Olela, and U. Schibler, "Restricted feeding uncouples circadian oscillators in peripheral tissues from the central pacemaker in the suprachiasmatic nucleus," *Genes Development*, vol. 14, p. 2950–2961, Dec 2000.

[83] S. A. Brown, G. Zumbrunn, F. Fleury-Olela, N. Preitner, and U. Schibler, "Rhythms of mammalian body temperature can sustain peripheral circadian clocks," *Current Biology*, vol. 12, p. 1574–1583, Sep 2002.

[84] M. H. Hastings, A. B. Reddy, and E. S. Maywood, "A clockwork web: circadian timing in brain and periphery, in health and disease," *Nature Reviews Neuroscience*, vol. 4, p. 649–661, Aug 2003.

[85] M. D. Anglin, C. Burke, B. Perrochet, E. Stamper, and S. Dawud-Noursi, "History of the methamphetamine problem," *Journal of Psychoactive Drugs*, vol. 32, no. 2, pp. 137–141, 2000.

[86] R. M. Julien, *A primer of drug action: A concise nontechnical guide to the actions, uses, and side effects of psychoactive drugs, revised and updated*. Holt Paperbacks, 2013.

[87] M. R. Ralph, R. G. Foster, F. C. Davis, and M. Menaker, "Transplanted

suprachiasmatic nucleus determines circadian period," *Science*, vol. 247, p. 975–978, Feb 1990.

[88] F. K. Stephan and I. Zucker, "Circadian rhythms in drinking behavior and locomotor activity of rats are eliminated by hypothalamic lesions," *Proceedings of The National Academy of Sciences*, vol. 69, p. 1583–1586, Jun 1972.

[89] J. A. Mohawk, M. L. Baer, and M. Menaker, "The methamphetamine-sensitive circadian oscillator does not employ canonical clock genes," *Proceedings of The National Academy of Sciences*, vol. 106, p. 3519–3524, Mar 2009.

[90] S. K. T. Taufique, D. E. Ehichioya, J. S. Pendergast, and S. Yamazaki, "Genetics and functional significance of the understudied methamphetamine sensitive circadian oscillator (masco)," *F1000Research*, vol. 11, p. 1018, Oct 2022.

[91] Tataroglu, A. J. Davidson, L. J. Benvenuto, and M. Menaker, "The methamphetamine-sensitive circadian oscillator (masco) in mice," *Journal of Biological Rhythms*, vol. 21, p. 185–194, Jun 2006.

[92] A. S. Fisk, *The effect of disruptive light conditions on sleep and circadian rhythms*. PhD thesis, University of Oxford, 2019.

[93] R. G. Foster and K. Wulff, "The rhythm of rest and excess," *Nature Reviews Neuroscience*, vol. 6, p. 407–414, May 2005.

[94] A. C. West and D. A. Bechtold, "The cost of circadian desynchrony: Evidence, insights and open questions," *BioEssays*, vol. 37, p. 777–788, May 2015.

[95] G. Vandewalle, C. Schmidt, G. Albouy, V. Sterpenich, A. Darsaud, G. Rauchs, P.-Y. Berken, E. Balteau, C. Degueldre, A. Luxen, P. Maquet, and D.-J. Dijk, "Brain responses to violet, blue, and green monochromatic light exposures in humans: Prominent role of blue light and the brainstem," *PLoS ONE*, vol. 2, p. e1247, Nov 2007.

[96] N. Park, S. Cheon, G. H. Son, S. Cho, and K. Kim, "Chronic circadian disturbance by a shortened light-dark cycle increases mortality," *Neurobiology of Aging*, vol. 33, pp. 1122.e11–1122.e22, Jun 2012.

[97] M. W. Hurd and M. R. Ralph, "The significance of circadian organization for longevity in the golden hamster," *Journal of Biological Rhythms*, vol. 13, p. 430–436, Oct 1998.

[98] T. A. Martino, G. Y. Oudit, A. M. Herzenberg, N. Tata, M. M. Koletar, G. M. Kabir, D. D. Belsham, P. H. Backx, M. R. Ralph, and M. J. Sole, "Circadian rhythm disorganization produces profound cardiovascular and renal disease in hamsters," *American Journal of Physiology-Regulatory, Integrative and Comparative Physiology*, vol. 294, p. R1675–R1683, May 2008.

[99] Y. Tahara, Y. Takatsu, T. Shiraishi, Y. Kikuchi, M. Yamazaki, H. Motohashi, A. Muto, H. Sasaki, A. Haraguchi, D. Kuriki, T. J. Nakamura, and S. Shibata, "Age-related circadian disorganization caused by sympathetic dysfunction in peripheral clock regulation," *NPJ Aging and Mechanisms of Disease*, vol. 3, Jan 2017.

[100] S. Strogatz, M. Friedman, A. J. Mallinckrodt, and S. McKay, "Nonlinear dynamics and chaos: With applications to physics, biology, chemistry, and engineering," *Journal of Computational Physics*, vol. 8, no. 5, pp. 532–532, 1994.

[101] A. Goldbeter, *Biochemical oscillations and cellular rhythms: the molecular bases of periodic and chaotic behaviour*. Cambridge University Press, 1997.

[102] P. E. Kloeden and C. Pötzsche, "Nonautonomous dynamical systems in the life sciences," in *Nonautonomous Dynamical Systems in the Life Sciences*, pp. 3–39, Springer, 2013.

[103] C. Chatfield, *The Analysis of Time Series: an Introduction*. CRC Press, 2016.

[104] D. Gabor, "Theory of communication. part 1: The analysis of information," *Journal of the Institution of Electrical Engineers*, vol. 93, no. 26, pp. 429–441, 1946.

[105] F. M. Pouzols and A. Lendasse, "Effect of different detrending approaches on computational intelligence models of time series," in *The 2010 International Joint Conference on Neural Networks (IJCNN)*, pp. 1–8, IEEE, 2010.

[106] J. Newman, G. Lancaster, and A. Stefanovska, "Multiscale oscillatory dynamics analysis (v1. 01, user manual)," *Department of Physics, Lancaster University*, 2018.

[107] D. Iatsenko, P. V. McClintock, and A. Stefanovska, "Linear and synchrosqueezed time–frequency representations revisited: Overview, standards of use, resolution, reconstruction, concentration, and algorithms," *Digital Signal Processing*, vol. 42, pp. 1–26, 2015.

[108] A. R. Kiselev, A. S. Karavaev, V. I. Gridnev, M. D. Prokhorov, V. I. Ponomarenko, E. I. Borovkova, V. A. Shvartz, Y. M. Ishbulatov, O. M. Posnenkova, and B. P. Bezruchko, "Method of estimation of synchronization strength between low-frequency oscillations in heart rate variability and photoplethysmographic waveform variability," *Russian Open Medical Journal*, vol. 5, no. 1, pp. 0101–0101, 2016.

[109] J. Rowland Adams, J. Newman, and A. Stefanovska, "Distinguishing between deterministic oscillations and noise," *The European Physical Journal Special Topics*, Sep 2023.

[110] A. Lerch, *An introduction to audio content analysis: Applications in signal processing and music informatics*. Wiley-IEEE Press, 2012.

[111] M. Bračič and A. Stefanovska, "Wavelet-based analysis of human blood-flow dynamics," *Bulletin of Mathematical Biology*, vol. 60, pp. 919–935, 1998.

[112] X. Yu, Z. Mei, C. Chen, and W. Chen, "Ranking power spectra: a proof of concept," *Entropy*, vol. 21, no. 11, p. 1057, 2019.

[113] J. N. Joe Rowland Adams and A. Stefanovska, "Distinguishing between deterministic oscillations and noise," *The European Physical Journal Special Topics*, vol. 232, no. 20, pp. 3435–3457, 2023.

[114] A. Guillet, A. Arneodo, and F. Argoul, "Tracking rhythms coherence from polysomnographic records: A time-frequency approach," *Frontiers in Applied Mathematics and Statistics*, vol. 7, p. 624456, 2021.

[115] B. Cazelles, M. Chavez, D. Berteaux, F. Ménard, J. O. Vik, S. Jenouvrier, and N. C. Stenseth, "Wavelet analysis of ecological time series," *Oecologia*, vol. 156, pp. 287–304, 2008.

[116] M. B. Lotric, A. Stefanovska, D. Stajer, and V. Urbancic-Rovan, "Spectral components of heart rate variability determined by wavelet analysis," *Physiological Measurement*, vol. 21, no. 4, p. 441, 2000.

[117] F. T. Yu and G. Lu, "Short-time fourier transform and wavelet transform with fourier-domain processing," *Applied Optics*, vol. 33, no. 23, pp. 5262–5270, 1994.

[118] D. Iatsenko, P. V. E. McClintock, and A. Stefanovska, "Extraction of instantaneous frequencies from ridges in time–frequency representations of signals," *Signal Processing*, vol. 125, pp. 290–303, 2016.

[119] N. Delprat, B. Escudié, P. Guillemain, R. Kronland-Martinet, P. Tchamitchian, and B. Torresani, "Asymptotic wavelet and Gabor analysis: Extraction of instantaneous frequencies," *IEEE Transactions on Information Theory*, vol. 38, no. 2, pp. 644–664, 1992.

[120] L. W. Sheppard, A. Stefanovska, and P. V. E. McClintock, "Detecting the harmonics of oscillations with time-variable frequencies," *Physics Review E*, vol. 83, no. 1, p. 016206, 2011.

[121] J. Newman, A. Pidde, and A. Stefanovska, "Defining the wavelet bispectrum," *Applied and Computational Harmonic Analysis*, vol. 51, pp. 171–224, 2021.

[122] J. Jamsek and A. Stefanovska, "The cardio-respiratory couplings observed in the ldf signal using wavelet bispectrum," in *2007 29th Annual International Conference of the IEEE Engineering in Medicine and Biology Society*, pp. 4072–4075, IEEE, 2007.

[123] T. Stankovski, A. Duggento, P. V. E. McClintock, and A. Stefanovska, "A tutorial on time-evolving dynamical Bayesian inference," *The European Physical Journal Special Topics*, vol. 223, no. 13, pp. 2685–2703, 2014.

[124] M. G. Rosenblum and A. S. Pikovsky, "Detecting direction of coupling in interacting oscillators," *Physics Review E*, vol. 64, no. 4, p. 045202, 2001.

[125] M. Paluš and A. Stefanovska, "Direction of coupling from phases of interacting oscillators: An information-theoretic approach," *Physics Review E*, vol. 67, no. 5, p. 055201, 2003.

[126] T. Stankovski, T. Pereira, P. V. E. McClintock, and A. Stefanovska, "Coupling functions: universal insights into dynamical interaction mechanisms," *Reviews of Modern Physics*, vol. 89, no. 4, p. 045001, 2017.

[127] A. Duggento, T. Stankovski, P. V. E. McClintock, and A. Stefanovska, "Dynamical Bayesian inference of time-evolving interactions: From a pair of coupled oscillators to networks of oscillators," *Physics Review E*, vol. 86, no. 6, p. 061126, 2012.

[128] F. Wilcoxon, "Individual comparisons by ranking methods," *Biometrics Bulletin*, vol. 1, p. 80, Dec 1945.

[129] B. Rosner, R. J. Glynn, and M.-L. T. Lee, "The wilcoxon signed rank test for paired comparisons of clustered data," *Biometrics*, vol. 62, no. 1, pp. 185–192, 2006.

[130] J. McDonald, "Student's t-test," *Handbook of Biological Statistics. 2nd ed. Sparky House Publishing. Baltimore, MD*, pp. 118–122, 2009.

[131] M. Bücker, "Jean dickinson gibbons, subhabrata chakraborti: Nonparametric statistical inferences," *Statistical Papers*, vol. 55, p. 1227–1228, Jun 2013.

[132] G. Lancaster, D. Iatsenko, A. Pidde, V. Ticcinelli, and A. Stefanovska, "Surrogate data for hypothesis testing of physical systems," *Physics Reports*, 2018.

[133] T. Schreiber and A. Schmitz, "Surrogate time series," *Physica D: Nonlinear Phenomena*, vol. 142, no. 3-4, pp. 346–382, 2000.

[134] S. J. Barnes, M. Alanazi, S. Yamazaki, and A. Stefanovska, "Methamphetamine alters the circadian oscillator and its couplings on multiple scales in per1/2/3 knockout mice," *PNAS Nexus*, p. 1–12, YEAR.

[135] J. S. O'Neill, G. Van Ooijen, L. E. Dixon, C. Troein, F. Corellou, F.-Y. Bouget, A. B. Reddy, and A. J. Millar, "Circadian rhythms persist without transcription in a eukaryote," *Nature*, vol. 469, no. 7331, pp. 554–558, 2011.

[136] R. W. Logan and C. A. McClung, "Rhythms of life: circadian disruption and brain disorders across the lifespan," *Nature Reviews Neuroscience*, vol. 20, no. 1, pp. 49–65, 2019.

[137] R. P. Ogeil, S. Arunogiri, and J. Grigg, "Methamphetamine addiction: do

biological rhythms matter, and could they play a role in treatment?," *Sleep*, vol. 44, no. 7, p. zsab052, 2021.

[138] M. Morris, S. Yamazaki, and A. Stefanovska, "Multiscale time-resolved analysis reveals remaining behavioral rhythms in mice without canonical circadian clocks," *Journal of Biological Rhythms*, vol. 37, no. 3, pp. 310–328, 2022.

[139] M. Shamir, Y. Bar-On, R. Phillips, and R. Milo, "Snapshot: timescales in cell biology," *Cell*, vol. 164, no. 6, pp. 1302–1302, 2016.

[140] S. Yamazaki, M. C. Kerbeshian, C. G. Hocker, G. D. Block, and M. Menaker, "Rhythmic properties of the hamster suprachiasmatic nucleusin vivo," *Journal of Neuroscience*, vol. 18, no. 24, pp. 10709–10723, 1998.

[141] J. J. Mahoney III, B. J. Jackson, A. D. Kalechstein, R. De La Garza II, and T. F. Newton, "Acute, low-dose methamphetamine administration improves attention/information processing speed and working memory in methamphetamine-dependent individuals displaying poorer cognitive performance at baseline," *Progress in Neuro-Psychopharmacology and Biological Psychiatry*, vol. 35, no. 2, pp. 459–465, 2011.

[142] L. W. Sheppard, A. Stefanovska, and P. V. E. McClintock, "Testing for time-localized coherence in bivariate data," *Physics Review E*, vol. 85, no. 4, p. 046205, 2012.

[143] A. Bandrivskyy, A. Bernjak, P. V. E. McClintock, and A. Stefanovska, "Wavelet phase coherence analysis: application to skin temperature and blood flow," *Cardiovascular Engineering: An International Journal*, vol. 4, no. 1, pp. 89–93, 2004.

[144] J.-P. Lachaux, A. Lutz, D. Rudrauf, D. Cosmelli, M. Le Van Quyen, J. Martinerie, and F. Varela, "Estimating the time-course of coherence between single-trial brain

signals: an introduction to wavelet coherence," *Clinical Neurophysiology*, vol. 32, no. 3, pp. 157–174, 2002.

[145] M. Le Van Quyen, J. Foucher, J.-P. Lachaux, E. Rodriguez, A. Lutz, J. Martinerie, and F. J. Varela, "Comparison of Hilbert transform and wavelet methods for the analysis of neuronal synchrony," *Journal of Neuroscience Methods*, vol. 111, no. 2, pp. 83–98, 2001.

[146] A. Grinsted, J. C. Moore, and S. Jevrejeva, "Application of the cross wavelet transform and wavelet coherence to geophysical time series," *Nonlinear Process. Geophys*, vol. 11, no. 5/6, pp. 561–566, 2004.

[147] D. Kugiumtzis, "Surrogate data test on time series," in *Modelling and Forecasting Financial Data*, pp. 267–282, Springer, 2002.